Bharat Jhamnani

Thesis_Zohaib_Minor_Revision

Thesis 2026

Document Details

Submission ID
trn:oid:::27535:139185248

Submission Date
May 16, 2026, 1:37 PM GMT+5:30

Download Date
May 16, 2026, 1:50 PM GMT+5:30

File Name
Thesis_Zohaib_Minor_Revision.pdf

File Size
7.9 MB

168 Pages

42,207 Words

246,119 Characters

8% Overall Similarity

The combined total of all matches, including overlapping sources, for each database.

Filtered from the Report

- Bibliography
- Quoted Text
- Cited Text
- Small Matches (less than 10 words)

Exclusions

- 2 Excluded Sources

Match Groups

186 Not Cited or Quoted 8%
Matches with neither in-text citation nor quotation marks

0 Missing Quotations 0%
Matches that are still very similar to source material

0 Missing Citation 0%
Matches that have quotation marks, but no in-text citation

0 Cited and Quoted 0%
Matches with in-text citation present, but no quotation marks

Top Sources

4% Internet sources
5% Publications
5% Submitted works (Student Papers)

Integrity Flags

0 Integrity Flags for Review

Our system's algorithms look deeply at a document for any inconsistencies that would set it apart from a normal submission. If we notice something strange, we flag it for you to review.

A Flag is not necessarily an indicator of a problem. However, we'd recommend you focus your attention there for further review.

Match Groups

- **186** Not Cited or Quoted 8%
  Matches with neither in-text citation nor quotation marks
- **0** Missing Quotations 0%
  Matches that are still very similar to source material
- **0** Missing Citation 0%
  Matches that have quotation marks, but no in-text citation
- **0** Cited and Quoted 0%
  Matches with in-text citation present, but no quotation marks

Top Sources

4% Internet sources
5% Publications
5% Submitted works (Student Papers)

Top Sources

The sources with the highest number of matches within the submission. Overlapping sources will not be displayed.

1	Student papers	Indian Institute of Technology Guwahati on 2025-01-06 <1%
2	Internet	www.mdpi.com <1%
3	Internet	idr.nitk.ac.in <1%
4	Student papers	Krea University on 2026-05-01 <1%
5	Internet	dtu.ac.in <1%
6	Internet	irgu.unigoa.ac.in <1%
7	Publication	"Laser Scanning Applications in Landslide Assessment", Springer Science and Bus... <1%
8	Publication	Sumit Das, Amitesh Gupta. "Multi-criteria decision based geospatial mapping of fl... <1%
9	Student papers	University of Moratuwa on 2026-04-29 <1%
10	Publication	Sumit Das. "Geospatial mapping of flood susceptibility and hydro-geomorphic res... <1%

11 Publication
Jesudasan Jacinth Jennifer, Subbarayan Saravanan. "Artificial neural network and... <1%

12 Publication
Amrie Singh, Vijay Sreeparvathy, Sengupta Debdut, Maria Pregnolato, Nigel Wrig... <1%

13 Publication
Aumed Rahman M Amen, Andam Mustafa, Dalshad Ahmed Kareem, Hasan Moha... <1%

14 Student papers
Loughborough University on 2024-04-30 <1%

15 Student papers
Sultan Qaboos University on 2022-07-26 <1%

16 Publication
Mahfuzur Rahman, Chen Ningsheng, Golam Iftekhar Mahmud, Md Monirul Islam ... <1%

17 Publication
Olabanji Aladejana. "Flood investigation and adaptation strategies through best ... <1%

18 Student papers
Delhi Technological University on 2026-04-30 <1%

19 Publication
Parthasarathy Kulithalai Shiyam Sundar, Subrahmanya Kundapura. "Spatial Map... <1%

20 Student papers
Sardar Vallabhbhai National Inst. of Tech.Surat on 2023-04-05 <1%

21 Student papers
University of Edinburgh on 2023-08-31 <1%

22 Student papers
Delhi Technological University on 2026-05-07 <1%

23 Publication
Munonde, Tshimangadzo Saddam. "Design and Development of Low Cost Materi... <1%

24 Publication
Biswajit Das, Subodh Chandra Pal. "Assessment of groundwater vulnerability to o... <1%

25 Internet

link.springer.com <1%

26 Publication

Ashish Juneja, Anil Joseph, Dasaka S. Murty. "GeoVadis - The Future of Geotechnic... <1%

27 Student papers

Hawassa University on 2025-10-23 <1%

28 Internet

repository.pauwes-cop.net <1%

29 Student papers

Anna University on 2025-07-07 <1%

30 Internet

docplayer.net <1%

31 Internet

www.researchgate.net <1%

32 Student papers

Anna University on 2025-12-13 <1%

33 Student papers

Anna University on 2026-03-26 <1%

34 Publication

Temesgen T. Mihret, Fasikaw F. Cherie, Fasikaw A. Zemale. "Flood susceptibility m... <1%

35 Internet

gyan.iitg.ac.in <1%

36 Student papers

Uttar Pradesh Technical University on 2022-03-21 <1%

37 Internet

ouci.dntb.gov.ua <1%

38 Internet

iwfm.buet.ac.bd <1%

39 Publication

Subbarayan Saravanan, Devanantham Abijith, Nagireddy Masthan Reddy, Partha... <1%

40 Student papers

Addis Ababa University on 2025-06-23 <1%

41 Publication

Debabrata Sarkar, Sunil Saha, Trishna Sarkar, Prolay Mondal. "Delineation of Floo... <1%

42 Publication

Jatan Debnath, Dhrubajyoti Sahariah, Meghna Mazumdar, Durlov Lahon et al. "Ev... <1%

43 Publication

Kyriakos Michaelides, Athos Agapiou. "An Open-Access Remote Sensing and AHP–... <1%

44 Student papers

University of Aberdeen on 2023-08-15 <1%

45 Internet

espace.curtin.edu.au <1%

46 Student papers

Addis Ababa University on 2024-05-07 <1%

47 Publication

Ananda Krishnan, S.G. Dhanil Dev, S. Arjun, V. Deepchand, Yogendra Singh, E. Sha... <1%

48 Publication

Boyuan Li, Na Lin, Xian Zhang, Chun Wang, Kai Yang, Kai Ding, Bin Wang. "Monito... <1%

49 Publication

Bulti Das, Tuhin Kanti Ray, Eshita Boral. "Identification of urban waterlogging ris... <1%

50 Publication

Biplab Mandal, Sujit Mandal. "Analytical hierarchy process (AHP) based landslide ... <1%

51 Student papers

Dibrugarh University,Assam on 2026-01-04 <1%

52 Publication

Manamno Beza Dinku, Habtamu Hailu Kebede. "Identification and mapping of su... <1%

53 Publication

Showmitra Sarkar, Swapan Talukdar, Atiqur Rahman, Shah fahad, Sujit Roy. "Gro... <1%

54 Internet

assets-eu.researchsquare.com <1%

55 Publication

"Water Security and Climate Change", Springer Science and Business Media LLC, ... <1%

56 Publication

Abdelkader Hamlat, Chadli Bendjedid Kadri, Azeddine Guidoum, Hadda Bekkaye. ... <1%

57 Publication

Câmara, Ariele. "Knowledge-Based Machine Learning Approach to Indirect Prosp... <1%

58 Student papers

Higher Education Commission Pakistan on 2020-11-24 <1%

59 Student papers

Kenyatta University on 2020-08-11 <1%

60 Student papers

Manipal Academy of Higher Education (MAHE) on 2023-02-08 <1%

61 Publication

Michael M. Msabi, Michael Makonyo. "Flood susceptibility mapping using GIS and... <1%

62 Student papers

The University of Manchester on 2026-03-20 <1%

63 Student papers

University of Leicester on 2024-10-14 <1%

64 Publication

Wahidullah Hussainzada, Han Soo Lee. "Effect of an improved agricultural irrigati... <1%

65 Internet

www.frontiersin.org <1%

66 Internet

www.uts.edu.au <1%

67 Student papers
Arba Minch University on 2024-08-27 <1%

68 Publication
Bhumika Uniyal, Madan K. Jha, Arvind Kumar Verma, Prajna Kasargodu Anebagil... <1%

69 Student papers
Douglas County Schools on 2022-04-20 <1%

70 Publication
Jesudasan Jacinth Jennifer, Subbarayan Saravanan, Biswajeet Pradhan. "Persisten... <1%

71 Student papers
National Institute of Technical Teachers Training and Research Chennai on 2026-... <1%

72 Student papers
Nottingham Trent University on 2025-09-12 <1%

73 Student papers
University Der Es Salaam on 2025-05-12 <1%

74 Student papers
University of Witwatersrand on 2026-02-24 <1%

75 Internet
core.ac.uk <1%

76 Publication
"Progress in Multicriteria Decision Making Models", Springer Science and Busines... <1%

77 Publication
Arpana Handique, Praduyt Dey, Santanu Kumar Patnaik. "Chapter 4 Modeling La... <1%

78 Student papers
Delhi Technological University on 2026-04-29 <1%

79 Student papers
Fakir Mohan University on 2024-10-25 <1%

80 Student papers
Higher Education Commission Pakistan on 2020-12-29 <1%

81 Student papers

Jawaharlal Nehru University (JNU) on 2022-05-23 <1%

82 Student papers

Kwame Nkrumah University of Science and Technology on 2016-12-29 <1%

83 Student papers

National Institute of Technology, Rourkela on 2014-05-25 <1%

84 Publication

Seyed Amir Naghibi, Hamid Reza Pourghasemi, Barnali Dixon. "GIS-based ground... <1%

85 Publication

Suman Patra, Pulak Mishra, Subhash Chandra Mahapatra. "Delineation of ground... <1%

86 Publication

Tariku Takele, Abraham Mechal, Berihu Abadi Berhe. "Evaluation of groundwater ... <1%

87 Student papers

University of Moratuwa on 2022-01-01 <1%

88 Internet

dokumen.pub <1%

89 Internet

etd.uwc.ac.za <1%

90 Internet

repository.maseno.ac.ke <1%

91 Internet

udsspace.uds.edu.gh <1%

92 Internet

www.universepg.com <1%

93 Publication

"Advanced GIScience in Hydro-Geological Hazards", Springer Science and Busines... <1%

94 Publication

"Advancements in Soil Conservation", Springer Science and Business Media LLC, 2... <1%

95 Publication

"Groundwater and Society", Springer Science and Business Media LLC, 2021 <1%

96 Publication

"Hydrological Extremes", Springer Science and Business Media LLC, 2021 <1%

97 Publication

Ajay Kumar Taloor, Varun Khajuria, Savati Sharma, Gurnam Parsad et al. "Integra... <1%

98 Student papers

Asian Institute of Technology on 2023-02-09 <1%

99 Publication

Brototi Biswas, Bhagwan Ghute, Jayanta Das. "Geoinformatics for Flood Risk Man... <1%

100 Student papers

Central University of Karnataka on 2025-07-23 <1%

101 Student papers

Cotton University on 2026-02-04 <1%

102 Publication

Deepak Kumar, Anil Kumar, Shekhar Singh. "Geospatial and Hydrological Modelli... <1%

103 Publication

Eltaher M. Shams, Ahmed A. Asmoay, Abrar Abdel-Salam, Sahar N. E. Tawfik, Rash... <1%

104 Publication

Hamed Taherdoost. "Navigating Qualitative Research - A Comprehensive Guide t... <1%

105 Publication

Logesh Natarajan, Tune Usha, Muthusankar Gowrappan, Bavinaya Palpanabhan ... <1%

106 Student papers

Maulana Azad National Institute of Technology Bhopal on 2022-04-21 <1%

107 Publication

Muluneh Legesse Edamo, Kedir Bushira, Tigistu Yisihak Ukumo. "Flood susceptibi... <1%

108 Student papers

North West University on 2023-11-22 <1%

109 Publication

Olubusola Stephen Ilugbo, Babatunde Adebo, Olayinka Olanike Alada, Boluwatife... <1%

110 Publication

Riaz Sheriff, Mohammad Suhail Meer, Rana Waqar Aslam, Yahia Said. "Machine L... <1%

111 Publication

Springer Earth System Sciences, 2015. <1%

112 Publication

Sumit Das. "Flood susceptibility mapping of the Western Ghat coastal belt using ... <1%

113 Student papers

UNESCO-IHE Institute for Water Education on 2021-03-30 <1%

114 Student papers

UNESCO-IHE Institute for Water Education on 2021-09-10 <1%

115 Student papers

University of Cape Town on 2022-11-18 <1%

116 Student papers

University of Cape Town on 2023-11-16 <1%

117 Student papers

University of Sheffield on 2017-08-31 <1%

118 Student papers

University of Witwatersrand on 2024-10-24 <1%

119 Student papers

University of Witwatersrand on 2025-03-20 <1%

120 Student papers

University of Wolverhampton on 2020-06-11 <1%

121 Publication

Yun Zhang, Guangtao Xu, Dan Li, Yinglin Lu et al. "Integrating spectral, texture, s... <1%

122 Internet

ebin.pub <1%

123 Internet

essay.utwente.nl <1%

124 Internet

gathacognition.com <1%

125 Internet

neptjournal.com <1%

126 Internet

opus4.kobv.de <1%

127 Internet

www.tnsroindia.org.in <1%

STUDY ON ASSESSMENT OF FLOODS & GROUNDWATER SUSCEPTIBLE ZONES IN IDUKKI DISTRICT, KERALA USING GIS BASED APPROACH

A Thesis Submitted

In Partial Fulfillment of the Requirements

For the Degree of

DOCTOR OF PHILOSOPHY

in

CIVIL ENGINEERING

by

ZOHAIB AHMED KHAN

(2K19/PHDCE/05)

Under the Supervision of

Dr. BHARAT JHAMNANI

Delhi Technological University

Department of Civil Engineering

DELHI TECHNOLOGICAL UNIVERSITY

(Formerly Delhi College of Engineering)

Shahbad Daulatpur, Main Bawana Road, Delhi-110042, India

April, 2026

ACKNOWLEDGEMENT

I sincerely acknowledge the support and direction that have been crucial to the successful completion of my doctoral research. I extend my profound appreciation to my research supervisor, Dr. Bharat Jhamnani, whose continuous encouragement, thoughtful guidance, and steadfast mentorship have been invaluable throughout this academic journey. His academic rigor, critical thinking, and encouragement have been instrumental in shaping this research and my growth as a scholar. I am truly privileged to have worked under his supervision. I express my sincere gratitude to Prof. Awadhesh Kumar, Head of the Department of Civil Engineering, Delhi Technological University, for his constant motivation, institutional guidance, and administrative assistance. His leadership and support have been instrumental in creating a research-conducive atmosphere that encourages scholarly growth and innovation. I also wish to acknowledge the faculty members and supporting staff of the Department of Civil Engineering for their valuable academic insights, technical assistance, and continued cooperation throughout the duration of this research work. The collaborative and intellectually stimulating environment of the department played a crucial role in enriching my research journey. I am especially thankful to my fellow research scholars and friends, whose companionship, support, and constructive feedback have been invaluable. The exchange of ideas and the shared challenges we faced together greatly contributed to my learning experience.

I owe my deepest gratitude to my family, whose unconditional love, patience, and unwavering belief in me have been the cornerstone of my academic pursuits. Their constant support gave me the strength to persevere through every phase of this journey. Finally, I extend my gratitude to all those who, in one way or another, contributed to the successful completion of this thesis. Your support has meant more than words can express.

5

DELHI TECHNOLOGICAL UNIVERSITY
(Formerly Delhi College of Engineering)
Shahbad Daulatpur, Main Bawana Road, Delhi-42

CANDIDATE'S DECLARATION

I **Zohaib Ahmed Khan** hereby certify that the work which is being presented in the thesis entitled **Study on Assessment of Floods & Groundwater susceptible zones in Idukki District, Kerala using GIS Based Approach** in partial fulfillment of the requirements for the award of the Degree of Doctor of Philosophy, submitted in the **Department of Civil Engineering**, Delhi Technological University is an authentic record of my own work carried out during the period from 01/08/2019 to 01/04/2026 under the supervision of **Dr. Bharat Jhamnani.**

5

4

The matter presented in the thesis has not been submitted by me for the award of any other degree of this or any other Institute.

Candidate's Signature

This is to certify that the student has incorporated all the corrections suggested by the examiners in the thesis and the statement made by the candidate is correct to the best of our knowledge.

Signature of Supervisor **Signature of External Examiner**

DELHI TECHNOLOGICAL UNIVERSITY

(Formerly Delhi College of Engineering)
Shahbad Daulatpur, Main Bawana Road, Delhi-42

CERTIFICATE BY THE SUPERVISOR(s)

Certified that **Zohaib Ahmed Khan** (2K19/PHDCE/05) has carried out their search work presented in this thesis entitled **"Study on Assessment of Floods & Groundwater susceptible zones in Idukki District, Kerala using GIS Based Approach"** for the award of **Doctor of Philosophy** from Department of Civil Engineering, Delhi Technological University, Delhi, under my supervision w.e.f. 01/08/2019. The thesis embodies results of original work, and studies are carried out by the student himself and the contents of the thesis do not form the basis for the award of any other degree to the candidate or to anybody else from this or any other University/Institution.

Signature

(Dr. Bharat Jhamnani)

(Assistant Professor)

Department of Civil Engineering, DTU

Date:

ABSTRACT

Floods constitute a recurrent and intensifying hydro-meteorological hazard in the Idukki district of Kerala, driven by the coupled influence of steep topography, high monsoonal rainfall variability, land use transitions, and complex catchment scale hydrological responses. This thesis undertakes a comprehensive assessment of flood susceptibility and its consequent impacts using an integrated geospatial and hydrological modelling framework, providing a scientific basis for understanding their broader environmental significance.

The study begins with the development of a flood susceptibility map for the Idukki district using twelve hydrological and geomorphological parameters such as geology, distance from river, land use, Topographic Wetness Index (TWI), elevation, slope, Topographic Roughness Index (TRI), soil, aspect, rainfall, Stream Power Index (SPI), and Sediment Transport Index (STI) within a GIS-based Analytical Hierarchy Process framework. The developed flood susceptibility map was categorized into five susceptibility categories namely very low, low, moderate, high, and very high and these classes occupied the areas of 609.0417 km^2, 1222.83 km^2, 1180.45 km^2, 950.48 km^2 and 395.9487 km^2 respectively. The analysis also identifies over 30% of the district as highly susceptible, with prominent hotspots in Thodupuzha and central Idukki where low terrain gradients, dense drainage networks, and proximity to major rivers enhance flood generation potential. To characterise subsurface conditions, groundwater potential zones were modelled using a GIS-enabled machine learning approach incorporating AdaBoost, Gradient Boosting, and Random Forest algorithms, capturing the influence of litho-structural features, slope, land use, and other recharge-controlling factors. These groundwater potential outputs were subsequently integrated with the flood susceptibility map to derive a groundwater susceptibility assessment, enabling evaluation of how flood affected areas respond in terms of recharge capacity. The coupled analysis reveals that regions repeatedly subjected to inundation experience elevated runoff coefficients, increased sediment detachment, and reduced infiltration, collectively constraining groundwater replenishment even in zones with otherwise favourable structural characteristics.

To evaluate how successive flood events alter the district's surface conditions, Land Use and Land Cover (LULC) changes associated with the major floods of August 2018

and October 2021 were analysed using multi-temporal satellite imagery classified with a Random Forest algorithm on the Google Earth Engine platform. The 2018 floods affected approximately 20.86 km², influencing built-up (0.48 km^2), forest (10.60 km^2), agricultural (5.11 km^2), and barren (4.67 km^2) areas, whereas the 2021 event impacted about 19.24 km² across built-up (0.24 km^2), agricultural (6.23 km^2), barren (2.82 km^2), and forest (9.95 km²) classes. These spatial patterns illustrate the substantial modifications to vegetation cover, agricultural land, and terrain stability driven by repeated high-intensity rainfall and flooding in the region.

The impact of flooding on surface runoff was further quantified using the Soil and Water Assessment Tool (SWAT) applied to the Periyar River Basin, the largest basin within the Idukki district. Model simulations indicate substantial amplification of runoff during extreme rainfall events, with several outlets exhibiting nearly a 128% rise and others showing increases exceeding nearly 126% compared to non flood conditions. These elevated discharge responses spatially coincide with the high and very high flood susceptibility zones, reinforcing the reliability of the susceptibility modelling and highlighting the presence of hydrologically sensitive regions within Idukki.

Collectively, the findings demonstrate strong interactions between surface flooding, groundwater recharge dynamics, landscape transformations, and basin scale runoff behaviour. The integration of multi-criteria analysis, machine-learning modelling, remote sensing, and hydrological simulation provides a comprehensive framework for characterising flood impacts in a complex mountainous environment. The outcomes offer valuable insights for flood mitigation planning, groundwater management, and sustainable land use decision making, while establishing a robust methodological foundation for future hydrological assessments in similar data-scarce regions.

Keywords: Remote Sensing, GIS, Flood Susceptibility Map, Groundwater Potential Zone, Hydrology, SWAT, Surface Runoff

LIST OF PUBLICATIONS

- Khan, Z. A., & Jhamnani, B. (2023). Development of flood susceptibility map using a GIS-based AHP approach: a novel case study on Idukki district, India. *Journal of Spatial Science*, *69*(2), 409–442. https://doi.org/10.1080/14498596.2023.2236051 (SCI IF - 1.6)
- Zohaib Ahmed Khan, Bharat Jhamnani; Identification of groundwater potential zones of Idukki district using remote sensing and GIS-based machine-learning approach. *Water Supply* 1 June 2023; 23 (6): 2426–2446. doi: https://doi.org/10.2166/ws.2023.134 (SCI - IF 1.768)
- Zohaib Ahmed Khan, Bharat Jhamnani; Effects of Torrential Rainfall and Floods on the Changing Landscapes and their Impact Assessment in Idukki District, India. 4th International Conference on River Corridor Research and Management (RCRM- 2024), IIT Jammu, 7th – 9th March 2024.
- Zohaib Ahmed Khan, Bharat Jhamnani; Evaluation of Surface Runoff in the Periyar River Basin using SWAT Model. First International Conference on Advances in Energy and Environmental Engineering 2024, 17th – 18th December 2024.

TABLE OF CONTENTS

LIST OF TABLES

LIST OF FIGURES

LIST OF ABBREVIATIONS

GIS = Geographic Information System

DEM = Digital Elevation Model

AHP = Analytic Hierarchy Process

SAR = Synthetic Aperture Radar

TRI = Topographic Roughness Index

TWI = Topographic Wetness Index

STI = Sediment Transport Index

DFR = Distance from River

RADAR = Radio Detection and Ranging

SPI = Stream Power Index

IMD = Indian Meteorological Department

SRTM = Shuttle Radar Topographic Mission

CR = Consistency Ratio

CI = Consistency Index

RI = Random Index

AUC = Area Under Curve

ROC = Receiver Operating Characteristics

SLC = Single Look Complex

VV = Vertical Transmit and Vertical Receive

GW = Ground Water

GWPZ = Ground Water Potential Zone

GWPM = Ground Water Potential Map

ML = Machine Learning

NDVI = Normalized Difference Vegetation Index

GSI = Geological Survey of India

DD = Drainage Density

LD = Lineament Density

RF = Random Forest

GB = Gradient Boosting

RFE = Recursive Feature Elimination

GEE = Google Earth Engine

LULC = Land use and Land Cover

KSDM = Kerala State Disaster Management Authority

WGS = World Geodetic System

UTM = Universal Transverse Mercator

SWAT = Soil & Water Assessment Tool

NSE = Nash–Sutcliffe Efficiency

ETM = Enhanced Thematic Mapper

PAN = Panchromatic

NBSS = National Bureau of Soil Survey

HRU = Hydrological Response Unit

FPZ = Flood Prone Zones

CHAPTER 1
INTRODUCTION

1.1 General

Floods are one of the most commonly occurring and highly destructive natural hazards in India, causing widespread loss of life, damage to infrastructure, and long term environmental degradation. The country's hydrological regime is predominantly controlled by the southwest monsoon, during which a substantial proportion of annual rainfall is received over a short duration. While this seasonal concentration of rainfall is vital for replenishing surface and subsurface water resources, it also increases the likelihood of extreme hydrometeorological events. Variability in rainfall intensity, combined with diverse physiographic conditions and land use patterns, often results in complex hydrological responses that manifest as flooding, landslides, and erosion across many regions of the country.

There is growing evidence of an escalation in the frequency and intensity of extreme precipitation events over several parts of India in recent times. This trend has raised concerns about the vulnerability of not only large river floodplains but also upland and mountainous regions, where steep slopes and rapid runoff generation can lead to sudden and severe flooding. The Western Ghats, a prominent mountain system along the west coast of India, exemplifies this growing hydrological sensitivity. Characterised by high monsoonal rainfall, rugged terrain, shallow soils, and dense drainage networks, the region is particularly prone to flash floods and slope instabilities triggered by intense precipitation.

Kerala, located along the windward side of the Western Ghats, has experienced several extreme flood events in recent years, highlighting the increasing exposure of mountainous landscapes to hydrological hazards. Among these, the floods of 2018 and 2021 stand out due to their scale, intensity, and widespread impacts. The 2018 Kerala floods were driven by exceptionally high monsoon rainfall, far exceeding long term averages, which led to catchment saturation, rapid rise in river levels, and extensive inundation across much of the state (Joseph et al., 2020). Similarly, the flood event of 2021, associated with intense rainfall episodes during the retreating monsoon, further demonstrated the region's vulnerability to consecutive hydrological extremes

(Vijaykumar et al., 2021). These events collectively underscore the growing challenge of managing flood risks in complex terrain under changing climatic conditions.

The Idukki district, situated in the central Western Ghats, is one of the most hydrologically sensitive regions in Kerala. Its mountainous landscape, steep slopes, dense forest and plantation cover, and hard rock terrain contribute to rapid runoff generation during periods of intense rainfall. The district also hosts major river systems, including the Periyar, along with large reservoirs that play a crucial role in regional water management. Extreme flood events in recent years have revealed how quickly hydrological conditions can shift in such settings, leading to widespread inundation, slope failures, and changes in surface and subsurface water processes.

Flooding in mountainous regions like Idukki does not act in isolation but influences multiple environmental components simultaneously. Flood susceptibility determines the spatial likelihood of inundation, while flood events can also alter groundwater recharge conditions, modify land use and land cover patterns, and intensify surface runoff responses. These interactions are highly dynamic and spatially variable, particularly in regions where natural terrain features intersect with human activities such as agriculture, settlements, and reservoir operations. Understanding these interlinked processes is therefore critical for effective watershed management, hazard mitigation, and sustainable use of water resources.

The assessment of flood impacts has been significantly enhanced by advancements in geospatial technologies and hydrological modelling tools (Young et al., 2022). Remote sensing and Geographic Information Systems (GIS) enable the spatial analysis of terrain characteristics, flood extents, land cover changes, and hydrological indicators at multiple scales (Gupta & Dixit (2022)). Analytical techniques, including multi-criteria decision making methods and machine learning algorithms, facilitate the integration of diverse datasets to produce more reliable flood susceptibility and groundwater potential maps. In parallel, SWAT, which is one of the most popularly used hydrological model allow for the simulation of discharge values and streamflow dynamics under varying climatic and land use conditions, offering valuable insights into basin scale hydrological responses during extreme events.

In this context, an integrated approach that combines flood susceptibility mapping, groundwater potential assessment, land use and land cover analysis, and hydrological modelling is essential to comprehensively evaluate flood impacts in mountainous

regions. Such an approach not only improves the understanding of flood related processes but also facilitates informed decision making for land and water resource management. The present study adopts this integrated geospatial and hydrological framework to analyse flood susceptibility and its associated impacts on groundwater potential, LULC dynamics, and surface runoff behaviour in the Idukki district of Kerala.

1.2 Floods

Flooding is one of the most widespread and damaging natural hazards, causing severe disruption to human life, infrastructure, agriculture, and ecosystems (Jha et al., 2012). Although moderate floods can contribute positively to ecosystem functioning by transporting nutrients, flushing pollutants, supporting groundwater recharge, and enhancing soil fertility (Kraus et al., 2019; Lyubimova et al., 2016; Mahato et al., 2021;), events that exceed the natural resilience of a system can lead to extensive environmental and socio-economic losses (George et al., 2022; Pradhan & Youssef, 2011). Floods commonly arise from prolonged heavy rainfall or rapid snowmelt that causes rivers to overflow and inundate adjacent land (Kron, 2005), while intense cloudbursts in steep or semi-arid regions may trigger destructive flash floods (Tehrany et al., 2013). Their occurrence is shaped by both natural controls such as topography, slope, channel proximity, and geological variability (Lim & Lee, 2017) and anthropogenic drivers including deforestation, urban expansion, poor land-use practices, and extensive impervious surface development (Bradshaw et al., 2007).

In recent decades, climate change has emerged as a major factor intensifying flood hazards (Sampson et al., 2015; Gebrechorkos et al., 2020). Alterations in precipitation regimes, increased storm intensity, and land cover modifications amplify runoff generation and elevate flood risk. Climate induced land use shifts may also increase imperviousness, reduce infiltration, and accelerate surface flow (Charlton et al., 2006). In urban environments, inadequate drainage capacity and rapid concretization further exacerbate waterlogging and flooding during extreme rainfall episodes (Bronstert, 2003). These combined natural and anthropogenic influences underscore the growing complexity of flood generation processes and the need for enhanced understanding of watershed responses.

India’s monsoon, extending from June to September, delivers substantial rainfall that sustains agriculture but also poses a high risk of inundation (Saha et al., 2021). Flood

vulnerability in the country is exacerbated by intense precipitation, inadequate drainage infrastructure, deforestation, unregulated urbanization, and unsustainable land practices. Climate variability and rapid urban growth continue to challenge flood management efforts nationwide (Neumann et al., 2015). Several states including Assam, Bihar, Uttar Pradesh, West Bengal, Odisha, Maharashtra, Karnataka, and Kerala regularly experience severe flooding due to these combined pressures (Parthasarathy et al., 2021). In this context, understanding the mechanisms, drivers, and evolving patterns of flooding has become crucial for developing resilient and sustainable water management strategies.

1.2.1 Multidimensional Impacts of Flooding

Flooding is a complex natural phenomenon that affects various aspects of the environment and society. Its impacts extend beyond immediate waterlogging, influencing land surface processes, groundwater systems, ecological stability, and human livelihoods (Hadipour et al., 2020; Bui et al., 2019). The effects can vary in intensity and duration, often triggering long term changes in landscape dynamics and water resource availability. Understanding these multidimensional consequences is essential for building resilient planning and management strategies in flood prone regions.

Annually, floods in India have a significant impact on a vast number of individuals. Natural hazards can result in losses of lives, displacement of people, damage to residential facilities, destruction of crops, hindrance of transportation and communication systems and spread of waterborne diseases. The groups that are most susceptible to adverse impacts are those that are marginalized and reside in regions with low elevation or in close proximity to river banks (Saravanan & Abijith, 2021). Flooding experienced in India has some noteworthy economic effects. The negative effects of this phenomenon spread to the structural integrity of different types of infrastructure, such as roads, bridges, railways, and buildings resulting into huge economic consequences. Through flooding fields may result in negative effects to the agriculture sector where crops and livestock are destroyed which subsequently can affect the production of food as well as the lives of individuals in the industry. Industries situated in regions susceptible to flooding also encounter interruptions in their operations (Pramanick et al., 2022). The Indian government, at both the central and state levels, has been engaged in the development of flood management strategies

and disaster response mechanisms. Flood control infrastructure such as earthen embankments, dams and barrages along with implementation of early warning systems and relief measure for communities which are impacted by the natural disasters encompass the broader flood mitigation measures and initiatives taken by the government. The National Disaster Management Authority (NDMA) and State Disaster Management Authorities (SDMAs) are pivotal entities in the realm of disaster preparedness and response (Parthasarathy et al., 2021).

In recent years, India had some of the most unusual severe precipitation occurrences, which have resulted in flooding and the loss of lives. For example, the Kosi River, commonly known as the "Sorrow of Bihar," is renowned for its catastrophic floods in Bihar. The river in controversy has its source in Nepal and subsequently flows into Bihar, where it has been known to alter its course over time, resulting in devastating inundations. Due to the substantial amount of sediment transported by the river, it is susceptible to obstructions and embankment breaches, resulting in extensive flooding.

Catastrophic rainfall and extensive flooding in Kerala recently demonstrated the magnitude of India's extreme rainfall and large scale floods. In August 2018, Kerala saw prolonged and excessive rains that impacted many elements of human life, including socioeconomic circumstances, transportation, infrastructure, agriculture, and livelihood. The Kerala floods of 2018, which is likely the worst flood in a century, has already drew the attention of the media, scientific community, and policymakers (Hunt & Menon, 2018). According to preliminary estimates, the Kerala floods killed over 440 people and inflicted $3 billion in economic damage (Young et.al., 2022). According to India Meteorological Department (IMD), Kerala recorded the highest daily rainfall in six decades in 2021. This resulted in excess rainfall which flooded most of the agricultural areas, due to which crop production got adversely affected which further impacted the livelihood of farmers.

Beyond the immediate destruction to life and infrastructure, flooding also exerts significant influence on water resources and landscape processes. One of the notable consequences is its effect on groundwater availability, where floodwaters may disrupt natural recharge mechanisms, particularly in flood prone zones. The accelerated surface runoff and heightened flow velocities often hinder infiltration, thereby reducing the potential for groundwater replenishment. Additionally, rapidly moving floodwaters tend to carry sediments that can clog soil pores, further limit percolation

and negatively impacting groundwater recharge capacity. On the other hand, in certain scenarios, flooding can contribute positively to aquifer recharge by allowing water to seep into the subsurface and raise groundwater levels. However, the increased exposure of aquifers to surface contaminants during such events raises concerns about groundwater quality and its suitability for consumption and domestic use (Resmi et al., 2025). In arid and semi-arid regions, studies by Ghazavi et al. (2012) observed a decline in groundwater levels following flood events, although they noted that implementing flood spreading techniques could potentially enhance recharge and stabilize water tables.

Flood events have a profound influence on land use and land cover (LULC) dynamics, often leading to substantial alterations in landscape composition. In various river basins, such as the Melamchi–Indrawati region, flood induced transformations have been observed in the form of declining agricultural areas and expanding barren land, highlighting shifts in land utility and vegetation cover (Thapa & Prasai, 2022). The comparative analysis of pre and post flood conditions in certain flood affected zones has revealed the inundation of aquatic vegetation and following these flood events, a significant portion of submerged areas was overtaken by sand and sediment deposits due to elevated levels of siltation, altering the land surface considerably (Ahmad et al., 2017). Similar consequences were reported during the 2010 floods in Muzaffargarh, Pakistan, where extensive damage was recorded in vegetated zones and built-up regions, demonstrating the vulnerability of both ecological and human modified landscapes to flood related disturbances (Mahmood et al., 2021).

1.3 Groundwater

Groundwater constitutes a crucial element of the global freshwater supply, playing an indispensable role in agriculture, domestic consumption, and industrial use particularly in areas where surface water is either insufficient or irregularly distributed (Chung et al., 2012). In the Indian context, groundwater underpins nearly two-thirds of agricultural irrigation and provides over 85% of the water needs in rural communities. However, groundwater availability is highly sensitive to climatic fluctuations, notably shifts in rainfall intensity and the occurrence of events of extreme nature, including floods and droughts. Such hydrological disturbances can alter recharge patterns, highlighting the need to examine their effects on groundwater systems at both regional and local levels.

While rainfall is the primary source of natural groundwater recharge, excessive and poorly managed rainfall can paradoxically diminish groundwater potential. In regions affected by torrential rainfall and flooding such as the Idukki district in Kerala, the high volume of water does not always translate into higher infiltration or aquifer recharge. Instead, steep slopes, soil erosion, increased surface runoff, and altered land cover associated with floods may actually reduce the rate of groundwater recharge.

Hydrogeological evaluations conducted after the 2018 Kerala floods revealed significant drops in dug-well water levels, implying that the event altered recharge dynamics and, in many locations, impeded effective groundwater replenishment (Shaji et al., 2018). Hence, despite record breaking rainfall and massive water accumulation in rivers and reservoirs, large parts of Idukki experienced water stress and inconsistent groundwater availability in the months following the disaster. This contradiction highlights the need to understand the spatial variability of groundwater potential in the context of flood prone environments.

In this context, Groundwater Potential Zonation (GWPZ) emerges as a powerful tool to evaluate the recharge potential of different areas based on multiple environmental and hydrological parameters. GWPZ involves the integration of different parameters such as LULC, soil type, slope, geology, rainfall and lineament density, all of which influence the occurrence and movement of groundwater. In flood prone regions, additional layers such as flood susceptibility and elevation become especially important, as they determine how water is distributed and whether it contributes to infiltration or rapid runoff.

Ultimately, understanding the spatial interdependence between flood prone zones and groundwater potential is essential for building long term resilience in hydro-geologically sensitive regions like Idukki, where the challenges of climate change, population pressure, and environmental degradation converge.

1.4 Alterations in Land Use and Land Cover

Flood events often induce substantial transformations in land use and land cover by altering the physical, biological, and socio-economic attributes of the landscape. Intense flooding can erode topsoil, deposit sediments, destroy vegetation, reduce agricultural productivity, and displace human settlements. These transformations may lead to long term or even irreversible shifts in land cover classes and disrupt ecological functioning as well as human livelihoods (Charlton et al., 2006). Variability in flood magnitude and landscape characteristics means that LULC responses are highly

context specific. In forested terrains, vegetation loss and canopy thinning may occur, while agricultural lands may experience waterlogging or sediment deposition that alters cropping patterns. Urban and peri-urban regions often exhibit post-flood land conversion due to infrastructure damage and relocation. These shifts in LULC subsequently influence hydrological behaviour by modifying runoff, infiltration, and erosion processes, thereby creating feedback loops that can intensify future flood vulnerability.

The Kerala floods of 2018 marked one of the most severe hydrometeorological disasters in the state's recent history, producing widespread LULC changes across both highland and lowland regions (Joseph et al., 2020). Exceptionally intense monsoon rainfall resulted in landslides, river overtopping, and dam releases, leading to extensive inundation and damage to forests, agricultural land, and built-up areas. Satellite based assessments showed substantial increases in barren or exposed surfaces and notable reductions in dense vegetation and cultivated land. Agricultural fields were submerged for extended periods, while forests in landslide prone hill slopes experienced canopy loss and extensive scarring. Built-up areas in several districts suffered structural damage or abandonment, contributing further to spatial reorganization of land cover.

The 2021 floods, although more localized than the 2018 event, again caused severe landscape disturbances, particularly in central and highland Kerala. Short duration, high intensity cloudbursts triggered flash floods and slope failures in areas already destabilized by the 2018 event, highlighting the cumulative weakening of terrain stability. Remote sensing observations indicated renewed increases in barren land, forest fragmentation, and damage to agricultural plots, especially along riverbanks and steep slopes. Settlements in vulnerable areas experienced repeated disruption, and patterns of reconstruction or relocation contributed to additional land-cover transitions.

Idukki district, situated within the Western Ghats, exemplifies these cumulative LULC impacts. As a topographically steep, high rainfall, and ecologically sensitive region, Idukki is highly prone to landslides and flash floods. During the 2018 floods, unprecedented rainfall and subsequent dam releases resulted in widespread damage across plantations, forests, agricultural valleys, and settlements. Tea, cardamom, and pepper plantations experienced topsoil loss and infrastructure damage, while low lying paddy fields remained submerged for prolonged periods. Forested slopes exhibited

extensive landslide scars and canopy removal. The 2021 floods further aggravated these conditions, producing new landslides, widening river channels, and degrading regenerated vegetation. The combined effects of repeated flooding, geomorphic instability, and post disaster human adjustments have led to persistent landscape transformation, altering land use patterns and increasing the district's susceptibility to future hydrological hazards.

1.5 Surface Runoff

Extreme rainfall and flood events disrupt the natural hydrological balance of a region by sharply increasing surface runoff and altering catchment response characteristics. In steep, high rainfall terrains such as Idukki, this elevated runoff accelerates soil erosion, slope instability, sediment transport, and fluctuations in streamflow regimes. Although the immediate impacts of flooding are often visible, the longer term hydrological implications, particularly those related to reduced infiltration and modified runoff pathways are equally significant. During intense rainfall episodes, soil saturation occurs rapidly, converting most additional rainfall directly into surface runoff. This rapid overland flow, observed prominently during the 2018 and 2021 Kerala floods, limits groundwater recharge and amplifies watershed sensitivity.

The hydrological response of Idukki during these events was marked by near-instantaneous runoff in several sub watersheds, reflecting the district's steep gradients and dense drainage network. Rivers such as the Periyar, Meenachil, and Pamba carried flows far exceeding their typical capacities, contributing to flash floods and landslides across the region. Identifying zones that produce disproportionate runoff is therefore essential for watershed management, as these hydrologically sensitive areas are prone to high soil loss, rapid streamflow variations, and recurrent flooding.

Hydrological modelling offers a scientific framework for assessing such behaviour. The Soil and Water Assessment Tool (SWAT) which is a popular semi-distributed model, enables simulation of streamflow, infiltration, evapotranspiration, and discharge at sub basin and hydrological response unit scales (Aladejana et al., 2020). By integrating rainfall, land use, soil characteristics, topography, and discharge records, SWAT can quantify shifts in runoff generation during extreme events and delineate sub-basins that exhibit elevated hydrological responses (Singh et al., 2020). These insights allow for targeted interventions such as slope stabilization, reforestation, land use regulation, and improved watershed planning.

Hydrological modelling thus serves as a critical tool for understanding evolving runoff dynamics and for identifying vulnerable zones that require focused management to enhance regional resilience.

1.6 Role of Remote Sensing, GIS, and Machine Learning

Advances in geospatial technologies have significantly transformed the way hydrological processes and landscape dynamics are assessed, offering powerful tools for analysing complex environmental systems with greater accuracy and spatial detail (Catani et al., 2013; Danumah et al., 2016; Moghaddam et al., 2019). Remote sensing enables continuous, multi-temporal observation of terrain, vegetation, land cover, and surface water features, making it indispensable for monitoring changes associated with floods, groundwater variability, and runoff behaviour (Devananatham et al., 2021). When integrated with Geographic Information Systems (GIS), these datasets can be systematically processed, visualized, and analysed to generate spatial layers that support decision-making in hazard assessment and resource management. The emergence of analytical techniques such as the Analytical Hierarchy Process (AHP) has further strengthened GIS-based modelling by enabling the incorporation of expert judgement and multi-criteria evaluation for flood susceptibility mapping. Similarly, machine learning algorithms such as Random Forest, AdaBoost, and Gradient Boosting have demonstrated remarkable efficiency in capturing nonlinear relationships among hydrological, geological, and land use variables, thereby enhancing the accuracy of groundwater potential mapping (Golkarin et al., 2018; Suthirat et al., 2020). In parallel, hydrological modelling tools such as SWAT provide a robust, process based framework for simulating runoff generation and discharge dynamics at watershed scales (Chu et al., 2020; Uniyal et al., 2020). The convergence of these geospatial, statistical, and hydrological approaches allows for a comprehensive assessment of environmental hazards and strengthens the capability to identify vulnerable zones, predict hydrological responses, and support sustainable water and land management in complex terrains such as the Idukki district.

1.7 Objectives of the Study

In order to comprehensively investigate the complex interactions between flooding, groundwater dynamics, land use changes, and surface hydrology within the Idukki district of Kerala, the current study employs an integrated geospatial approach. The present research utilizes a combination of GIS-based Analytical Hierarchy Process

(AHP), remote sensing data analysis, machine learning algorithms, Google Earth Engine (GEE), and the Soil and Water Assessment Tool (SWAT) to examine the spatial and temporal dimensions of flood related processes. These methodological tools enable a systematic and data driven exploration of flood susceptibility, groundwater potential, land use transformations, and runoff behaviour. Accordingly, the research has been structured around the following four interrelated objectives:

- **Objective 1**: To develop a flood susceptibility map for the Idukki district, Kerala, using a GIS based Analytical Hierarchy Process (AHP) approach, serving as a foundational spatial layer for integrated flood related assessments.
- **Objective 2**: To assess the impact of flood prone areas on groundwater potential in Idukki district through the identification of groundwater potential zones using a remote sensing and GIS based machine learning approach.
- **Objective 3**: To evaluate the impact of torrential rainfall and flooding on land use and land cover (LULC) patterns in the Idukki district by analysing landscape changes in relation to the delineated flood susceptible zones.
- **Objective 4**: To model the increase in surface runoff in the Idukki region using a hydrological approach, with the objective of assessing the impact of flood events on discharge variations and identifying hydrologically sensitive zones.

1.8 Organization of the thesis

Chapter 1 provides a general introduction, focusing on the broader context of flooding and its multidimensional impacts on land use, land cover, groundwater, and runoff patterns. Chapter 2 presents a detailed literature review related to flood susceptibility mapping, groundwater zonation, and the effects of flooding on land use and land cover. synthesizing key findings from previous studies to establish the research background. Chapter 3 describes the study area, which is the Idukki district of Kerala, highlighting its physiographic features, climatic conditions, and geological characteristics relevant to the study. Chapter 4 outlines the methodologies utilized to meet the research goal. Chapter 5 discusses the results and discussions derived from the analysis, interpreting the spatial patterns and changes observed across flood susceptibility, groundwater potential, land use dynamics, and runoff variations. Chapter 6 concludes the thesis by summarizing the key results, defining the implications of the study, and suggesting future scope of work.

29

CHAPTER 2
REVIEW OF LITERATURE

2.1 General

A thorough review of existing academic and scientific literature was carried out to understand the progress made in fields relevant to this study. The focus was placed on research concerning flood susceptibility mapping, identifying key parameters involved in generating reliable flood hazard maps, delineation of groundwater potential zones using geospatial tools, and evaluating the influence of flood events on LULC changes and runoff behaviour. This review was designed to align with the thematic scope of the present research and to guide the selection of appropriate methodologies.

Efforts were made to study and analyse the contributions of previous researchers who have explored the spatial distribution of flood prone zones, the effectiveness of various validation strategies, and the impact of floods on both surface and subsurface hydrological systems. Particular attention was given to factors that affect groundwater recharge during and after flooding, as well as the extent to which land cover changes occur in flood affected regions over time.

Additionally, a range of literature was examined to understand the potential of geospatial technologies often integrated with machine learning techniques in improving the accuracy of spatial predictions and environmental assessments. These studies illustrate the evolution of flood and groundwater modeling from conventional mapping practices to data driven, technology enhanced approaches.

The following sections provide a detailed account of these previous studies, highlighting key findings, methodological innovations, and their relevance to the current research context.

2.2 Overview of Existing Literature

Shrestha et al. (2025) employed a combined GIS–AHP framework to evaluate flood susceptibility in Davidson County. Ten flood conditioning factors were analysed, with soil type, LULC, TWI, and slope identified as the most influential. A weighted overlay in GIS produced a flood susceptibility map categorized into five risk levels. Most areas were found to be in low to moderate risk zones. Validation with the Federal Emergency Management Agency (FEMA) flood hazard map confirmed the model's reliability, supporting its use for future flood mitigation planning.

Ashfaq et al. (2025) conducted a study in District Nowshera, Pakistan, used AHP and FR models with GIS and remote sensing to map flood susceptibility. Twelve flood conditioning factors were analysed, identifying high-risk areas mainly near the Kabul River. Validation using AUC-ROC showed high accuracy (92.1% for AHP). The study highlights the vulnerability of settlements and croplands in flood-prone zones. It recommends strengthening flood protection infrastructure and applying advanced modeling techniques in future work.

Sharker et al. (2025) used AHP and GIS with MCDA to identify flood prone lower reach areas that have experienced severe damage. The flood risk map aids public awareness and supports government planning for better flood management. Model validation confirmed its accuracy with real flood data.

Shadman & Hassan (2024) used an integrated AHP and GIS approach to assess flood susceptibility in Sylhet district, identifying rainfall as the most influential factor and road proximity as the least. Flood susceptibility zones were categorized into five classes, with 33.41% of the area falling under high to very high risk regions. High risk regions are characterized by lower elevation values, flat slopes, high drainage density, and proximity to rivers. The study acknowledges limitations due to reliance on expert judgment for weighting and exclusion of soil and infrastructure data. Despite this, the findings offer valuable insights for pre-flood planning and disaster risk reduction in Sylhet.

Kader et al. (2024) conducted a study using GIS-AHP approach to map flood susceptibility in Bangladesh, identifying 16.03% of the country, especially Dhaka division, as highly flood-prone. Elevation, slope, rainfall, and drainage density were key influencing factors. However, limitations such as subjective weighting, static data, and low-resolution inputs affected accuracy. Despite this, the study offers a baseline for improving flood risk assessment using more advanced and data-driven models.

Rebouh et al. (2024) utilized a GIS-AHP approach combined with Remote Sensing and Google Earth Engine to assess flood susceptibility in Ain Smara, Algeria, using ten key criteria. Results showed 4% of the area is highly flood prone, mainly near the Rhumel River, with 66% moderately susceptible. The findings align well with recent flood events, demonstrating the method's effectiveness for flood risk mapping.

Ayadi et al. (2024) explored the integration of Geospatial AI (Geo-AI) with traditional GIS and Remote Sensing to map Groundwater Potential Zones (GWPZs) in the Majerda transboundary basin shared by Tunisia and Algeria. Geo-AI, particularly

using Artificial Neural Networks, outperformed AHP in accuracy and adaptability to complex data. High groundwater potential was linked to areas with high rainfall, low slope, and favourable lithology. Findings support sustainable groundwater management and informed water allocation strategies in arid areas.

Nugroho et al. (2024) used supervised machine learning Random Forest (RF), SVM, and ANN to map groundwater potential in West Java, Indonesia, with RF achieving the highest accuracy (0.8). Key factors influencing groundwater potential included land system, lithology, and NDVI. Approximately, 50% of the region was categorized as having very low to low groundwater potential, with less than 16% in high to very high potential zones. The validation for the study was done using well locations and geoelectric measurements in sample areas. The study highlights the need for sustainable groundwater management to prevent resource depletion in West Java.

Asrade (2024) used AHP and Frequency Ratio (FR) models combined with GIS and Remote Sensing to evaluate groundwater potential zones (GWPZs) in the Jedeb watershed. The FR model outperformed AHP with an AUC of 88.3% versus 85.6%. Both models identified zones ranging from very high to low groundwater potential, aiding well site selection and resource management. The results offer valuable guidance for planners and policymakers, though further fieldwork is recommended for more precise local mapping.

Arfasa et al. (2024) reviewed the impacts of climate change and land use/land cover (LULC) dynamics on the sustainability of irrigation water in West Africa. The study highlighted that rising temperatures, altered precipitation patterns, and rapid LULC changes significantly influence key hydrological processes, including evapotranspiration, runoff, groundwater flow, and river discharge. Declining forest cover and expanding agricultural and urban areas, combined with increasing irrigation demand driven by population growth and climate change, are expected to intensify water stress. The authors emphasized the need for effective adaptation and mitigation strategies to ensure long-term irrigation water availability in the region.

Abraham et al. (2022) analysed spatio-temporal land use/land cover (LULC) changes in the Meenachil and Manimala river basins of Kerala using Random Forest classification in Google Earth Engine and Land Change Modeler (LCM). The study produced highly accurate multi-temporal LULC maps and successfully validated future LULC predictions. Results indicated a pronounced expansion of built-up areas

and a continuous decline in agricultural land, with projections up to 2050 showing accelerated urban growth in both basins. The findings highlight development-driven landscape transformation and provide useful inputs for long term land use planning and management.

Das & Gupta (2021) conducted a detailed study on floods in Subarnarekha River basin, India using flood hydrology and GIS based AHP technique. It was found that monsoon peak discharges were approximately fivefold higher than average flows at all gauging stations, leading to overbank flooding in the shallow sections of the Subarnarekha and 38% of total area comes under very high to high probability of flooding and it is validated through discharge data, where Ghatshila, a gauging station also showed maximum value for discharge.

D. Nsangou et al. (2021) evaluated flood susceptible regions in Mfoundi catchment, Cameroon through AHP method considering ten parameters namely elevation, drainage density, slope, rainfall, distance from river, topographic humidity, hydraulic conductivity, groundwater level, geology and landcover and findings revealed that around 20% area came under very flood prone region and validation of AHP method using Area under curve technique showed a very high accuracy.

Abu Reza Md Towfiqul Islam et al. (2021) utilized five different machine learning models which were ANN, SVM, RF, Subspace random and Dagging for flood susceptibility mapping in Teesta river basin of northern Bangladesh and it was reported that among all machine learning models, dagging model produced the most accurate results of flood prone regions

Natarajan et al. (2021) employed frequency ratio method to identify the flood susceptible areas in Chennai corporation region and suggested that a greater number of inputs will result in better accuracy of the maps. Developed flood maps showed very high accuracy and indicated that more than one third area comes under high flood susceptible zone and maps were validated using news reports and satellite data of pre and post flood events.

Hamlat et al. (2021) utilized AHP methodology to map the flood hazard potential areas of M'zi wadi catchment, Algeria and it taking into account seven parameters, namely, the flow accumulation, the elevation, the rainfall intensity, the basin's slope, the drainage density, Land use/land cover and the soil types and results indicated that 3% of the total area is under very high risk and flood mitigation strategy will be a key

factor in safeguarding of these areas. Furthermore, to assess the hydrological behaviour of the basin, rainfall runoff inundation model (RRI) was employed which showed that the widening of wadi near the outlet of the basin can reduce the water level substantially.

Anil & Das (2021) applied Fuzzy AHP technique for identification of high prone soil erosion sub watersheds of Agrani Watershed and findings indicated that more than 65% area of watershed was in very high to moderate soil erosion prone zones which further indicates that with the utilization of GIS techniques better soil resource management can be achieved.

E. Herman et al. (2021) mitigated the devastating effects of flash floods in new urban areas of Ras Gharib, Egypt, optical and radar satellite images acquired before and after the flash flood events were analysed to detect the affected areas results indicated that accurate active distributing channel maps through the satellite images were useful in knowing the conveyance of floods so that these paths can be blocked and construction of storage dams near the upstream areas could also help in mitigating the effect of floods to some extent.

B.K. Osei et al. (2021) delineated flood prone areas in the Tarkwa mining area in Ghana by utilizing slope map and streamflow network map in ArcGIS and results indicated that more than 40% of area is under very high flood susceptible zones and it was recommended that proper drainage systems should be constructed for runoff from floods and proper land use police should be introduced.

Desalegn & Mulu (2020) used HEC-RAS coupled with GIS to achieve good results in flood inundation mapping. The mapping of flood inundated areas of Fetam river in Ethiopia was evaluated using flood frequency approach and HEC-GeoRAS tool and reliable results in terms of flood depth and flooded areas were obtained which were very useful for future river training works and construction of dykes and levees.

Saha and Agrawal (2020) conducted a study in Prayagraj district of India for flood prone areas using integration of GIS with analytical Hierarchy process (AHP). They considered 7 parameters namely elevation, Slope, Flow accumulation, TWI, drainage density, roughness, LULC & made two flood risk maps, one by considering LANDSAT images of dry and wet seasons of 3 consecutive years and other map was constructed using AHP process and the results were successfully validated using area under curve technique.

Koc et al. (2020) utilized Fuzzy Analytical hierarchy process (FAHP), districts of Istanbul prioritized with respect to flood risk using vulnerability criteria and hazard criteria and results indicated that land use, population density, return period, imperviousness and storm water pipe network were the most parameters for flood risk.

Akay & Baduna (2020) employed traditional methods such as compound factor, hazard degree and statistical methods were compared with Multi criteria decision making (MCDM) methods such as AHP and ANP & results indicated that amongst all methods, methodology of AHP is better suitable for evaluating the sub basins for flash flood potential than the traditional methods.

Msabi & Makonya (2020) performed flood susceptibility mapping of Dodoma region using AHP methodology considering seven factors namely elevation, slope, drainage density, flow accumulation, land use, geology and soil and the technique used was successful as it was successfully validated by historical flood locations with the susceptible areas of the region.

Suthirat et al. (2020) employed AHP method integrated with GIS to model the flood risk zones to safeguard the Ayutthaya which is a World Heritage Site. The developed flood hazard maps for Ayutthaya and surrounding communities assists in emergency preparedness and help in mitigation strategies.

Surwase et al. (2019) conducted research for a more realistic identification of flood hazard zones in Mahanadi River in Odisha with the help of Spatial flood frequency maps (SFFM). These maps were produced and analysed from 100 historic satellite images between 2001 and 2008 and results were compared with AHP methodology which eventually helped in correctly identifying the towns which are at a higher risk of flooding during the monsoon season.

Das (2019) employed AHP model for determining flood risk maps and vulnerability index for the entire western coast area of India by using eleven environmental predictor variables and four economic parameters as well to accurately identify the impact of floods on the people residing near flood zone areas. The developed maps indicated that 50% areas come under high flood susceptibility and vulnerability index indicated that 25% of coastal belt population is under high flood risk.

Mahmoud & Gan (2018) employed AHP coupled with GIS to model the flood susceptibility zones in the Riyadh province, Saudi Arabia, using ten flood conditioning factors such as flow accumulation, annual rainfall, slope, runoff, land use and land cover, elevation, geology, soil type, distance from drainage network and drainage

density. The developed flood susceptibility model was successfully validated with historic flood records and analysis indicated that some factors have more significance over others.

Jia et al. (2019) examined the characteristics of rainstorm-induced flooding in Henan Province, China. In their study, the likelihood of flood hazards, the sensitivity of the disaster environment, and the vulnerability of exposed elements were assessed using the Analytic Hierarchy Process integrated with fuzzy variable set theory.

Das (2019) considered geospatial mapping of flood susceptibility for Ulhas basin in Maharashtra considering twelve flood conditioning factors i.e. elevation, slope, distance from drainage network, geomorphology, drainage density, flow accumulation, rainfall, land use, geology, stream power index, topographic wetness index and curvature of topography and reported that only three factors elevation, drainage density and slope have much more significance than others in flood mapping.

Das (2018) modelled the flood hazard zones in Vaitarna basin of Maharashtra using AHP (Analytical Hierarchy Process) method considering 9 important factors namely elevation, slope, distance from the river, rainfall, flow accumulation, land use, geology, TWI and curvature and results indicated that 22 % of the total area in the south-central part of Vaitarna basin comes under high flood zones.

M.Haq et al. (2013) assessed that Remote sensing and GIS have immense scope in rapid damage assessments caused due to floods with the help of high quality satellite images to assess the flood inundated areas along with the affected population.

Yang et al. (2013) developed a new scientific method by combining Fuzzy AHP and triangular fuzzy number (TFN) for flood risk prediction by considering four factors and 16 sub factors for the lower Yangtze River in China which yielded good results.

Yang et al. (2013) developed a new scientific method by combining Fuzzy AHP and triangular fuzzy number (TFN) for flood risk prediction by considering only four factors and 16 sub factors for the lower Yangtze River in China which yielded good results.

Aydin et al. (2021) carried out flood hazard zoning mapping in the Biltis province of Turkey using AHP method integrated with GIS considering 5 factors namely precipitation, distance from the river, geology, slope and aspect. Results indicated that south western regions are more prone to flood risk where stream density and precipitation is high.

Aggarwal et al. (2019) delineated groundwater potential zones in the hard-rock terrain of the Gundihalla watershed, Bellary district, Karnataka, by integrating remote sensing, GIS and multi-criteria decision analysis. Using Saaty's Analytical Hierarchy Process, key thematic layers including geomorphology, soil, drainage density, lineament density, rainfall and slope were weighted and combined to generate a groundwater potential map. The study classified the watershed into five groundwater potential categories ranging from very good to very poor, revealing a heterogeneous spatial distribution of groundwater availability. The results demonstrate the effectiveness of GIS-based AHP approaches for groundwater assessment and provide valuable guidance for groundwater planning and management in hard-rock regions.

Pavelic et al. (2012) carried out the studies on impact of floods on groundwater zones and suggested that in Chao river basin, Thailand, practices such as rain water harvesting which stores water at the surface and managed aquifer recharge in which stores water below the surface when flooding occurs. Results also indicated that surplus water is diverted during very high flows and allowed to percolate through soil zones for groundwater recharge and due to this large amount of flood water has been harvested for agricultural production.

Golian et al. (2021) conducted a study to evaluate the effect of rainstorms and floods of 2019 on water resources present in Iran. The high intensity rainfall in Iran also known as Dena rainstorm caused extreme precipitation which caused a lot of damage; however, it also replenished groundwater resources a large extent.

Patra et al. (2017) utilized GIS based AHP methodology in delineating groundwater potential zones of Hooghly district which lies in the Ganga alluvial plain area using LULC, geology, geomorphology, soil, elevation, slope, rainfall, NDVI, recharge rate, post monsoon groundwater depth and pre monsoon groundwater depth. Results indicated that good, moderate and poor groundwater potential zones covering 71.61%, 23.04% and 6% areas respectively are delineated. Furthermore, the validation of the obtained results shows that 75% of well data matches with the zones of groundwater potential maps.

Chakraborty et al. (2018) studied the influence of geology, land use, lineament density, soil, drainage density, rainfall, slope, infiltration rate, groundwater fluctuation on groundwater potential zones of Raniganj block, Paschim Bardhhaman, West Bengal using integration of GIS and AHP methodology. Geology, land use and land cover, drainage density and lineament density, were found to be the most sensitive

parameters. The outcomes of groundwater potential zones were successfully validated with groundwater depth data from CGWB (Central Groundwater Board).

Rajasekhar et al. (2019) conducted studies on groundwater potential zones using 8 thematic layers which are geomorphology map, LULC, geology map, slope, lineament map, soil map, rainfall data, drainage density and concluded that north western region has high groundwater potential while south eastern part has low groundwater potential.

Mukherjee and Singh (2020) employed a combination of Geographical Information System (GIS) and Analytical Hierarchical Process (AHP) techniques to delineate the Groundwater Potential Zones (GPZs) of the semi-arid Birbhum district in eastern India which suffers from seasonal drought considering geology, geomorphology, Land Use/Land Cover (LULC), fault and lineament density, drainage density, rainfall, soil type, slope, roughness, topographic wetness index. The groundwater potential map achieved an accuracy of 80.49% when validated against observation tube well data, while ROC curve–based cross-validation indicated a satisfactory predictive performance of 71.50%.

Bera et al. (2020) conducted a study in the Karha river basin, Maharashtra State for the exploration of groundwater resources with the help of integration of remote sensing data and GIS with AHP method and considering ten thematic layers such as geomorphology, LULC, slope angle, lineament density, drainage density, rainfall distribution map, curvature, TWI, geology, and soil map were integrated in a GIS environment. The analysis indicated that the western sector of the basin, especially the Ghorawadi, Garade, and Saswad areas, exhibits highly favorable conditions for groundwater exploration.

Doke et al. (2021) employed GIS based AHP approach to evaluate groundwater potential zones using rainfall, lineament density, geology, distance from the river, geomorphology, slope, land use, drainage density, soil in Ulhas basin is located in Western Maharashtra, India. Approximately 14% of the study area is classified as the High Groundwater Potential Zone (HGPZ), 34% as the Moderate Groundwater Potential Zone (MGPZ), 27% as the Low Groundwater Potential Zone (LGPZ), and the remaining 24% as the Poor Groundwater Potential Zone (PGPZ), with the zonation validated using well data.

Muthu & Sadalaimuthu (2021) conducted a study intended to demarcate groundwater potential zones (GWPZ) using remote sensing and geographical information system (GIS) with analytical hierarchy process (AHP) for Pattukottai

Taluk belongs to Thanjavur district, Tamil Nadu, India. Researchers utilized eight parameters which are geomorphology, LULC, soil, lineament density, drainage density, slope, geology and rainfall.

Rajesh et al. (2021) applied a GIS-based Analytical Hierarchy Process using factors such as land use, geology, elevation, slope, lineament characteristics, drainage density, and geomorphology to delineate groundwater potential zones in the Godavari River basin, India. Their results showed that 49.71% of the area falls within good, 41.05% within moderate, and 9.22% within poor groundwater potential zones, with the highest potential observed in the lower basin owing to favorable runoff accumulation, infiltration conditions, and subsurface storage capacity.

Jena et al. (2020) employed GIS and RS technique and AHP method for the delineation of ground water storage and recharge potential zones in Rana groundwater basin considering SPI, elevation, topographic wetness index, aspect, plan curvature, drainage density and geology.

Saranya & Saravanan (2020) utilized AHP method integrated with GIS and RS delineated groundwater potential zoning in Kancheepuram district, Tamil Nadu, India considering topography, geology, drainage density, geomorphology, soil, land use, lineament density, rainfall and validated well yield data and post monsoon water level obtained from the Central Ground Water Board.

Thomas & Raghunath (2020) employed AHP coupled with GIS and RS for the delineation of groundwater potential zones in Manimala river basin, Kerala, India using factors such as lithology, geomorphology, land use, density of lineaments and stream network, slope and soil texture and results of the research validated with Central Ground Water Board.

Das & Pal (2020) used AHP and Fuzzy Logic in the assessment of groundwater vulnerability to over exploitation in Ghoghat-I and II blocks of West Bengal, India considering parameters such as groundwater recharge, geology, elevation, groundwater level in the pre-monsoon season, land use land cover and results were validated yield from the well from the Central Ground Water Board report.

S. Biswas et al. (2020) utilized AHP coupled with GIS and RS in Uttar Dinajpur district, West Bengal considering Geomorphology, slope, soil, geology, LULC, rainfall, curvature, NDWI, and drainage density and the results were well validated with Groundwater Fluctuation level from the Central Ground Water Board reports.

Hamdani & Baali (2020) employed AHP coupled with GIS for the characterization of ground water potential zones in Central Middle Atlas, Morocco considering parameters such as elevation, slope, precipitation, geology, geomorphology and lineament density.

Nigussie et al. (2019) utilized AHP coupled with GIS for mapping of ground water potential zones in Ketar watershed, Main Ethiopian taking into consideration all the groundwater conditioning factors and validated the findings with point data of boreholes, hand-dug wells and springs.

Bhumika Uniyal et al. (2020) evaluated the effectiveness of structural as well as agricultural best management practices (BMP's) for reducing sediment production at sub watershed levels in the Upper Baitarani river basin using SWAT model and identification of critical sub watersheds were also done to assess the soil loss so that proper remedial measures can be taken to control soil erosion and reduce sedimentation in the region. Results indicated that structural best management practices are more effective in reduction of sediment yields.

Olabanji Aladejana et al. (2020) established a relationship between the basin geologic properties and streamflow response by suggesting best management practices based on the SWAT model in Northwest Benin Owena River Basin. The results proved that the application of model tested best management practices results in the substantial reduction in runoff and helps in mitigating the floods in the area by adopting terracing system on arable lands.

Leelambar Singh & Subbarayan Saravanan (2020) used SWAT for simulating discharge and estimation of the components of water balance of Ib river watershed of Mahanadi basin. The study used TRMM rainfall data and results from the hydrological modelling reported that 26-50% of the rainfall was dissipated by evapotranspiration, Percolation and groundwater flow contributed 15-21% and 13-18% respectively from total precipitation.

Marian Amoakowaah Osei et al. (2019) carried out a hydroclimatic modelling using SWAT on small Owabi catchment of Ghana to evaluate the impact of changes in LULC on the catchment. SWAT model simulated historic and projected streamflow and water balance while SUFI2 algorithm in the SWAT CUP was employed for calibration and validation of the results derived from the model.

Hasan and Wyseure (2018) used SWAT for investigating the effect of climate change on hydropower generation in Rio Jubones basin, Equador. SWAT model was

successfully simulated the hydrological processes for forecasting streamflow under three different climate scenarios to analyse the impact of climate change and it was inferred that the hydropower generation will increase in the wet season due to increased rainfall and plant will witness a substantial power drop in the dry season with 17% reduced discharge and 2.9 degrees increments in temperature.

Hallouz et al. (2018) evaluated the applicability of the SWAT model in the Harraza basin (Northwest of Algeria). The study reported that the model was calibrated and validated only against the monthly streamflow measurements using SUFI2 and based on the good performance for discharge, model was used to predict the sediment concentration in the basin.

Sushil et al. (2017) estimated the hydrology and sediment concentration of Ken River basin which is a semi-arid region of central India. The study reported accurate daily and monthly values for runoff and sediment concentration and further assessed that evapotranspiration, runoff and soil erosion is predominant in the region which implies that better management practices are required in the basin to utilize the water resources judiciously.

Ghoraba (2015) used ArcSWAT to model the hydrology of watershed in Simly Dam, Pakistan and estimated the monthly inflow to Simly dam. The model was initially calibrated using annual data and subsequently refined at the monthly scale. The outcomes indicate a strong agreement between the calibration results and the corresponding validation data.

Odewole et al. (2020) conducted the study to examine the pre flood and post flood nature of floodplain along hadejia to Tiga dam in Kano state using sentinel 2 data. The findings indicate that, before the flood event, the floodplain was predominantly characterized by bare surfaces, interspersed agricultural and vegetated patches, built-up areas, and water bodies. However, after floods, there are substantial changes in the settlements, waterbodies, vegetation and water body which helped in evaluating damages occurred due to floods.

Rehman et al. (2016) determined the land cover patterns of pre-flood period, flood period and post flood period in the year 2015 on upper part of Sindh region. Three satellite images of Landsat-8 OLI were used in the study acquired on April 11, 2015, August 17, 2015 and October 20, 2015. Findings indicated a decrease in the vegetation and hazardous results of destruction and deterioration of crops with other infrastructure

and it also provides some beneficial information like refreshing of fertile soil by flooded water.

Ahmad et al. (2017) conducted study to find out the impact of floods on Wular lake, Kashmir Valley, India using satellite images. Comparative analysis of the two images showed substantial post-flood declines in agricultural land (−43.65%), water bodies (−39.94%), and terrestrial vegetation (−23.71%). Additionally, high siltation resulted in sand deposition over approximately 8.19 km² (20.5%) of the area.

Elmahdy and Mohamed (2013) delineated groundwater potential zones using ASTER DEM and Landsat imagery by integrating structural, topographic and hydrological factors within a GIS framework. The analysis identified high groundwater potential areas primarily along the foothills of the Oman Mountains and the Al Dhaid Depression. Validation using well and aquifer hydraulic data showed good agreement with the mapped groundwater potential zones, confirming the reliability of the approach for groundwater assessment.

Meyer et al. (2012) examined limitations in current flood mapping practices in Europe, highlighting that flood maps are often developed as technical information products rather than effective communication tools. Through participatory case studies across five European regions, the study demonstrated that incorporating stakeholder input and local knowledge significantly improves the relevance, clarity, and usability of flood maps. The authors proposed user-specific recommendations for map content, stakeholder engagement, and visualization design, emphasizing the importance of tailored flood maps to support strategic planning and emergency management.

Pulvirenti et al. (2011) developed a fuzzy logic based algorithm for mapping flood extents from synthetic aperture radar (SAR) imagery, designed for operational use in flood management systems. The method integrates radar backscatter modelling, basic hydraulic principles, and ancillary data such as land cover and digital elevation models to improve flood detection in complex conditions, including vegetated areas.

Arthur et al. (2007) developed the Florida Aquifer Vulnerability Assessment (FAVA) to support groundwater protection and management using a Bayesian weights-of-evidence modelling framework. The approach integrated key hydrogeological factors with groundwater quality indicators to map relative aquifer vulnerability across Florida, with rigorous sensitivity and validation testing. The study demonstrated the effectiveness of data-driven probabilistic models for large-scale groundwater vulnerability assessment and informed subsequent spring-protection initiatives.

Ahern et al. (2005) reviewed epidemiological evidence on the health impacts of floods, highlighting floods as one of the most frequent and damaging natural hazards worldwide. The study emphasized that health outcomes vary widely depending on population vulnerability and flood characteristics and warned that climate change driven increases in extreme rainfall and sea level rise are likely to intensify flood related health risks in the future.

2.3 Research Gaps

The Idukki district of Kerala, with its steep terrain, high intensity monsoonal rainfall, and fragile ecological landscape, is one of the most severely flood affected regions in the state. Despite experiencing devastating flood events in recent years most notably in 2018 and 2021 there remains a significant void in scientific research that holistically investigates the interconnections between flood susceptibility, surface runoff dynamics, and groundwater potential in this region.

To date, no comprehensive or spatially integrated study has been undertaken to assess how extreme flood events influence both surface and subsurface hydrological systems within Idukki. The district lacks flood susceptibility mapping, groundwater potential zoning, and runoff modeling that are interlinked within a unified geospatial framework. As a result, the hydrological behaviour of this flood prone and topographically complex region remains poorly understood in the context of flood driven impacts.

The following gaps emphasize the novelty and necessity of the present research:

- A comprehensive GIS-based mapping of groundwater potential has not previously been undertaken for the Idukki district, making this the first study to generate such spatially detailed groundwater assessments for the region.
- The influence of flooding on groundwater-susceptible regions in high relief terrains such as Idukki has not been systematically investigated before. No prior studies have explicitly linked flood susceptibility with groundwater susceptibility in this context.
- Groundwater susceptibility representing how vulnerable zones respond to reduced recharge under flood conditions has not been studied or spatially delineated for Idukki.

- A GIS-based flood susceptibility assessment has not previously been undertaken for the Idukki district, and this study provides the first systematically developed flood susceptibility map for the region.
- There is a lack of comprehensive research that links surface hydrological extremes (such as flood induced runoff) with flood susceptibility map and subsurface groundwater dynamics, particularly in complex terrain and highly variable climatic settings like Idukki.
- Land use and land cover changes, though frequently studied, are rarely analysed in direct relation to flood zones or validated against hydrological extremes such as the 2018 flood event.
- Hydrological modelling tools, such as SWAT, have not yet been applied in Idukki to simulate runoff dynamics in connection with spatial flood vulnerability, missing a crucial opportunity to identify hydrologically active and risk prone areas.

The thesis addresses a fundamental void in flood and water resource studies by developing a holistic, spatially explicit framework that connects flood susceptibility, surface and subsurface hydrology, and land system evolution. In doing so, it offers not only a novel methodological approach but also a timely and region specific contribution to the broader discourse on integrated flood management and groundwater sustainability in mountainous, flood vulnerable environments.

CHAPTER 3
STUDY AREA

The Idukki district, situated in the Western Ghats of Kerala, India, is located at approximately 9.85°N latitude and 76.94°E longitude. The district is predominantly forested, with limited urbanization and scattered rural settlements, and tea plantations forming the core of its agricultural economy. Spanning an area of about 4,358 km², nearly 97% of the district is under forest cover. The terrain is largely rugged and mountainous. The region experiences a tropical climate, with a mean annual temperature of about 24.4 °C and an average annual rainfall of approximately 2,226 mm, characterized by consistent and high intensity precipitation throughout the year.

Geologically, the district comprises three major lithological units: the Peninsular Gneissic Complex in the north, the Migmatitic Complex in the central part, and the Charnockite Group in the south. Granite gneiss, representing the oldest formation, exhibits well developed foliation and localized folding. The landscape is dominated by structural denudational hills formed of Precambrian basement rocks with thin soil cover. While most of the district lies within the Western Ghats, the Thodupuzha and western Elamdesam blocks fall within the midland region, characterized by undulating terrain with small hillocks and deeply incised valleys. The district is primarily drained by the Periyar River, with the Pambar and Muvattupuzha rivers draining the northeastern and western sectors, respectively.

The soil characteristics of the district are influenced by the predominance of hard crystalline rocks and rugged terrain. The major soil types include clay, loam, and gravelly clay, which occur as shallow to moderately deep profiles across much of the area. Steep to very steep slopes is widespread, particularly within the hilly tracts, promoting rapid surface runoff and limiting infiltration during intense rainfall events. The combined presence of hard rock formations, thin soil cover, and steep slopes plays an important role in governing the hydrological response of the district, especially in terms of runoff generation and flood behaviour. Figure *3.1* shows the location of the Idukki district.

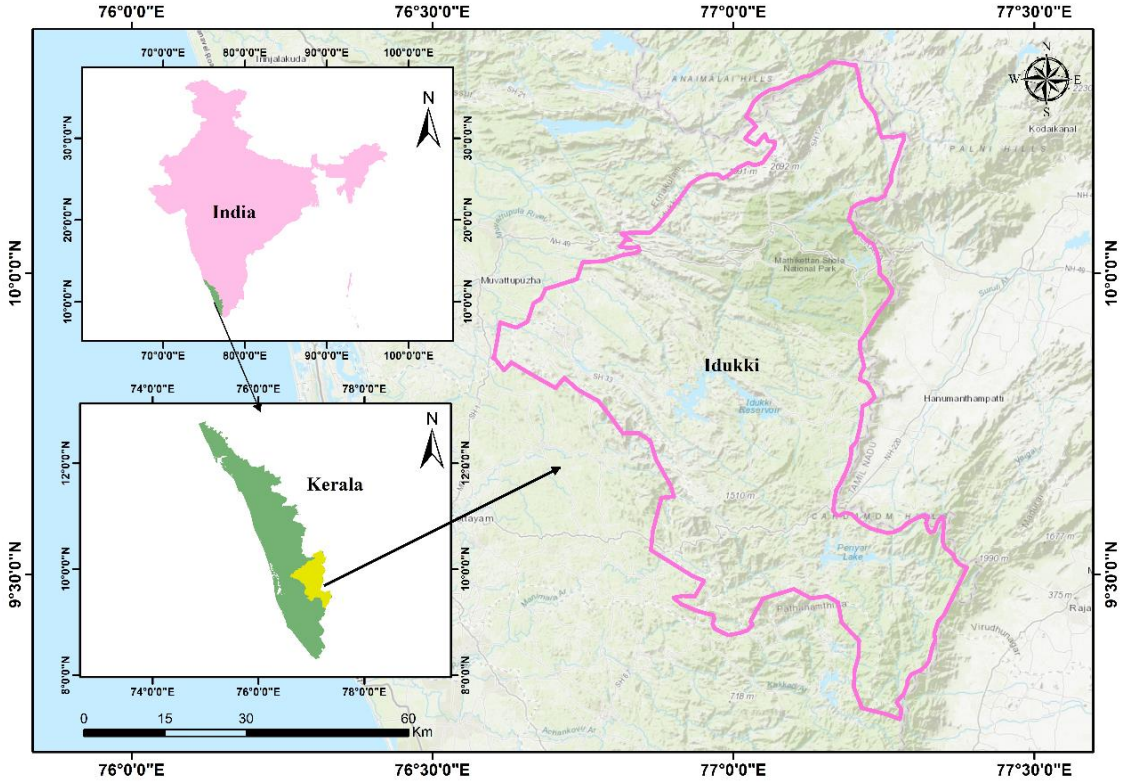

Figure 3.1 : Study Area: Idukki District, Kerala, India

CHAPTER 4
METHODOLOGY

4.1 General

In academic research, methodology serves as the structural backbone that guides the entire study. It provides the framework through which research questions are systematically investigated, hypotheses are tested, and meaningful conclusions are drawn. A well defined methodology ensures that the research process is coherent, replicable, and scientifically valid. It determines the credibility of the results and helps in maintaining transparency throughout the course of the study. For geographically and environmentally complex issues like floods and their effects, the choice of appropriate methods becomes even more critical, as these phenomena are inherently spatial, dynamic, and multifactorial.

The methodological design of a research study is deeply rooted in the nature of its objectives. It defines the tools, techniques, and processes adopted to collect, analyze, and interpret data. In geospatial and environmental studies, this often involves integrating qualitative and quantitative approaches, adopting both traditional and modern technologies, and employing spatial modeling, satellite data processing, and predictive analytics. Selecting a suitable methodology is not merely a procedural step, but a deliberate and strategic decision that directly influences the accuracy and depth of the findings.

For research that seeks to examine the multidimensional impacts of floods such as their influence on groundwater recharge, land use patterns, and surface runoff dynamics, the methodology must not only be technically sound but also adaptable to complex interactions within natural systems. Spatial variability, temporal fluctuations, topographical nuances, and hydrological responses must all be accounted for, necessitating a robust and multifaceted methodological framework. Furthermore, the use of modern computational tools, geospatial techniques, and machine learning enhances the analytical precision, offering new insights into spatial processes and environmental change.

In the present study, a comprehensive and integrative methodology has been employed to investigate the various dimensions of flooding within the Idukki district of Kerala, a region characterized by complex topography and frequent extreme rainfall events.

The approach brings together multiple tools and techniques drawn from the domains of GIS, remote sensing, machine learning, and hydrological modeling to holistically assess the impact of floods on key environmental components.

The subsequent section outlines the detailed methodological approaches adopted for each of the defined research objectives, accompanied by corresponding flowcharts that illustrate the procedural framework.

4.2 Methodology for Objective 1

The first objective emphasizes on the identification of flood prone zones within the Idukki district of Kerala by employing Analytic Hierarchy Process (AHP). In this process, a set of twelve flood contributing parameters namely geology, elevation, distance from river, Sediment transport index (STI), rainfall, land use, soil, Topographic Wetness Index (TWI), slope, aspect, Stream Power Index (SPI) and Topographic Roughness Index (TRI), were selected based on their hydrological and topographical relevance and are considered to evaluate their relative influence on flood susceptibility. The database information for the parameters is indicated in Table 4.1. These parameters are systematically weighted through pairwise comparisons, following the AHP framework, to generate a flood susceptibility map for Idukki district.

Table 4.1 Database information of Flood susceptibility Mapping

Data Layers	Source of Data
Rainfall	IMD https://mausam.imd.gov.in/
Geology/Lithology	GSI https://www.gsi.gov.in/
Soil	NBSSLUP https://www.nbsslup.in/
Digital Elevation Model (DEM)	SRTM https://earthexplorer.usgs.gov/
LULC	Landsat 8 Imagery https://earthexplorer.usgs.gov/

4.2.1 Analytic Hierarchy Process (AHP) Model

The analytical hierarchy process method is a versatile and well-structured technique for interpreting complex decision scenarios involving several factors (Saaty, 1980). It

is a widely accepted technique for addressing complex decision-making challenges. The key strength of this approach is its ability to assign user defined weights within a hierarchical framework of criteria and sub-criteria. Therefore, AHP facilitates the user to assess different parameters which are of utmost significance as per the requirement and comprehend the problem statement with deeper understanding. Comparison of different parameters is done by assigning scores based on their relative influences and importance (i.e., 1 denotes equally significant; 3 denotes moderately more significant; 5 denotes strongly more significant; 7 denotes very strong more significant; 2, 4 and 6 are the transition scores) as shown in Table 4.2. In various problems such as flood susceptible mapping, landslide mapping and Groundwater potential zones assessment, AHP is found to be a powerful and a beneficial tool having high accuracy (Mahmoud & Gan 2018; Surwase et.al., 2019; Suthirat et.al., 2020). The reason for wide popularity of AHP model is its capability to handle quantitative as well as qualitative data in assessing natural hazards like floods (Chakraborty & Mukhopadhyay (2019)). Implementation of AHP model has been successful in comprehending problems of various natural hazards such as assessment of floods and landslides susceptible regions (Jazouli et.al. 2019; Danumah et.al. 2016).

For investigating problems of flood modelling or susceptibility studies, the AHP model is utilized to determine the weights and rankings of various parameters. Steps involved in the AHP method for delineation of flood susceptibility zones in a region is described below:

- The first stage of the AHP involves constructing a pairwise comparison matrix for all parameters influencing the system.
- The weights or values then are assigned to each parameter is built upon the knowledge or the expertise of the user in pairwise comparison matrix. For instance, when rainfall is compared with elevation, a value of 4 is assigned which indicates intensity of importance for rainfall is 4 times more than that of elevation.
- Similarly, when same parameters are compared in the standard pairwise comparison matrix, for instance when slope is compared with slope, assigned weight has a value equal to 1 as both the parameters hold equal importance. This further explains the reason of assigning a value of 1 to all the diagonal elements in pairwise comparison matrix. Evaluation of all the attributes is

generally performed on a nine-point scale as explained by Saaty (1980) in Table 4.2.

- The second step is to sum all the assigned weights at the end of a column and then each assigned weight is divided by sum of all the assigned weights. The normalized principal Eigen vector or priority vector is obtained by averaging all the weights and normalized values is obtained for each parameter. The priority vector indicates the final weights assigned to each parameter.
- To evaluate the consistency of weights with respect to one another, consistency ratio is calculated.
- After verifying consistency, the normalized weights are multiplied by the ranks of the respective subclasses of each parameter to derive the composite weights for all thematic layers.
- The assigned weight values were incorporated into the ArcGIS environment to develop the final flood susceptibility map.

Detailed mathematical expression of the AHP approach is given below.

Let X = $\{X_j | j = 1, 2\ldots\ldots n\}$ be the arrangement of the model. Result of the pairwise comparison on n criteria can be done in a (n_n) assessment matrix A where each component a_{ij} (i, j = 1, 2…..n) is the range of the weight of the attribute, as given in the condition below

$$A = \begin{bmatrix} a_{11} & a_{12} & \ldots & a_{1n} \\ a_{21} & a_{22} & \ldots & a_{2n} \\ \ldots & \ldots & \ldots & \ldots \\ a_{n1} & a_{n2} & \ldots & a_{nn} \end{bmatrix}, a_{ii} = 1, a_{ji} = \frac{1}{a_{ij}}, a_{ij} \neq 0$$

The scores obtained from the pairwise comparison matrix are normalized to derive the standardized matrix using the weighted arithmetic mean approach. The relative importance of each component is then calculated through the mean row method applied to the standardized pairwise comparison matrix. Maximum eigenvalue is expressed as:

A w = λmax w, Here A represents the standard pairwise comparison matrix, w is the eigen vector, λmax represents the matrix's principal eigenvalue

For having consistent pairwise comparison, the matrix A has rank equivalent to 1 and λmax is equivalent to n. Consistency of the pairwise judgements among the different parameters are of utmost importance as it regulates the accuracy of the

results through AHP model. The consistency of the AHP method is checked by employing the below equation (Saaty 1980):

$$CR = \frac{CI}{RI}$$

$$CI = \frac{\lambda max - n}{n - 1}$$

Where, CR represents consistency ratio, CI represents consistency index, RI represents random index, λmax represents the matrix's principal eigenvalue, and n denotes the number of parameters or factors. In Saaty's (1980) paper, a significant number of components are used to obtain RI values as shown in Table 4.3.

Observations indicate that RI is governed by a range of influencing conditions. According to Saaty's (1980) study, for instance, the comparable value of RI is 1.45 when the components are nine as indicated in Table 4.3. The consistency ratio (CR) is acceptable if it is less than 10% or 0.10 which indicates a fair level for the pairwise comparison matrix.

Table 4.2 Saaty's 1-9 scale of pairwise comparison matrix

Numerical Value	Description	Explanation
1	Equal Importance	Two activities contribute equally to the objective
3	Slight Importance of one over another	Experience and judgement slightly favour one activity over another
5	Moderate importance of one over another	Experience and judgement strongly favour one activity over another
7	Very strong importance	Activity is favoured very strongly over other
9	Extreme importance of one over another	Evidence favouring one activity over the other is of the highest importance
2,4,6,8	Intermediate values	-

Table 4.3 Saaty's Random Index (RI) Table

N	1	2	3	4	5	6	7	8	9	10	11	12	13	14	15
RI	0.00	0.00	0.58	0.90	1.12	1.24	1.32	1.41	1.45	1.49	1.51	1.48	1.56	1.57	1.58

4.2.2 Validation of the AHP Model

A critical aspect of any spatial modelling approach lies in its validation against real-world data to confirm the accuracy and credibility of the results (Band et al., 2020). In the case of the AHP-based flood susceptibility mapping, the model's predictive performance was evaluated using a success rate analysis. For this purpose, historical flood extent data were compiled by integrating secondary sources, including records from the Survey of India and satellite derived inundation information. Specifically, Sentinel-1 Synthetic Aperture Radar (SAR) imagery in VV polarization was utilized, with one acquisition date representing the pre-flood scenario (17 May 2018) and another corresponding to the peak flood period (21 August 2018). This temporal comparison enabled the delineation of actual flood-affected areas, which were subsequently used to assess the agreement between observed flood extents and the susceptibility zones identified by the model. The performance and reliability of the AHP-based flood susceptibility model were evaluated using the AUC-ROC approach. The AUC-ROC curve was generated by comparing the predicted flood susceptibility classes with observed flood occurrence points, providing a quantitative measure of the model's discriminatory capability. A comprehensive methodological workflow outlining the steps involved in developing the flood susceptibility map for Idukki District is presented below.

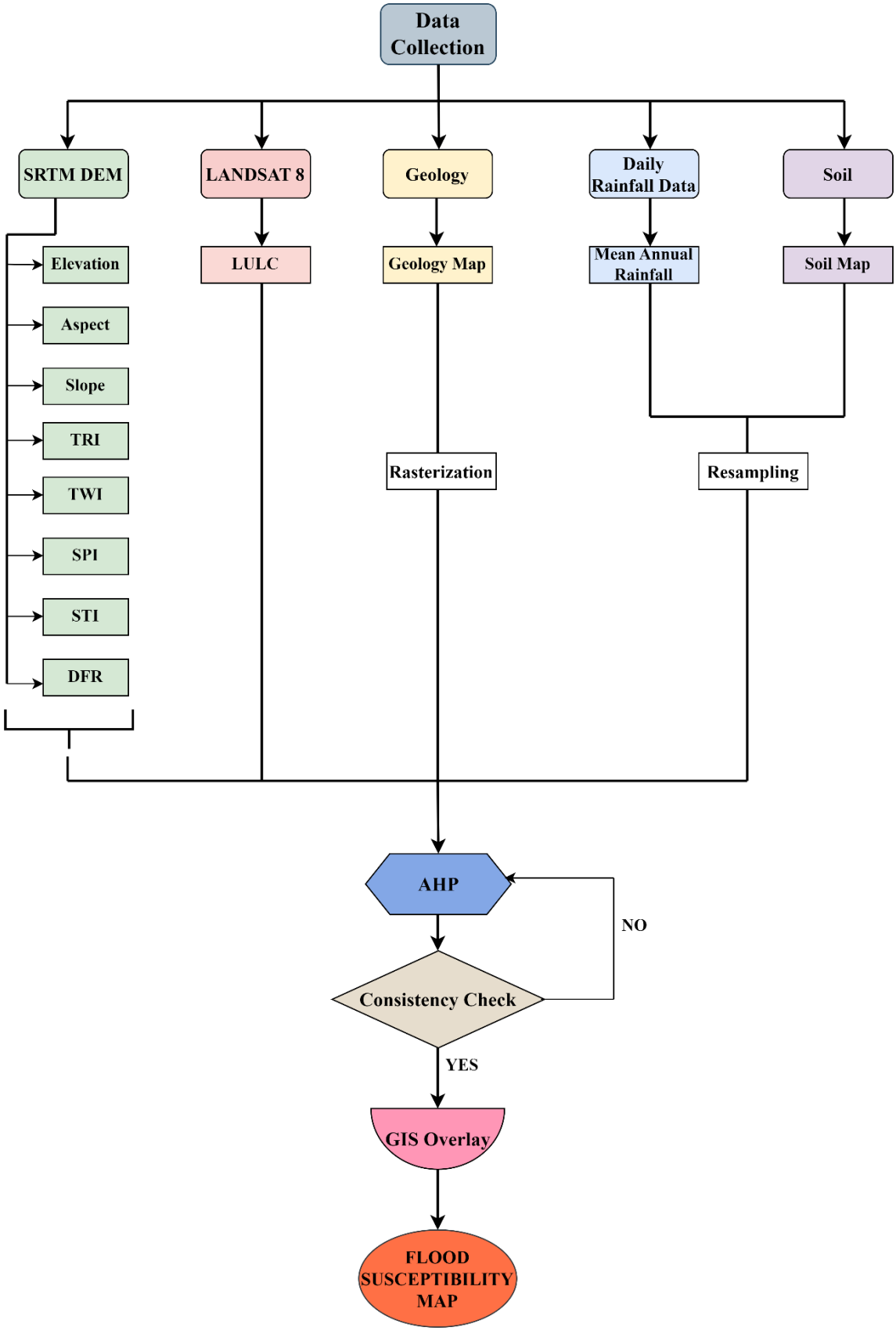

Figure 4.1 : Methodology for preparing flood susceptibility map of Idukki district

4.3 Methodology for Objective 2

A rigorous evaluation of how flood dynamics influence groundwater availability necessitates an accurate delineation of groundwater potential zones. In pursuit of this objective, the research employs an advanced GIS-based machine learning methodology capable of capturing intricate spatial patterns governing groundwater occurrence. Fourteen conditioning factors were considered in this study based on field verifications and literature studies (Chenini et al. 2010; Naghibi et al. 2016; Prasad et al. 2020; Devanantham et al. 2020). The conditioning parameters include elevation, slope, lineament density, soil, geology, topographic wetness index (TWI), curvature, sediment transport index (STI), rainfall, land use and land cover (LULC), Normalised Differential Vegetation Index (NDVI), topographic roughness index (TRI), geomorphology and drainage density. Each of these thematic layers were obtained from different sources as shown in Table 4.4 and then resampled to a uniform grid size of 30 x 30m in the ArcGIS 10.2.1 software.

Table 4.4 Database information of Groundwater Potential Mapping

Data Layers	**Source of Data**
Well Locations	Central Groundwater Board http://cgwb.gov.in/ Field Survey
Rainfall	IMD https://mausam.imd.gov.in/
Geology Geomorphology	Geological Survey of India https://www.gsi.gov.in
Soil	National Bureau of Soil Survey and Land Use Planning https://www.nbsslup.in/
Lineament Density	Landsat ETM+ & PAN
Digital Elevation Model (DEM)	SRTM https://earthexplorer.usgs.gov/
Land-use/land-cover NDVI	Sentinel – 1

Figure 4.2 presents the comprehensive methodological structure adopted for groundwater potential zones, illustrated in the form of a flowchart.

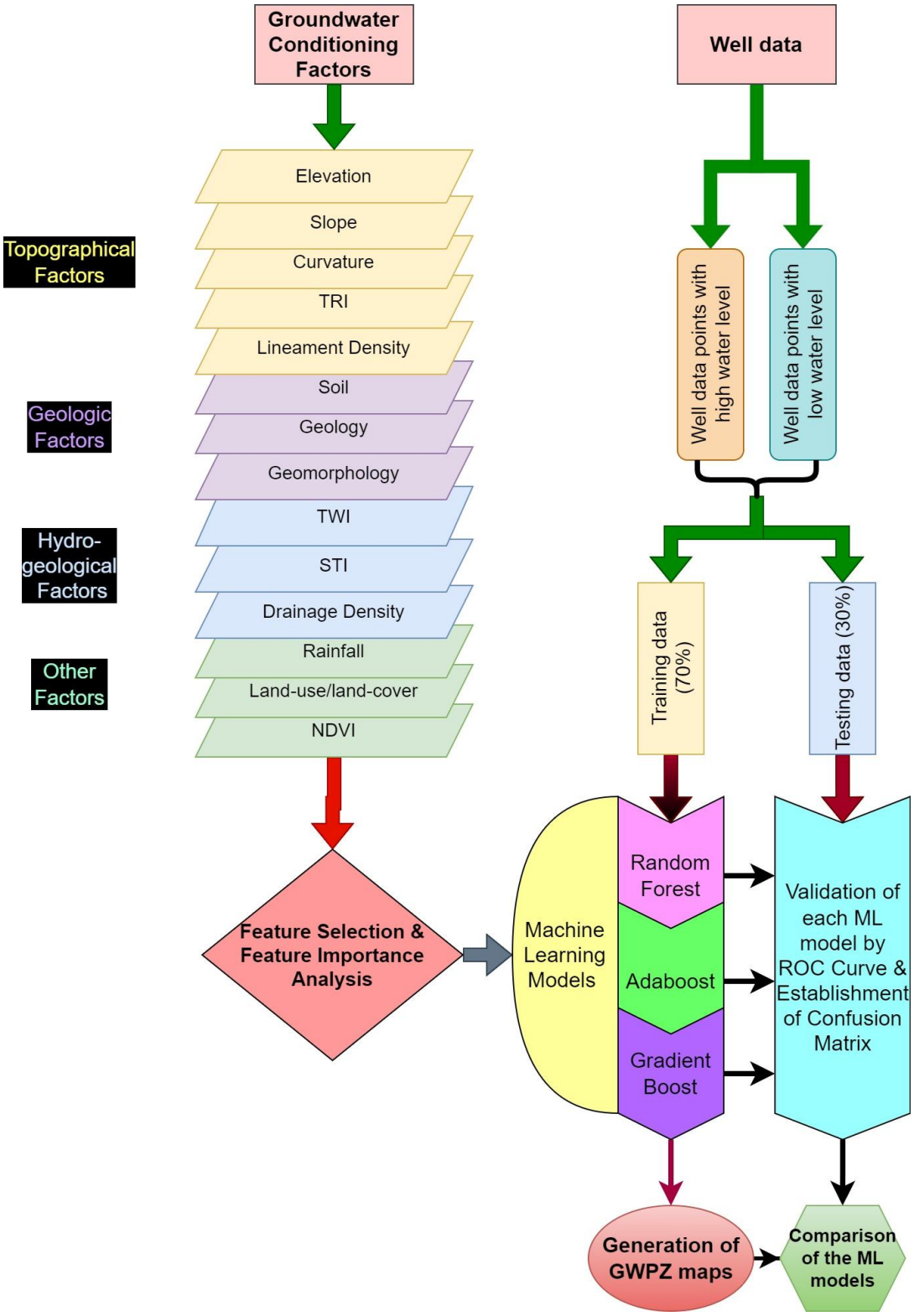

Figure 4.2 : Methodological Framework for GWPZ

For estimating and analysing the groundwater potential of the Idukki district, three machine learning algorithms including random forest, adaboost, and gradient boost were employed. The fourteen conditioning factors' 'variable importance' were measured before the modelling process in order to assess their significance. The well

locations and the raster layers of the conditioning factors were exported into the Google Colab environment, where the machine learning models were developed using python programming. Each ML model's final output values were exported to the ArcGIS software in order to generate the GWPM. The effectiveness of the ML models in predicting the GWP mapping was evaluated and compared, and models were validated using the AUROC method.

4.3.1 Variable Importance

Each factor's efficiency was evaluated using the "Variable importance" feature of the RF model. It is a generic method for estimating the value of a feature using learned algorithms (Kuhn 2015). A filter strategy was used to assess each factor on its own. The relevance ratings for the features vary from 0 to 100. Higher the importance value, the larger the influence of the factor, and vice versa.

4.3.2 Random Forest Algorithm

The RF model was initially developed by building several decision trees using various dataset subsets (Breiman 2001). The class that receives the most votes is the class that the random forest's decision trees each anticipate will belong to. The forest of tree classifiers increases the generalisation error built upon the strength of the individual trees and their associations. The significance of a variable can be ascertained with the use of internal estimations. The success of the model is largely due to the low correlation. Uncorrelated individual trees offer ensemble projections that are more precise than individual forecasts. By avoiding overfitting conclusions, random forests improve accuracy in classification and regression problems. Each tree also protects the others from its own defects. Most of the trees stay upright and move forwards together in the same direction, while a few may wander (Breiman 2001; Chen et al., 2014; Pourghasemi and Kerle 2016; Youssef et al., 2016; Jesudasan 2022; Mohebzadah et al., 2022). The key benefits of this approach are that it can handle huge datasets with high dimensionality and prevent over fitting of the datasets, that it requires no assumptions about explanatory variables and response variables, and that it doesn't need any prior data for transformation and rescaling (Prasad et al., 2020).

4.3.3 AdaBoost Algorithm

The Adaptive Boosting model also known as the AdaBoost algorithm is a robust classifier from a set of weak classifiers (Kearns and Valiant 1994; Freund and Schapire 1995, 1997). In order to construct poor learners across the training dataset, the

AdaBoost approach keeps a set of weights and modifies them after each cycle of weak learners. At the beginning, all weights are initialised evenly. The weight of the incorrectly identified samples rises each round, while the weight of the correctly classified samples falls. But for this boosting method, no prior knowledge of the effectiveness of the weak algorithm used is necessary.

4.3.4 Gradient Boosting Algorithm

Gradient boosting constructs additive regression models by iteratively fitting new models to the pseudo residuals using a least squares framework. These pseudo-residuals shows the gradient of the loss function being minimized with respect to the current model predictions at each training instance. Introducing controlled randomness into this process has been shown to markedly enhance both the predictive accuracy and computational efficiency of the gradient boosting algorithm. In particular, a subsample of the training data is randomly selected (without replacement) from the entire training data set at each cycle. The base learner and the model update for the current iteration are then computed using this randomly chosen subsample rather than the entire sample. This randomised technique also improves robustness against the base learner's overcapacity (Friedman 2002).

4.3.5 Validation and Comparison of ML models

The validation stage of any prediction modelling is crucial since it establishes the model's scientific validity. Therefore, to validate the outputs of the machine learning models, data from the well were employed as the primary reference dataset for assessing groundwater potential across the study area. A total of 253 well locations were collected and analysed into two categories: 121 wells exhibiting low groundwater levels and 132 wells indicating high groundwater levels. The dataset was then partitioned into training and validation subsets using a random sampling procedure, wherein 177 wells (70%) were allocated for model training and the remaining 76 wells (30%) were reserved for independent validation.

The accuracy, kappa value, and ROC were then used to assess the efficiency of the prediction rule (Aslam et. al 2022). An indicator of how well a classification model performs is the classification accuracy. By dividing the total number of projections by the number of accurate estimates, it is calculated. The Cohen's kappa, also referred to as the Kappa values, is a trustworthy statistic for determining inter- and intra-rate dependability. It is a standardised value that resembles correlation coefficients in

appearance. AUC serves as a model's overall accuracy statistic, independent of the discriminant criterion in question. The machine learning model's success rate and prediction rate are measured using the ROC (Landis and Koch 1977; Zweig and Campbell 1993; Pascale et al. 2013). Using these validation methods the ML models were compared for their prediction efficacy and reliability.

4.3.6 Uncertainty and Limitations of Machine Learning Models

Although machine learning algorithms such as AdaBoost, Gradient Boosting, and Random Forest provide robust predictive capabilities, certain sources of uncertainty may influence the reliability of the model outputs. One important factor relates to the quality and representativeness of the training dataset. The predictive performance of these algorithms depends on the accuracy of the input thematic layers and the spatial distribution of training samples. If the training data are limited, unevenly distributed, or contain inherent errors from source datasets, the model predictions may reflect these uncertainties. In addition, the ability of machine learning models to generalize beyond the conditions represented in the training dataset may be constrained, particularly in heterogeneous terrains where geological and hydrological characteristics vary significantly. Another potential limitation arises from classification bias, where models may favour dominant patterns present in the dataset, leading to overrepresentation of certain classes in the predicted outputs. To reduce these uncertainties, different machine learning algorithms were implemented in this study and their results compared. The use of different machine learning techniques helps improve prediction stability and reduces the influence of individual model bias, thereby enhancing the reliability of groundwater potential zone delineation.

4.4 Methodology for Objective 3

To evaluate the impact of floods on LULC, the research conducted a detailed examination of changes in LULC patterns. The focus was on two significant flood events that occurred in Kerala during 2018 and 2021. To accomplish this objective, Landsat 8 satellite imagery corresponding to periods before and after the flood events was acquired. The investigation was carried out using the Google Earth Engine (GEE) platform, enabling efficient comparison of pre flood and post flood LULC conditions.

To analyse the effects of the torrential rainfall and floods on land use and land cover (LULC), rainfall for the month of August 2018 and October 2021, has been analysed and subsequently rainfall for the Idukki district for the month of August 2018 and

October 2021 has been prepared in the ArcMap interface. Land use and land cover information was generated using the Random Forest technique, a widely applied machine learning algorithm. The processing was performed within the Google Earth Engine (GEE) platform, a cloud-based geospatial analysis system developed by Google. GEE provides an interactive framework that enables rapid data visualization and analysis through an online application programming interface (API).

The platform hosts a vast repository of freely available satellite datasets, encompassing optical, thermal, and microwave observations (Bhuyan et al., 2020). For evaluating effect of floods on LULC, readily available remote sensing data from the complete Landsat archive and Sentinel satellite missions were utilized. A key advantage of GEE is its access to extensive, pre-processed datasets, including land cover products, environmental variables, meteorological data, and climate related information, which significantly simplifies data retrieval and analysis workflows.

The satellite imagery is trained using a classification model which categories it into difference land use classes. Every class was trained using 60 Region of Interests (ROIs) and verified using 50 ROI points, following a widely accepted guideline (Lillesand and Kiefer 1979). The accuracy of the map is assessed after satisfactory results have been achieved. Flood extent mapping was performed using GEE, employing an image ratio based technique to identify the inundated regions as done in Flood susceptibility mapping in objective 1. The methodology for examining the changes in land use and land cover pattern is described in the flow chart below.

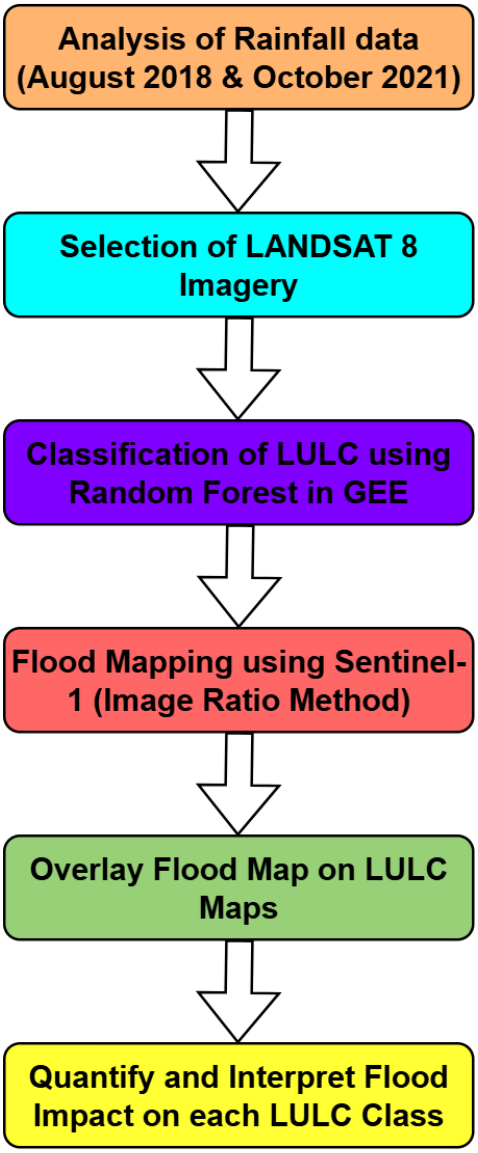

Figure 4.3 : Methodological Flowchart for Evaluating Flood-Induced LULC Changes

4.5 Methodology for Objective 4

To effectively evaluate the influence of extreme rainfall events and flooding on surface runoff in the Idukki district, a hydrological modeling approach was adopted. The Soil and Water Assessment Tool (SWAT), a well established hydrological model, was selected for simulating runoff dynamics. SWAT enables the quantification of various hydrological processes, particularly surface runoff and discharge fluctuations, at the watershed scale over extended periods.

The Periyar River Basin, which is the largest and most prominent drainage system in the Idukki district, was selected as the focal area for this objective. The modelling

process began with the delineation of the watershed boundaries within the Idukki region using high-resolution DEM data. The 30 meter spatial resolution DEM was obtained from the Shuttle Radar Topography Mission and processed within the ArcSWAT interface, an extension of ArcGIS designed to support SWAT-based analysis.

4.5.1 Input Datasets for SWAT

Key input datasets required for SWAT simulation were prepared and integrated into the model environment. These included:

- **Topographic data (DEM)**: Used for watershed delineation and stream network generation.
- **Land Use and Land Cover (LULC) maps**: Extracted from remote sensing imagery and classified using machine learning techniques, these maps define surface characteristics and influence hydrological response.
- **Soil data**: Sourced from national or regional soil databases, including information on texture, depth, hydraulic conductivity, and other relevant properties.
- **Meteorological data**: Daily precipitation, temperature, wind speed, solar radiation and relative humidity data were gathered from the Indian Meteorological Department (IMD) and other reliable sources for both pre flood and post flood periods, particularly around 2018 and 2021.

After assembling and formatting the input datasets, the model setup involved defining Hydrological Response Units (HRUs) by overlaying soil, land use, and slope classes. These HRUs represent unique combinations that respond similarly to hydrological inputs. The source for the data used in the SWAT model is presented below.

Table 4.5 Database and their sources for SWAT Model

S.No.	Data Type	Resolution	Data Source
1	Meteorological Data		
	Precipitation	0.25˚ x 0.25˚	IMD
	Temperature	0.5˚ x 0.5˚	NASA Power

	Wind Speed	0.5˚ x 0.5˚	NASA Power
	Solar radiation	0.5˚ x 0.5˚	NASA Power
2	Digital Elevation Model	30 m x 30 m	SRTM
3	Soil Texture	30 arc second	FAO
4	LULC	10 m x 10 m	Sentinel - 2
5	Gauge Discharge	Daily, Monthly, annually	CWC

4.5.2 Validation of SWAT Model

The calibration and validation of the model was conducted using observed discharge data from relevant gauging stations located within the Periyar basin. The accuracy of the model was assessed using statistical indicators namely the Nash-Sutcliffe Efficiency (NSE) and Coefficient of Determination (R^2) to ensure simulation's reliability.

Post calibration, the model was applied to simulate runoff behaviour during major flood events. Rainfall data for the flood months (August 2018 and October 2021) were used to observe shifts in discharge levels and runoff contributions from various sub basins. Areas with abrupt increases in runoff were identified as hydrologically sensitive and prone to flood induced erosion or waterlogging.

By integrating multiple datasets and simulation tools, this methodology allowed for a comprehensive understanding of runoff variability and the identification of zones within the Periyar basin that are most vulnerable to hydrological stress during flood events. The figure below outlines the methodological workflow employed for surface runoff assessment using the SWAT model.

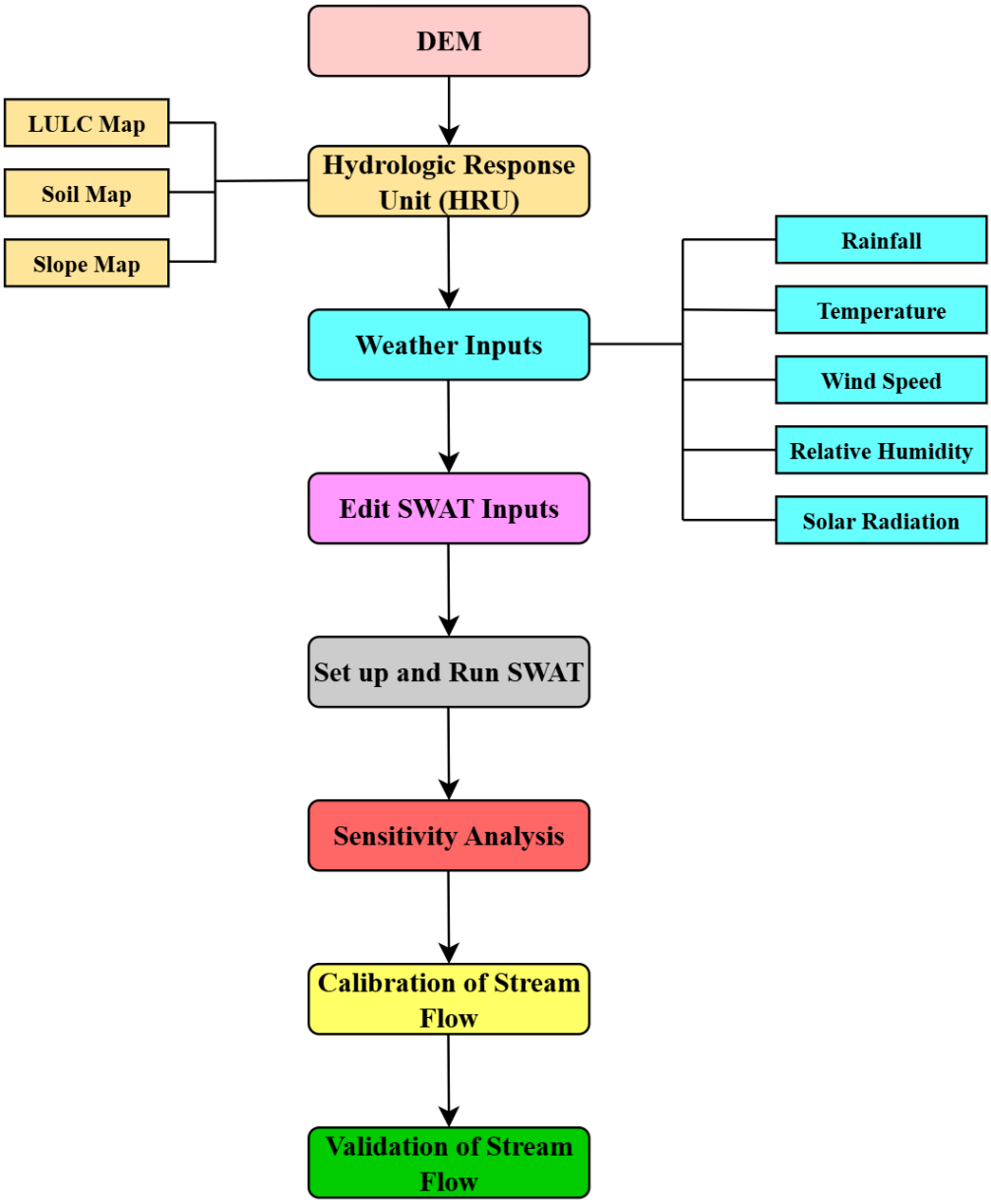

Figure 4.4 : Methodological framework for computation of Surface Runoff

CHAPTER 5
RESULTS AND DISCUSSIONS

5.1 Generation of Thematic Layers

In alignment with the stated research objectives, an extensive suite of geospatial parameters governing both flood susceptibility and groundwater behaviour was assembled and processed within a GIS analytical framework. In addition to the datasets prepared for flood susceptibility mapping and Groundwater zones, parameters required to evaluate the influence of flood events on land use and land cover (LULC) dynamics were also compiled. This included the acquisition of long term rainfall records and multispectral Landsat 8 imagery, which formed the basis for generating pre- and post-flood LULC classifications. These datasets enabled the examination of how extreme rainfall and subsequent flooding altered vegetation cover, built-up areas, agricultural land, and other surface features within the study region.

Furthermore, in order to investigate the effect of floods on surface runoff behaviour, a separate set of hydrological inputs was assembled. This included Digital Elevation Models, slope and terrain derivatives, soil attributes, land-cover information, and a suite of climatic variables such as rainfall, temperature, solar radiation, humidity, and wind speed. These parameters were essential for setting up the hydrological model and for quantifying changes in runoff generation during extreme rainfall episodes.

The collection, preprocessing, and integration of these datasets formed a critical component of the data preparation phase, ensuring that all necessary thematic layers were available for the subsequent analyses. Together, these spatial datasets provided a comprehensive foundation for understanding how floods influence groundwater potential, land surface characteristics and hydrological responses across the study area.

5.1.1 Generation of Spatial Inputs for Flood Susceptibility

For the flood susceptibility assessment, twelve thematic datasets were developed: geology, elevation, proximity to river channels, rainfall, land use, soil, Topographic Wetness Index (TWI), slope, Topographic Roughness Index (TRI), aspect, Stream Power Index (SPI), and Sediment Transport Index (STI). The generation of these layers involved the integration of DEM derived terrain attributes, hydrological records, remote sensing products, and available geospatial repositories at various spatial scales.

The derivation of each index based layer incorporated specific computational formulations and raster operations executed within the ArcMap environment. The hydrological and geomorphometric equations utilised for generating TWI, TRI, SPI, STI, and other model-based layers were applied through raster-based map algebra functions, spatial analyst tools, and digital terrain preprocessing routines. The corresponding input datasets, calculation expressions, reclassification schemes, and processing workflows are documented to ensure methodological clarity and reproducibility.

For flood modelling, topographic parameters are critical because they influence the hydrological properties of the studied region both directly and indirectly (Arabameri et al., 2020; Lei et al., 2020). In the first phase, the Shuttle Radar Topography Mission (SRTM) Digital Elevation Model (DEM) for the research region was downloaded from the Earth Explorer. It is a 1 arc second 30 m resolution freely available DEM data widely used in various applications of remote sensing analysis. This data is reprojected to UTM zone 43N in projected coordinate system. The data is void filled, mosaicked and extracted by mask for further processing in the ArcGIS 10.2 environment. These pre-processed SRTM DEMs can provide more accurate and reliable elevation data for flood modelling. We used DEM to compute aspect, curvature, stream power index (SPI), sediment transport index (STI), topographic wetness index (TWI), slope, and topographic roughness index (TRI) in the ArcGIS environment. Each of the thematic layers were derived from various sources as shown in the Table 4.1 above in the methodology section.

The most important aspect in flood modelling is elevation (Dodangeh et al., 2020). Flooding is inversely proportional to elevation. When heavy rainfall occurs, water flows quickly from higher elevation regions such as mountainous and hilly areas to low lying areas or flat regions of lower elevation and thereby making these low-lying areas more prone to flooding. (Chen et al., 2020, Veerappan & Sayed (2020)). As a result, floods are more likely to occur on flat or lower elevated areas. Figure 5.1 (a) shows the elevation map of the study region. Aspect is another parameter that affects the spatial orientation of flood-prone areas. It is derived from the DEM data spatial analyst tool in ArcGIS. It is considered to be a significant factor as it determines the direction of flow of water and hence assists in the evaluation of flooded regions (Rehman et.al., 2016). As a result, the aspect plays an indirect role on flood dynamics. Figure 5.1 (b) shows the aspect of the study area. The slope, which affects the flowing

water's flooded pace, is another major aspect that influences the flood (Stevaux et al., 2020). Slope is derived from the DEM data using the spatial analyst tool in ArcGIS. In regions where slope is steep, water flows with a high velocity during a rainfall event and hence disposes the surface runoff very quickly, whereas areas of flatter or gentle slopes are more prone to floods and water logging, as runoff gets stored over these regions for a longer time. Figure 5.2 (a) demonstrate the slope of the study area. TRI is also a key contributing variable for flood episodes as it assists in investigating basin's local topography. It is calculated by deriving the focal mean, focal minimum and focal maximum of the raster in each pixel in ArcGIS environment and using the following equation in raster calculator.

$$\boldsymbol{TRI} = \frac{(\boldsymbol{Focal\ mean - Focal\ minimum})}{(\boldsymbol{Focal\ maximum - Focal\ minimum})}$$

It describes the amount of difference in elevation between adjacent cells in a DEM. Higher magnitude of floods is always related with lower TRI values and high value of TRI leads to low magnitude of floods (Talukdar et.al., 2020). The TRI (Topographic Roughness Index) map was stored in the raster format for the analysis, with values spanning from 0.11- 0.89 (Figure 5.2 (b)). TWI (Topographic Wetness Index) is also an important aspect in the occurrence of floods (Abdel Hamid et al., 2020), since it allows the difference in the wetness of a basin to be visualised spatially (Meles et al., 2020). This index presents the water quantity present in each pixel of the area, and it is determined by employing the following equation in raster calculator in ArcGIS environment.

$$\boldsymbol{TWI} = \boldsymbol{ln}\left(\frac{\boldsymbol{A_S}}{\boldsymbol{\beta}}\right)$$

A_s indicates catchment area (m^2m^{-1}) and β represents local slope gradient (in degrees). Flood susceptibility is strongly linked to higher TWI values. In the study region, the TWI value ranges from 1.72 to 24.28.

The Stream power index (SPI) exerts a strong impact on the river network. Higher value of SPI is indictive of large erosion and heavy flowing water. SPI is calculated using the equation in raster calculator in ArcGIS environment.

$$\boldsymbol{SPI} = \boldsymbol{A_s\, tan\beta}$$

The specific catchment area is represented by A_s ($m^2\ m^{-1}$) and the local slope gradient is denoted by β (in degrees) (Wu et al., 2020). SPI map is shown in Figure 5.3 (b).

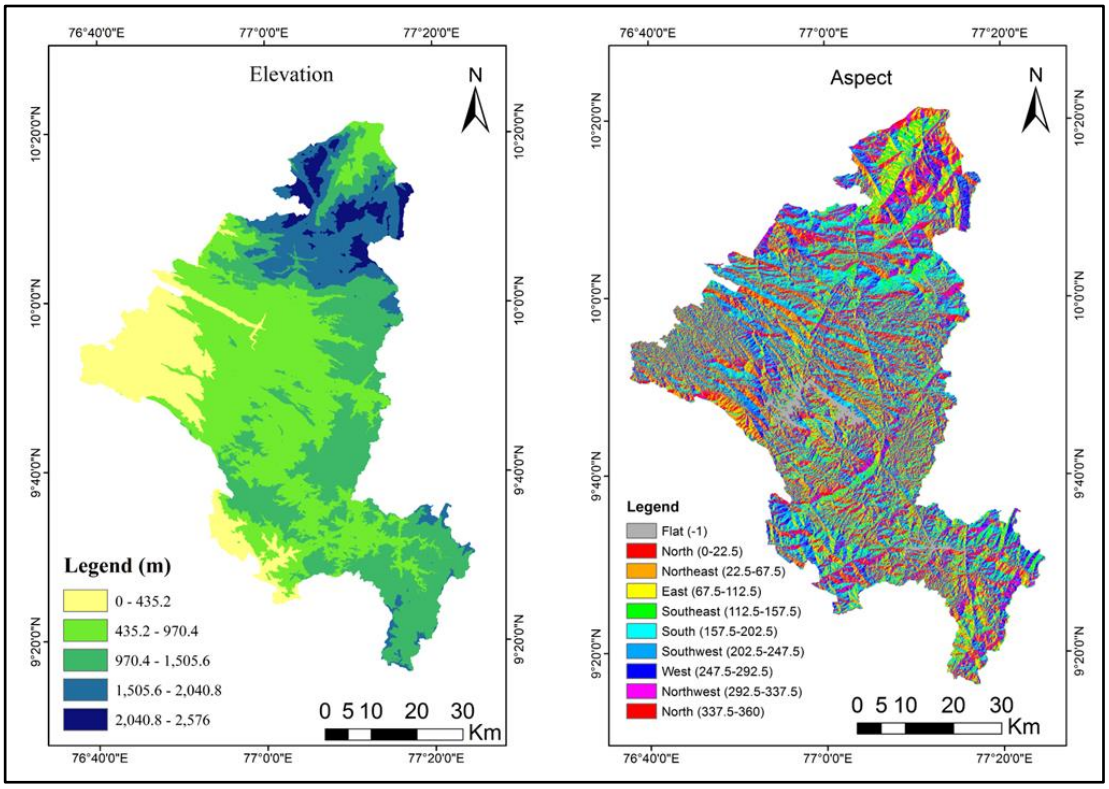

87

Figure 5.1 : (a) Elevation (b) Aspect

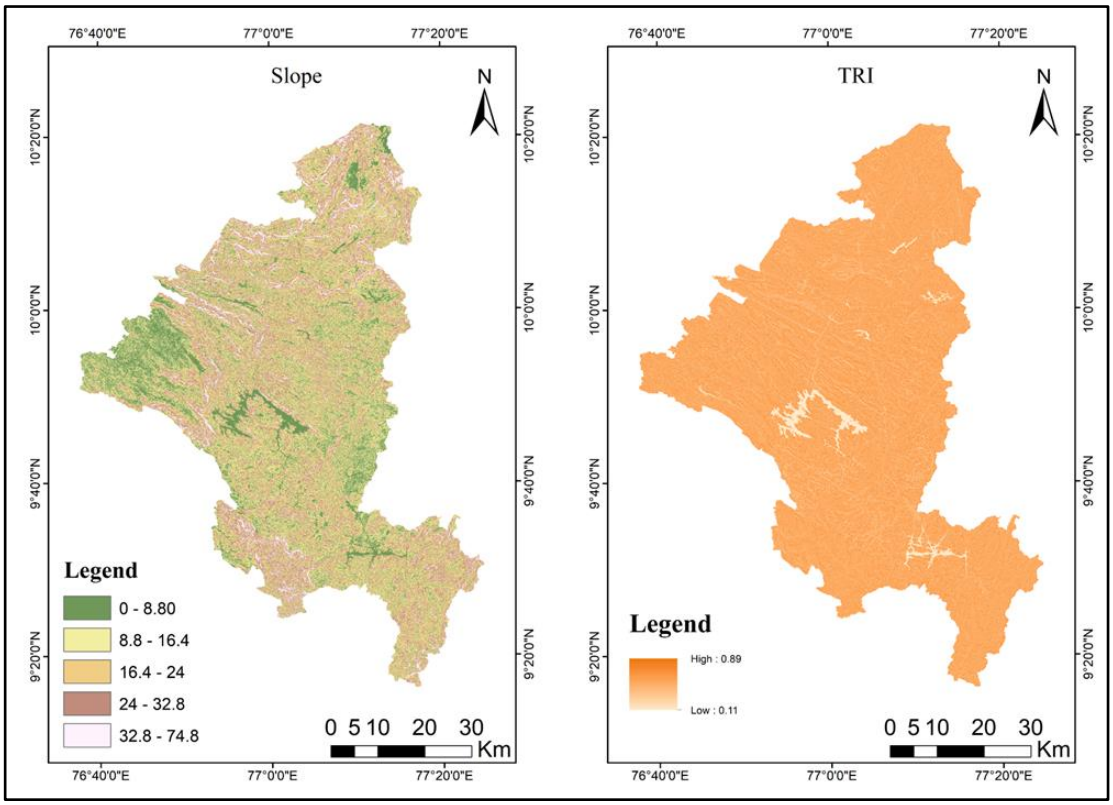

Figure 5.2 : (a) Slope (b) TRI

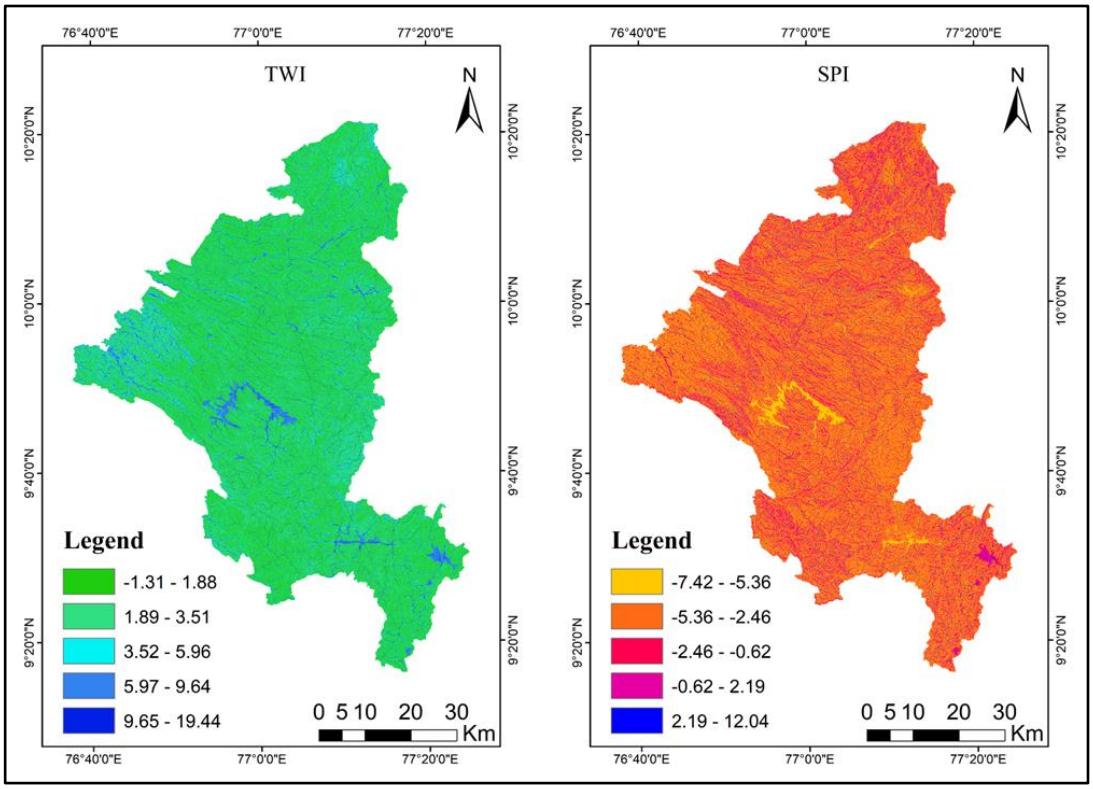

Figure 5.3 : (a) TWI (b) SPI

Sediment transport index (STI) describes the topographical effect on loss of soil and erosive capacity of a terrain. It is derived from DEM using following equation in raster calculator in ArcGIS environment.

$$STI = \left(\frac{A_s}{22.13}\right)^{0.6} \left(\frac{Sin\beta}{0.0896}\right)^{1.3}$$

Where β denotes each pixel of the local slope (in degrees) and area of the upstream section is denoted by A_s (m^2 m^{-1}). STI value were classed from low to high (Figure 5.4 (a)).

Surface runoff and sediment transport are influenced by land use, which has a direct impact on the frequency of floods (Benito et al., 2010). Land use has a direct influence on amount of streamflow generation and infiltration. Because regions in metropolitan areas do not permit water to enter the ground as a result of which flooding is more prevalent. The land use map created from LANDSAT 8 satellite imagery was divided into five categories: forest, agriculture, settlements, waste land and waterbodies as shown in Figure 5.4 (b). Supervised classification was employed to categorize land use. In supervised classification, the user identifies representative sample pixels for predefined land cover classes, which are then used by the image

processing algorithm as training data to assign all remaining pixels in the image to their respective classes. Training samples are chosen based on the knowledge and expertise of the user. For instance, training areas for urban areas, vegetation and water body can be selected by drawing a polygon around it. After having enough training samples for each class, signature files are generated in the ArcGIS software. Using the supervised classification tool, the study region is then classified into different land use features. The precision of the classification process is determined by selecting spatially balanced points within the research area and cross-referencing them with manually verified ground truth data obtained through the use of Google Earth Pro software. Subsequently, a confusion matrix was generated to evaluate the precision and reliability of the classified map. The results indicate an accuracy rate of approximately 83.35%, which is considered acceptable. Most flood inundation areas are often located in the vicinity of a river or a stream. Distance from the river plays a crucial role in delineating flood susceptible areas of a basin by controlling flood frequency and flow behaviour. The underlying concept is, less is the distance from the river, more likely that region will get flooded. We computed the distance to the river map using a 1:50,000 scale topographic map and Google Earth. The distance from the river map is depicted in Figure 5.5 (a). Soil types are one of the most important influencing elements in the process of runoff computation. Other variables such as local meteorological conditions and erosion regulate rainfall-runoff production, but soil qualities directly limit water infiltration, which determines rainfall-runoff generation. For flood susceptibility studies, we have used the National Bureau of Soil Survey and Land Use Planning to prepare the soil map. Figure 5.6 (a) shows the soil map of the study area. The lithological properties of a region influence porosity and permeability. The lithology map was developed using Geological survey of India data (1:250000 scale). Most of the region of Idukki is occupied with charnockite and followed by biotite gneiss, granite gneiss, etc. Rainfall is widely recognized as a key driver of flood occurrence, as intense precipitation over short durations can rapidly trigger flooding. Annual average rainfall data was collected from 15 Indian meteorological stations and with the help of Inverse Distance Weighted (IDW) interpolation technique, rainfall maps were created in the ArcGIS environment. IDW estimates the values of cell by averaging the values of sample data points in the neighbourhood of each processing cell. The closer a point is to the centre of the cell being estimated, the more influence

it has in the averaging process. The annual rainfall ranges from 2000 to 3700 mm in the study area as shown in Figure 5.6 (b).

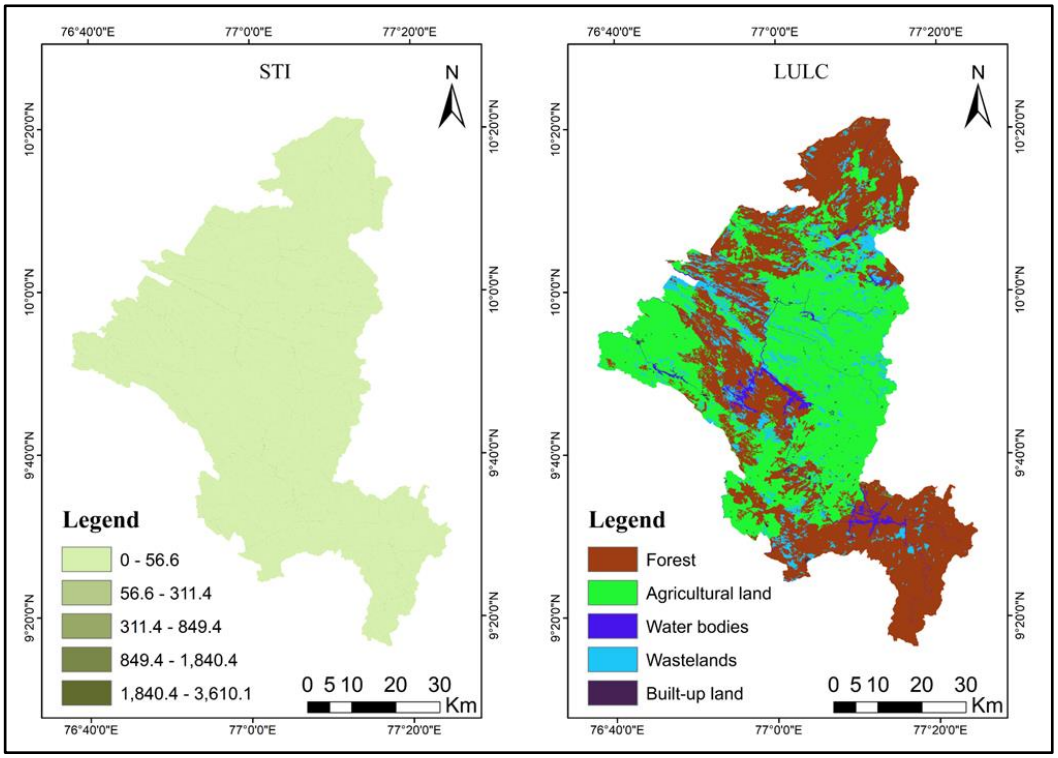

Figure 5.4 : (a) STI (b) LULC

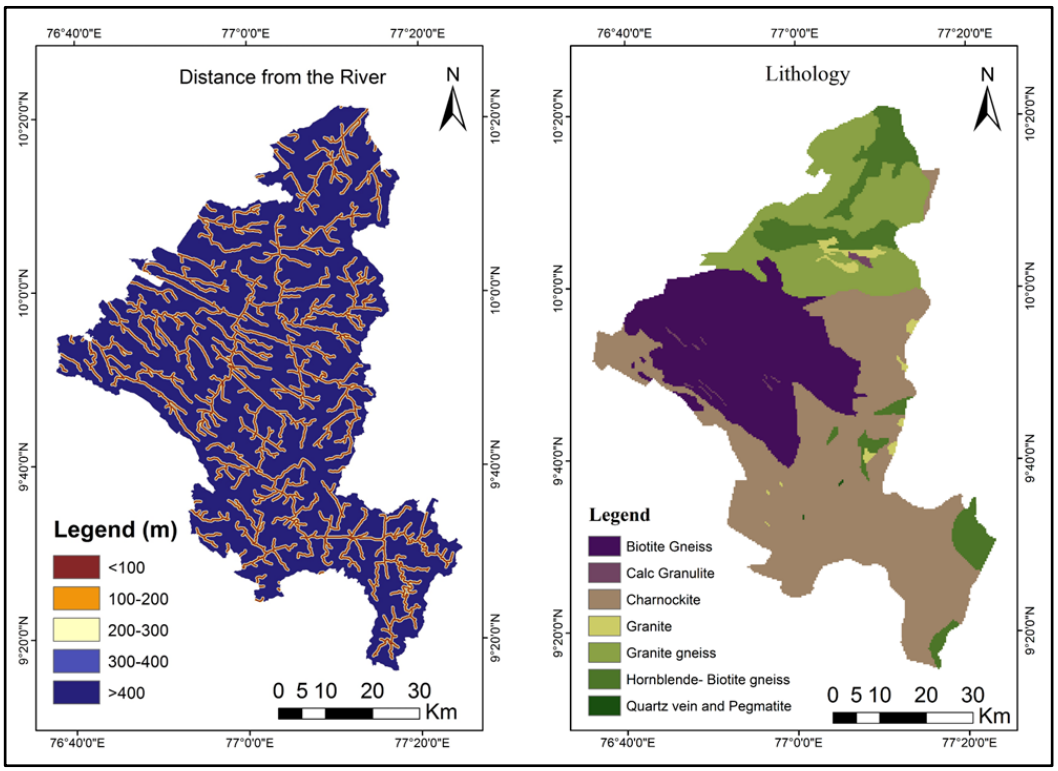

Figure 5.5 : (a) Distance from River (b) Lithology

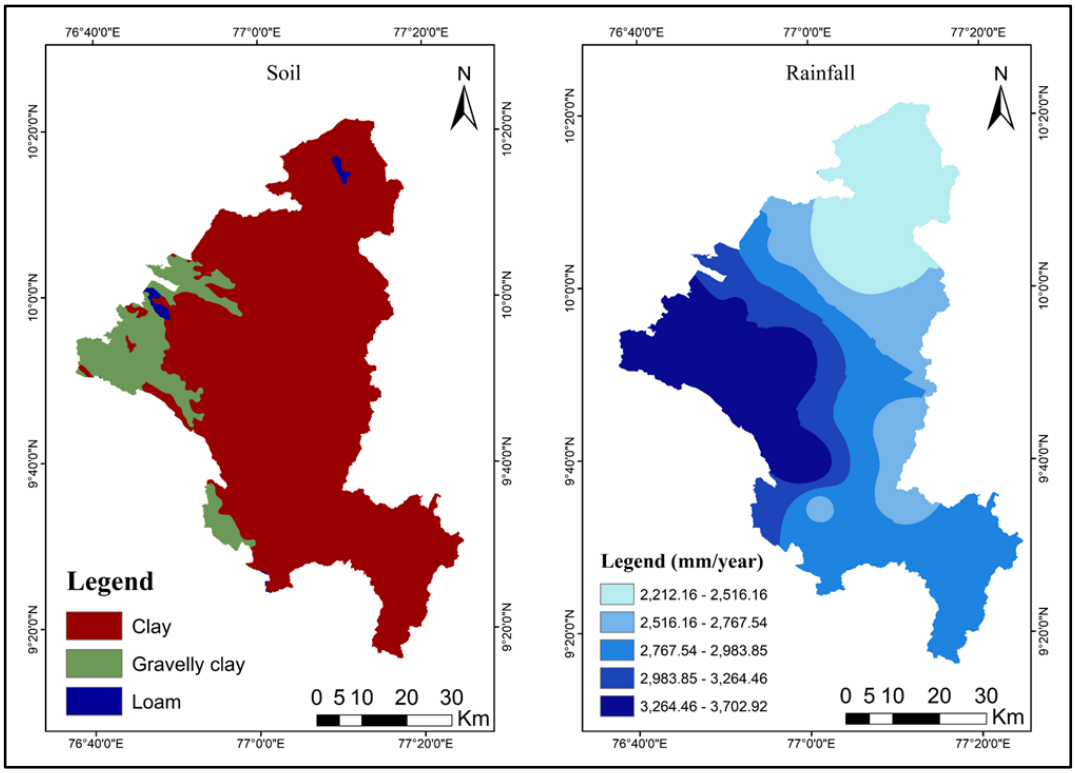

Figure 5.6 : (a) Soil Type (b) Rainfall

5.1.2 Development of Spatial datasets for GWPM

To evaluate the groundwater potential zones, fourteen spatial parameters used for groundwater potential assessment, outlining their hydrogeological relevance and individual contributions to the machine learning model. The preparation of all these spatial layers along and their significance for Groundwater potentiality is illustrated below:

Fourteen thematic layers relevant to groundwater conditioning were developed, which include: elevation, slope, curvature, TRI, lineament density (LD), rainfall, soil, drainage density (DD), geology, geomorphology, TWI, STI, LULC, and the normalized difference vegetation index (NDVI). Each layer was spatially referenced to a common coordinate system and resampled to a uniform grid resolution to ensure consistency in multi-criteria modeling and subsequent analyses.

Although certain flood conditioning factors overlap with those used in groundwater potential assessment, they are presented again to enhance clarity and to clearly distinguish the results and parameter sets employed in each analysis.

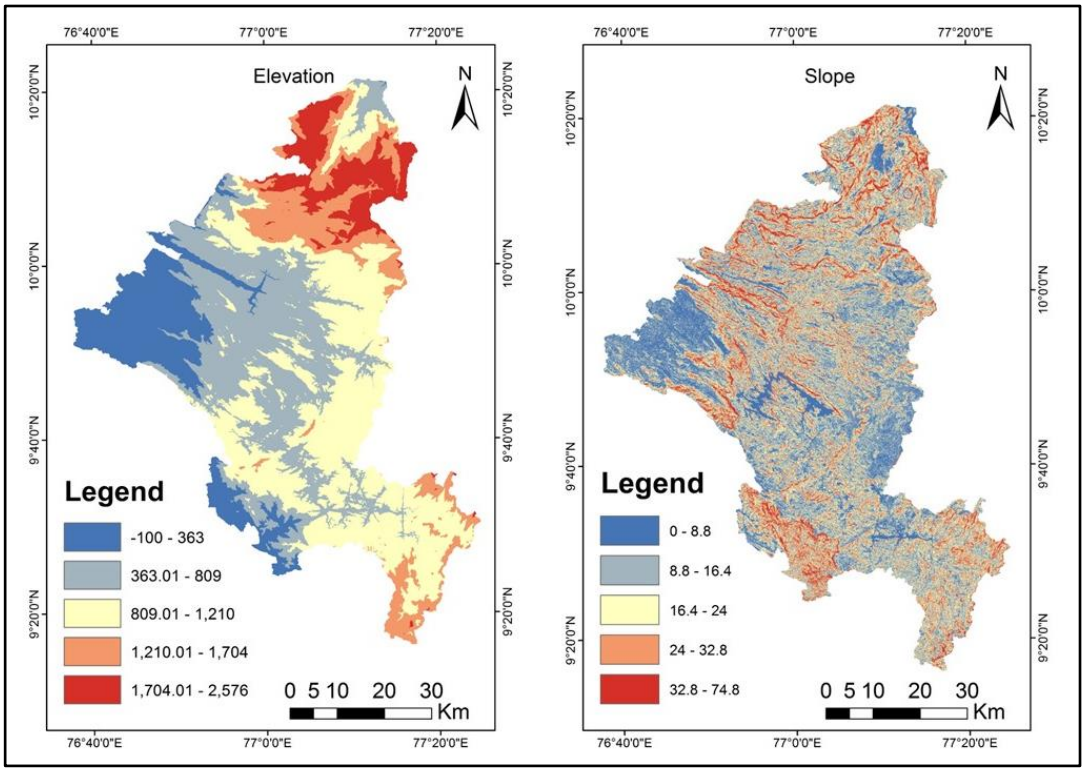

Figure 5.7 : (a) Elevation (b) Slope

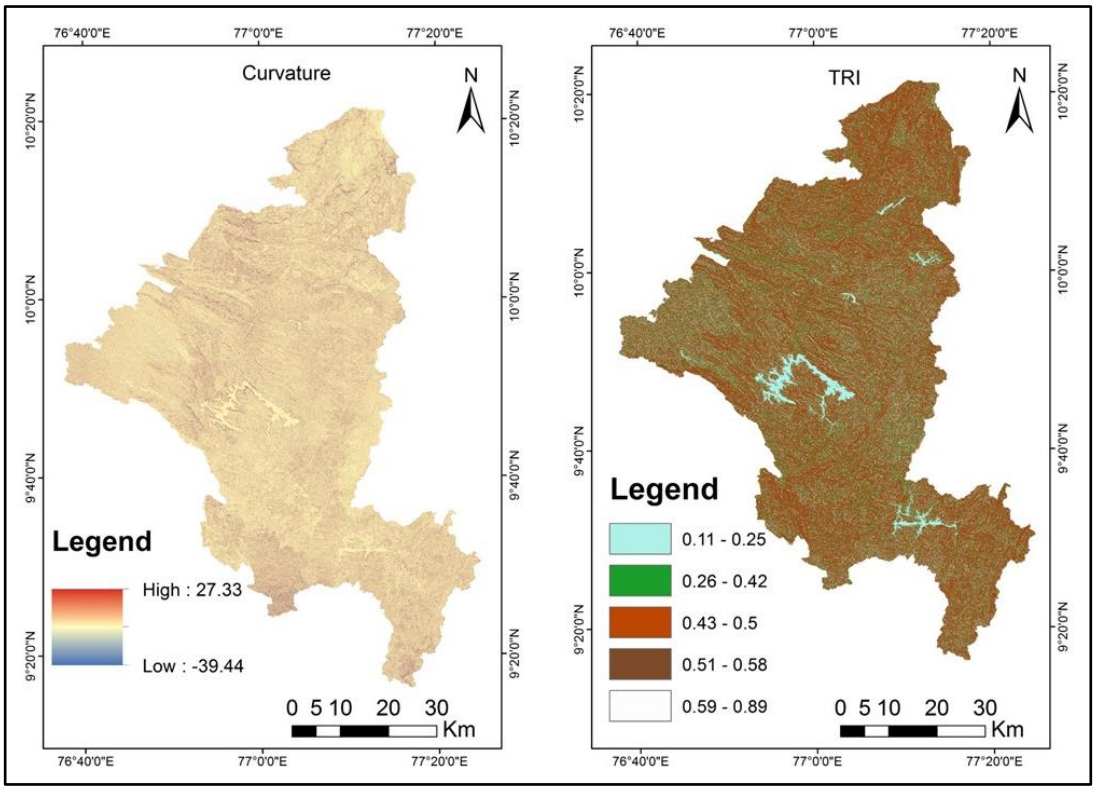

Figure 5.8 : (a) Curvature (b) TRI

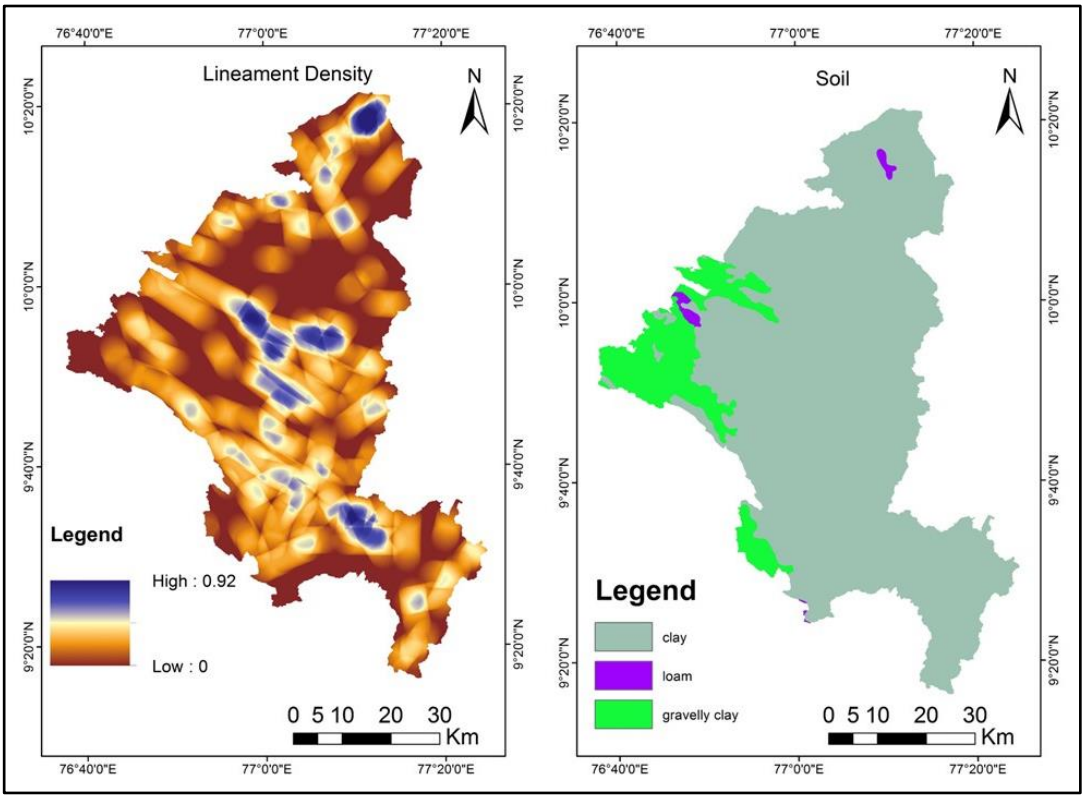

Figure 5.9 : (a) Lineament Density (b) Soil

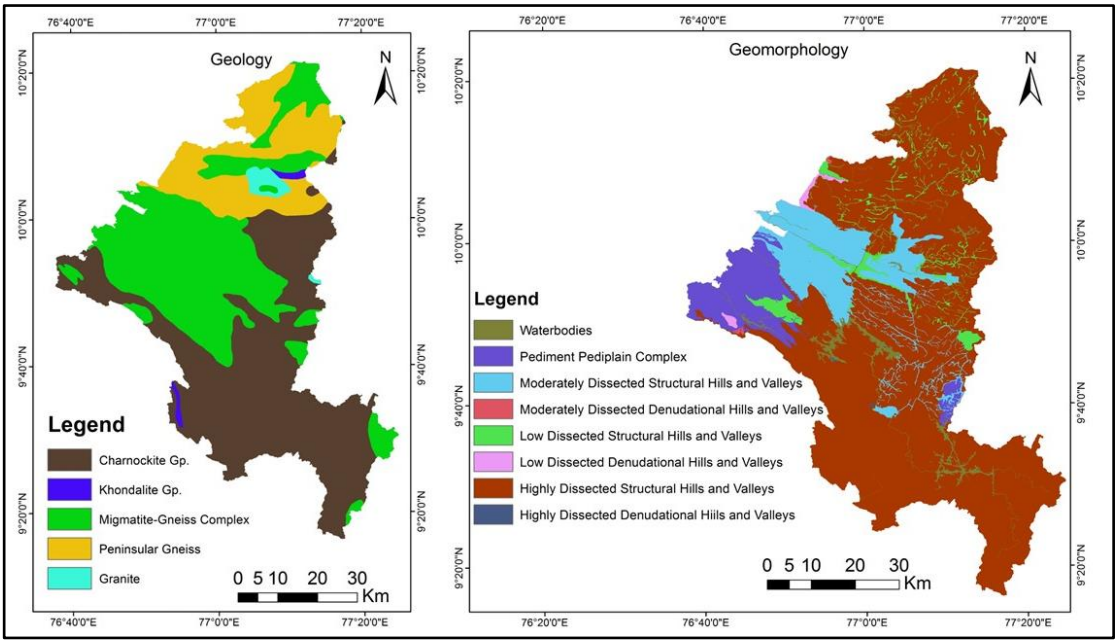

Figure 5.10 : (a) Geology (b) Geomorphology

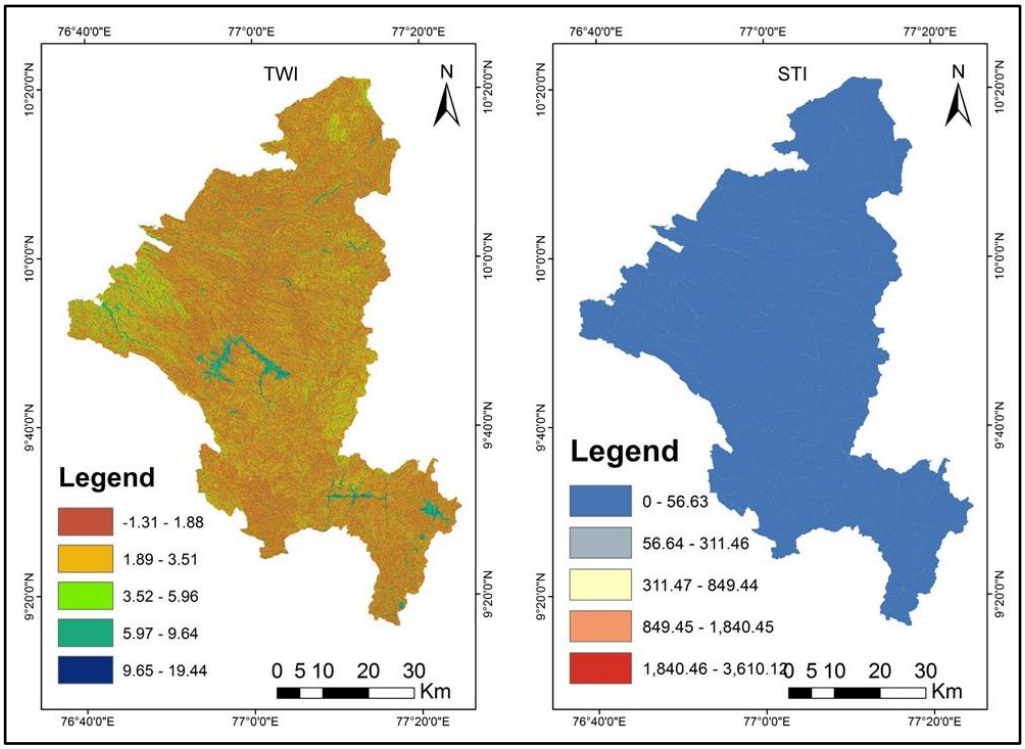

Figure 5.11 : (a) TWI (b) STI

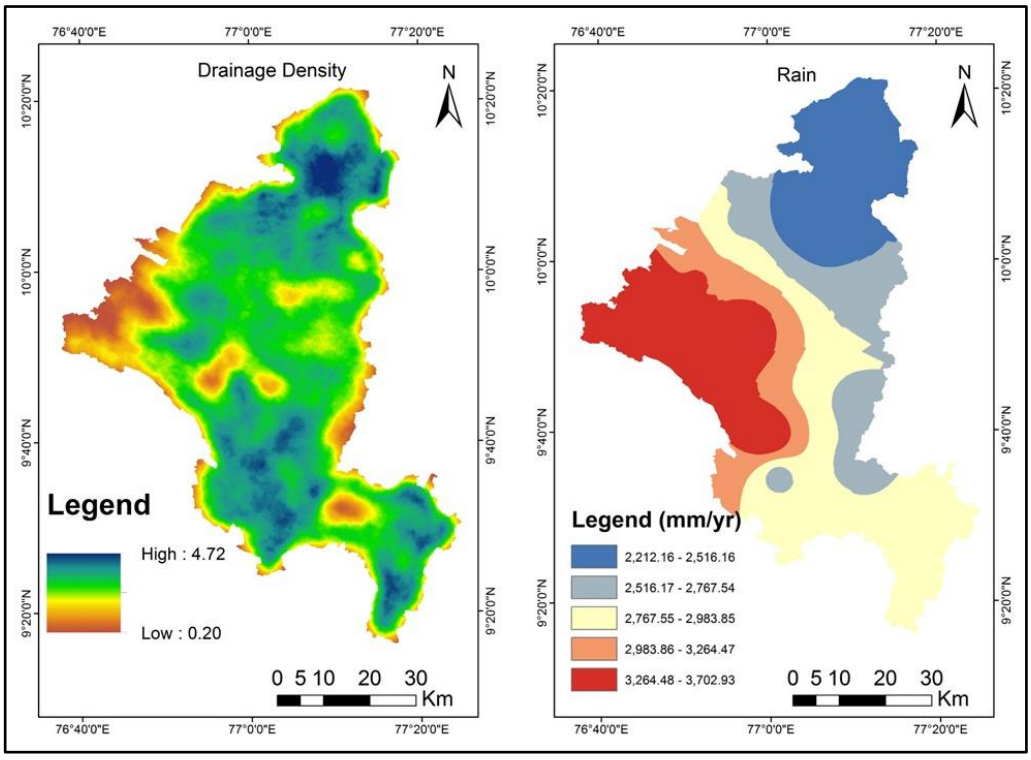

Figure 5.12 : (a) Drainage Density (b) Rain

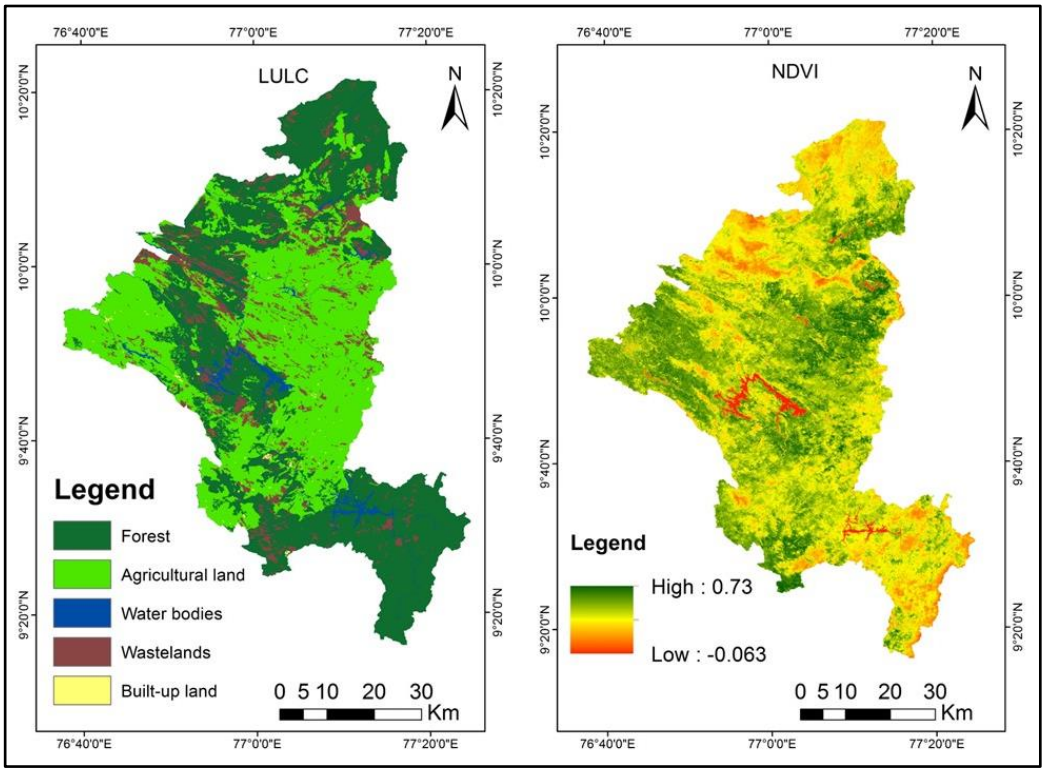

Figure 5.13 : (a) Land Use & Land Cover (b) NDVI

Elevation (Figure 5.7(a)) information obtained from the DEM data (SRTM 30m resolution) is one of the potential indicators of groundwater level and it plays a vital role as many other data products like slope, curvature, and TRI are derived from it (Oh et al., 2011; Naghibi et al., 2016). The slope as shown in Figure 5.7(b), which is characterised to be the upward or downward incline of a surface, symbolises the assemblages of the terrain. Compared to a region with a low slope, a high slope region offers poorer prospects for groundwater since it experiences greater erosion and less infiltration. The Idukki district has a slope that can reach 74.8 degrees, with most of the area having moderate to high slopes (Suresh et al., 2018; Jesudasan 2022).

The curvature of the topography (Figure *5.8* (a)) regulates the surface and subsurface hydrology. The maximum slope in a perpendicular direction is defined by the plan curvature reported in this study. The negative and positive values, respectively, represent the convergence and divergence in the water flow that are described (Prasad et al., 2020). The topographic roughness index (TRI) as shown in Figure *5.8* (b), which reflects the amount of difference in values of elevation between the adjacent cells of the DEM, has been used to calculate the roughness of the terrain. It gives topographic heterogeneity a precise, objective measurement (Riley et al., 1999; Jesudasan and Saravanan 2022).

Linear elements of a landscape that express the underlying geological structures are called lineaments. Given their high porosity and hydraulic conductivity, lineaments are seen as boon in the cases of groundwater potential. These linear features are easily extractable from the satellite and aerial imagery (Suresh et al., 2018). Landsat ETM+ and PAN data were utilised to delineate the lineaments and the lineament density map as shown in Figure *5.9* (a) was generated in the ArcGIS environment. The soil as shown in Figure *5.9* (b) type also plays a vital role in GWP due to its porosity and infiltration capacity. The Idukki region consists of thick or weathered rock and generally they are classified into clay, loam and gravelly clay.

The bedrock characteristics are explained by the local geology as shown in Figure *5.10* (a). Pore water pressure is influenced by the impact of water on the bedrock and its interaction with the landmass, which in turn affects infiltration and GWP. The geological types found in the Idukki district include granite, charnockites, khondalite, migmatite gneiss complex, and peninsular gneiss (Jesudasan and Saravanan 2022).

The geomorphology as shown in Figure *5.10* (b) of the area is influenced by the interaction of the geology, hydrology, and biological phenomena (Ramasamy et al., 2020). Eight geomorphological formations, including highly, moderately, and low dissected structural hills and valleys, highly, moderately, and low dissected denudational hills and valleys, pediment pediplain complex, and water bodies, have been identified in the Idukki district.

The topographic wetness index (TWI) as shown in Figure *5.11* (a) quantifies the influence of topography on hydrologic processes and is correlated with the local soil type.

The catchment evolution erosion theory and the transport capacity restricting sediment flux are considered to generate the sediment transport index (STI) (Figure *5.11* (b)), which describes the erosion and deposition process (Yilmaz 2010; Conforti et al., 2014; Chen et al., 2018a).

In stream-eroded topography, drainage density (DD) as depicted in Figure *5.12* (a) is a key measure of the linear scale of landform components. Less infiltration occurs at higher drainage densities. This is because a large portion of rainfall turns into runoff. The Idukki district experiences extremely high annual rainfall of roughly 3700 mm, and because the area has steep slopes, runoff frequently causes flooding. As a result,

there is high drainage density, which lowers GWP. The distribution, duration, and intensity of rainfall (Figure *5.12* (b)) all play a significant role in determining infiltration, runoff, and recharge conditions. Runoff and infiltration in the area are greatly influenced by short lived rainstorms and longer periods of intermittent rainfall. Soil erosion occurs during these flooded conditions as a result of the terrain's low void ratio. This adversely influences the groundwater potential of the region. The Indian Meteorological Department's yearly rainfall data was acquired, and the rainfall intensity map was produced by interpolation. Rainfall intensity in the Idukki district ranges from 2212 to 3703 mm.

An essential influencing factor for the evaluation of groundwater potential that considers the regional circumstances and anthropogenic activities in the area is a land use map. The land use map of Idukki district was divided into five classes (Figure *5.13* (a)) viz., forest, agricultural land, waterbodies, wastelands and built-up lands. Built-up land increases runoff, which lowers the ground's ability to recharge. Likewise, deforestation also reduces penetration of water into the soil, and promotes runoff. Thus, the need for identifying the vegetation cover is essential in the analysis of GWP. The Normalised Differential Vegetation Index (NDVI) as illustrated in Figure *5.13* (b) was thus included as one of the conditioning factors.

All fourteen thematic layers generated for delineating groundwater potential zones were subsequently incorporated as input variables in the machine learning modelling framework. These layers served as the fundamental predictors for the Random Forest, AdaBoost, and Gradient Boost algorithms, enabling a comprehensive and data-driven assessment of groundwater potential across the Idukki District.

5.1.3 Spatial Data Preparation for LULC Change

To investigate the relationship between precipitation, flooding behaviour, and land use & land cover dynamics, a long term rainfall dataset was assembled based on daily precipitation records obtained from the Indian Meteorological Department (IMD). The dataset was constructed from measurements collected by 6,955 rain gauge stations distributed across the country and used to generate a spatially gridded precipitation product covering a 123 year period (1901–2023) at a spatial resolution of 0.25° × 0.25°. The large station density and improved interpolation methodology resulted in a significantly enhanced representation of India’s rainfall climatology, particularly in regions characterised by strong orographic influences such as the elevated

precipitation along the windward slopes of the Western Ghats and north–eastern ranges and the markedly lower rainfall observed in the rain-shadow zones lying leeward of these mountain systems.

The rainfall assessment is performed using the gridded rainfall dataset for the Idukki district in order to analyse the temporal and spatial characteristics of precipitation associated with two major flood triggering events in Kerala: the extreme monsoon rainfall of August 2018 and the intense precipitation episode of October 2021. These events, both of which resulted in widespread flooding, were used as hydrometeorological reference points for evaluating rainfall behaviour under extreme climatic stress.

The district scale rainfall patterns corresponding to these flood episodes are depicted in Figure *5.14* and Figure *5.15*. Complementing this temporal assessment, spatial rainfall distribution maps were produced in the ArcMap environment to visualise the distribution of rainfall across Idukki during these events. The GIS derived spatial precipitation maps, presented in Figure *5.16* and Figure *5.17*, reveal the variability in rainfall intensity over contrasting physiographic settings and provide insight into the role of topography in modulating flood inducing rainfall accumulation.

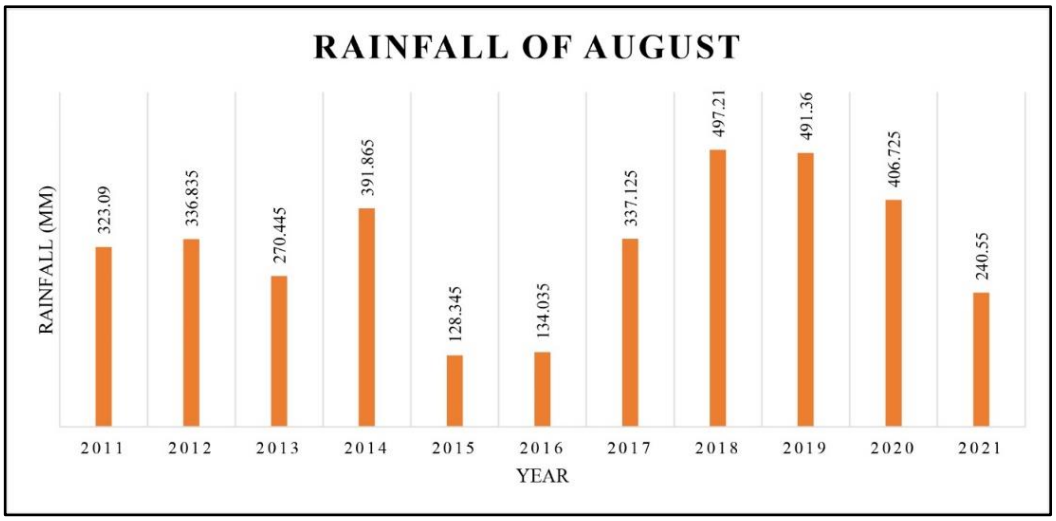

Figure 5.14 : Mean rainfall during August (2011 – 2021)

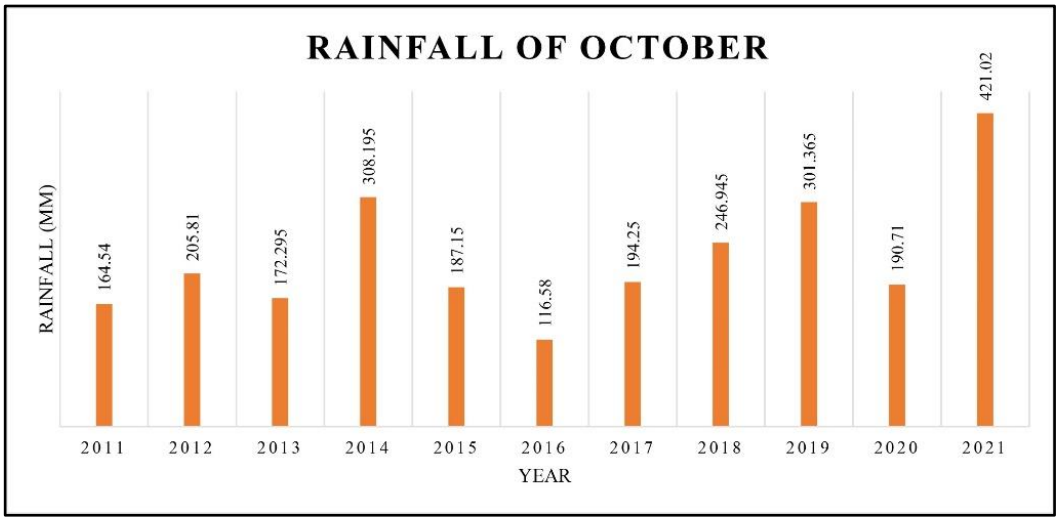

Figure 5.15 : Mean rainfall during October (2011 – 2021)

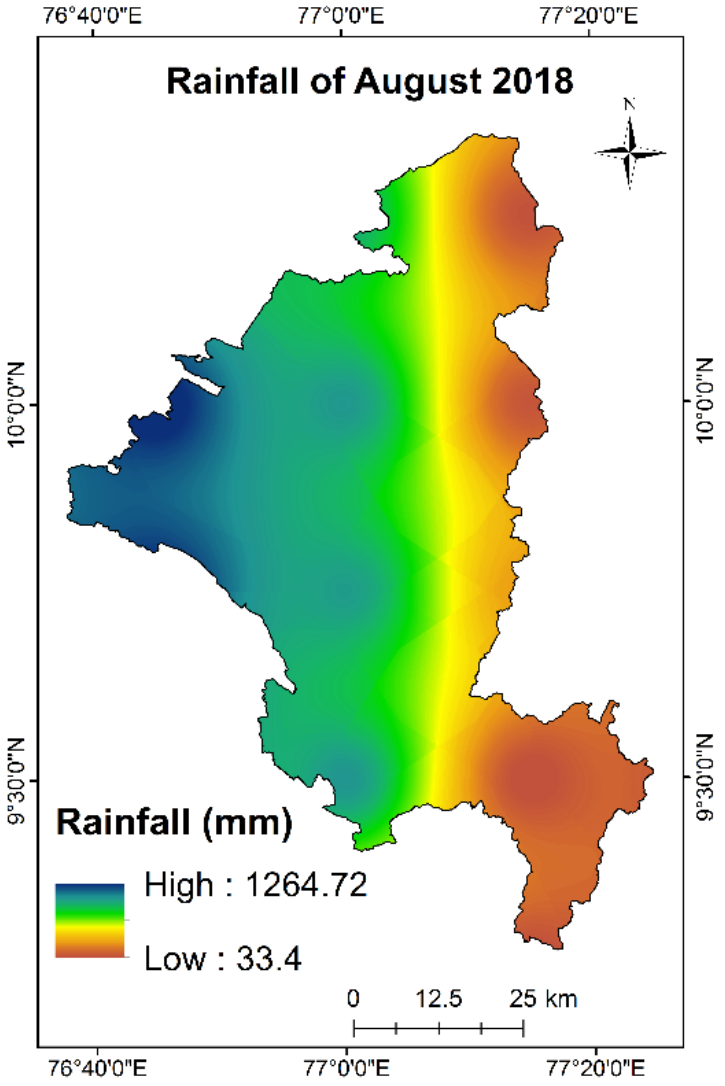

Figure 5.16 : Spatial distribution of rainfall during August 2018

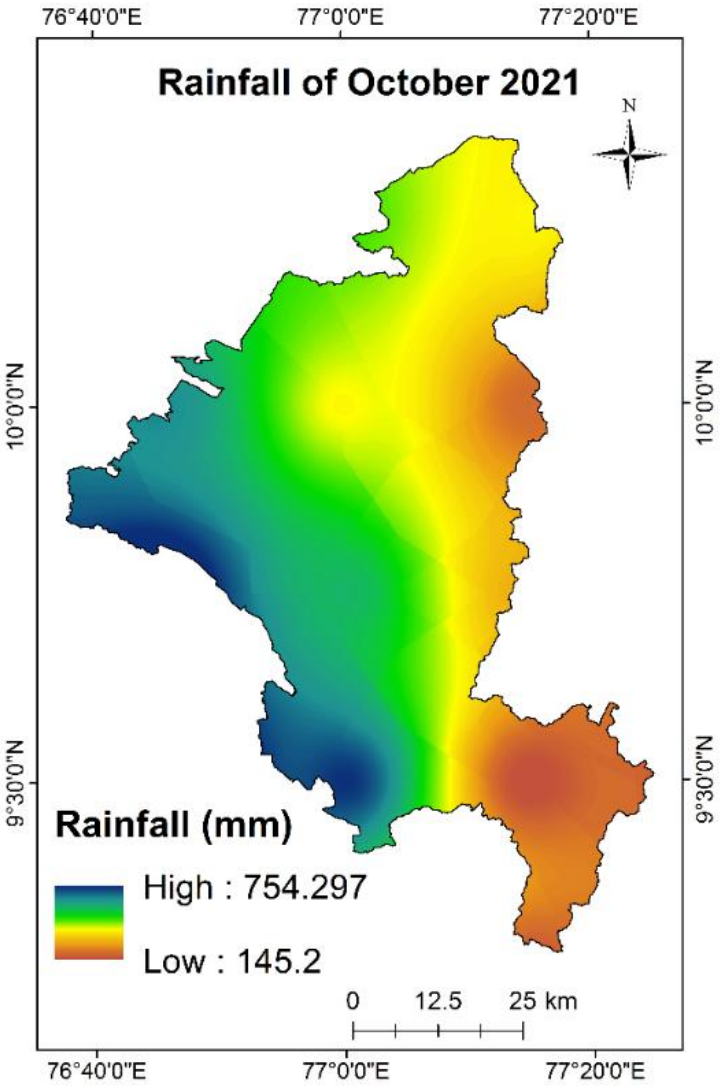

Figure 5.17 : Spatial distribution of rainfall during October 2021

To quantify the influence of flood events on landscape conditions, land use and land cover (LULC) maps were generated utilizing multispectral imagery from the LANDSAT 8 data. Satellite data were processed and classified within the Google Earth Engine (GEE) computational platform, wherein a supervised classification procedure was implemented to differentiate key land cover categories. Separate classifications were executed for pre-flood and post-flood temporal snapshots corresponding to the 2018 and 2021 flood events, enabling a comparative analysis of land cover transitions.

5.1.4 Spatial Inputs for Runoff Modelling

The final component of the research focused on evaluating how sustained heavy rainfall and resulting flood conditions influenced surface runoff dynamics within the Periyar River Basin, the largest hydrological catchment within the Idukki District of Kerala. Understanding runoff generation under extreme precipitation is particularly

critical in this basin, given its steep topographic gradients, dense drainage network, and sensitivity to monsoon driven hydrological extremes.

To support this analysis, multiple datasets representing topographic, land surface, soil, and atmospheric controls on runoff were integrated. The Digital Elevation Model (DEM) provided the foundational terrain morphology from which slope, flow direction, and hydrological connectivity were derived. The slope map, along with the LULC classification, enabled assessment of how vegetation cover, built up surfaces, bare land, and water bodies influenced infiltration and overland flow behaviour. Soil data contributed essential information regarding infiltration capacity, porosity, and moisture retention characteristics.

These spatial parameters were supplemented with climatic inputs including daily rainfall values, maximum and minimum temperature, wind speed, humidity and solar radiation.

5.2 Delineation of Flood Prone Zones in Idukki District

This section presents the outcomes of delineating flood-prone zones in Idukki District, Kerala, using a GIS-based Analytic Hierarchy Process (AHP) approach. The flood susceptibility analysis integrates 12 flood conditioning parameters, each selected for its demonstrated influence on runoff behaviour, terrain instability, and hydrological response.

The results of the flood susceptibility mapping are presented in the subsequent section, highlighting the spatial distribution of flood risk zones across the district. This is followed by a brief validation assessment to evaluate the reliability and predictive performance of the generated flood map. Together, these components offer a comprehensive understanding of the model outputs and their relevance for flood risk planning in Idukki.

5.2.1 Flood Susceptibility Map

All the thematic layers of twelve flood conditioning factors are prepared in GIS interface as shown in Figure *5.1* to Figure *5.6* . After preparation of all the thematic layers, relative weights are given to all the flood conditioning parameters, and a comparison matrix is made as shown in Table 5.1.

Table 5.1 Each parameter's comparison matrix and relative score

Parameters	Rainfall	Elevation	DFR	TWI	Slope	TRI	SPI	STI	LULC	Geology	Aspect	Soil
Rainfall	1.00	4.00	5.00	4.00	3.00	3.00	4.50	6.50	7.00	6.50	8.50	8.50
Elevation	0.25	1.00	3.00	2.00	3.00	2.50	3.00	4.00	5.00	4.00	7.50	7.00
DFR	0.20	0.33	1.00	5.00	4.50	3.00	2.00	3.50	5.00	3.50	5.50	7.00
TWI	0.25	0.50	0.20	1.00	4.00	2.00	3.00	3.00	3.50	4.50	4.00	5.50
Slope	0.33	0.33	0.22	0.25	1.00	4.00	3.50	4.00	3.50	3.50	4.50	5.00
TRI	0.33	0.40	0.33	0.50	0.25	1.00	2.00	3.00	2.00	2.50	4.00	3.00
SPI	0.22	0.33	0.50	0.33	0.25	0.50	1.00	5.00	2.50	2.00	3.00	3.50
STI	0.15	0.25	0.29	0.33	0.25	0.33	0.20	1.00	3.00	3.00	2.00	2.50
LULC	0.14	0.20	0.20	0.29	0.29	0.50	0.40	0.33	1.00	2.00	2.00	4.00
Geology	0.15	0.25	0.29	0.22	0.29	0.40	0.50	0.33	0.50	1.00	2.00	3.00
Aspect	0.12	0.13	0.18	0.25	0.22	0.25	0.33	0.50	0.50	0.50	1.00	2.00
Soil	0.12	0.14	0.14	0.18	0.20	0.33	0.29	0.40	0.25	0.33	0.50	1.00
Sum	3.27	7.88	11.35	14.36	17.24	17.82	20.72	31.57	33.75	33.33	44.50	52.00

The consistent weights are then calculated for every parameter in the standard pairwise comparison matrix. Since a lot of parameters are utilized for preparing a flood susceptibility map, consistency check is of utmost importance to ensure that weightages given to parameters are consistent with each other. The weights were assigned based on each variable's influence on flooding. Rainfall received the highest weight as the main trigger of floods, while distance from river (DFR) and TWI were given higher importance as they indicate flood-prone and water accumulation zones.

The consistency check for all the flood conditioning parameters is evaluated, where consistency ratio is found to be 0.09706. For maintaining consistency between parameters, consistency ratio must be less than 10%, and hence weightage given to every flood conditioning parameter is consistent with one another. AHP derived weights were assigned to all the thematic layers namely rainfall, elevation, distance

from river, TWI, Slope, TRI, SPI, STI, LULC, geology, Aspect and soil is 0.25, 0.15, 0.14, 0.10, 0.10, 0.06, 0.06, 0.04, 0.03, 0.03, 0.03 and 0.02 respectively. This weightage values are further multiplied with all the classes and ranks to determine the effect of each parameter as shown in Table 5.2. The weighted layers were then integrated to develop the final flood susceptibility map, illustrated in Figure 5.18.

Table 5.2 Sub-criteria of each parameter and their weights

Parameter	Factor	Weight	Rank	Overall weight
Elevation	0 – 435.2	0.15	5	0.75
	435.2 – 970.4		4	0.60
	970.4 – 1505.6		3	0.45
	1505.6 – 2040.8		2	0.30
	2040.8 - 2576		1	0.15
Slope	0 – 8.8	0.10	5	0.50
	8.8 – 16.4		4	0.40
	16.4 – 24		3	0.30
	24 – 32.8		2	0.20
	32.8 – 74.8		1	0.10
Distance from River	<100	0.14	5	0.70
	100 – 200		4	0.64
	200 – 300		3	0.42
	300 – 400		2	0.28
	>400		1	0.14
LULC	Built Up	0.03	5	0.15
	Agricultural Land		4	0.12
	Water Body		2	0.06
	Waste Land		3	0.09
	Forest		1	0.03
Geology	Biotite Gneiss	0.03	2	0.06
	Calc Granulite		3	0.09
	Charnockite		5	0.15
	Granite		5	0.15
	Granite Gneiss		4	0.12
	Hornblende- Biotite gneiss		2	0.06
	Quartz vein and Pegmatite		4	0.12
Soil	Clayey	0.02	5	0.10
	Loam		4	0.08
	Gravelly Clay		3	0.06
TWI	-1.31 - 1.88	0.10	1	0.01
	1.89 - 3.51		2	0.02
	3.52 - 5.96		3	0.03
	5.97 - 9.64		4	0.04
	9.65 - 19.44		5	0.05
Rainfall	2212.16 – 2516.16	0.25	1	0.25
	2516.16 – 2767.54		2	0.50

	2767.54 – 2983.85		3	0.75
	2983.85 – 3264.46		4	1.00
	3264.46 – 3702.92		5	1.25
	0.11 - 0.25		1	0.06
	0.25 – 0.41		2	0.12
	0.41 – 0.49		3	0.18
	0.49 – 0.58		4	0.24
TRI	0.58 – 0.89	0.06	5	0.30
	Flat		3	0.09
	North		4	0.12
	Northeast		2	0.06
	East		1	0.03
	Southeast		2	0.06
	South		4	0.12
	Southwest		5	0.15
	West		5	0.15
	Northwest		5	0.15
Aspect	North	0.03	4	0.12
	-7.42 - -5.36		1	0.06
	-5.36 - - 2.46		2	0.12
	-2.46 - -0.62		3	0.18
	-0.62 - 2.19		4	0.24
SPI	2.19 -12.04	0.06	5	0.30
	0 – 56.6		1	0.04
	56.6 – 311.4		2	0.08
	311.4 – 849.4		3	0.12
	849.4 – 1840.4		4	0.16
STI	1840.4 – 3610.1	0.04	5	0.20

The final flood susceptibility classes are ranged from 0.25 to 0.02 and it was classified using natural break classification into five categories namely very low, low, moderate, high, and very high and these classes occupied the areas of 609.0417 km^2, 1222.83 km^2, 1180.45 km^2, 950.48 km^2 and 395.9487 km^2 respectively (Table 5.3). More than 30% of the Idukki region is covered with high and very high flood susceptible zones as shown in Figure 5.18. These very high and high flood risk zones were derived from the areas of low elevation region, low slope area (less than 10°, distance from the river less than 100 m, highest topographic wetness index region (>15), very high rainfall region (~3700 mm), highest stream power and sediment transport index region and finally hard rock terrain and low permeability soil type region. Figure 5.18 displays the flood susceptibility map of the current study area. The very high and high flood prone regions are occupied in NW, Central and SE region of the study area.

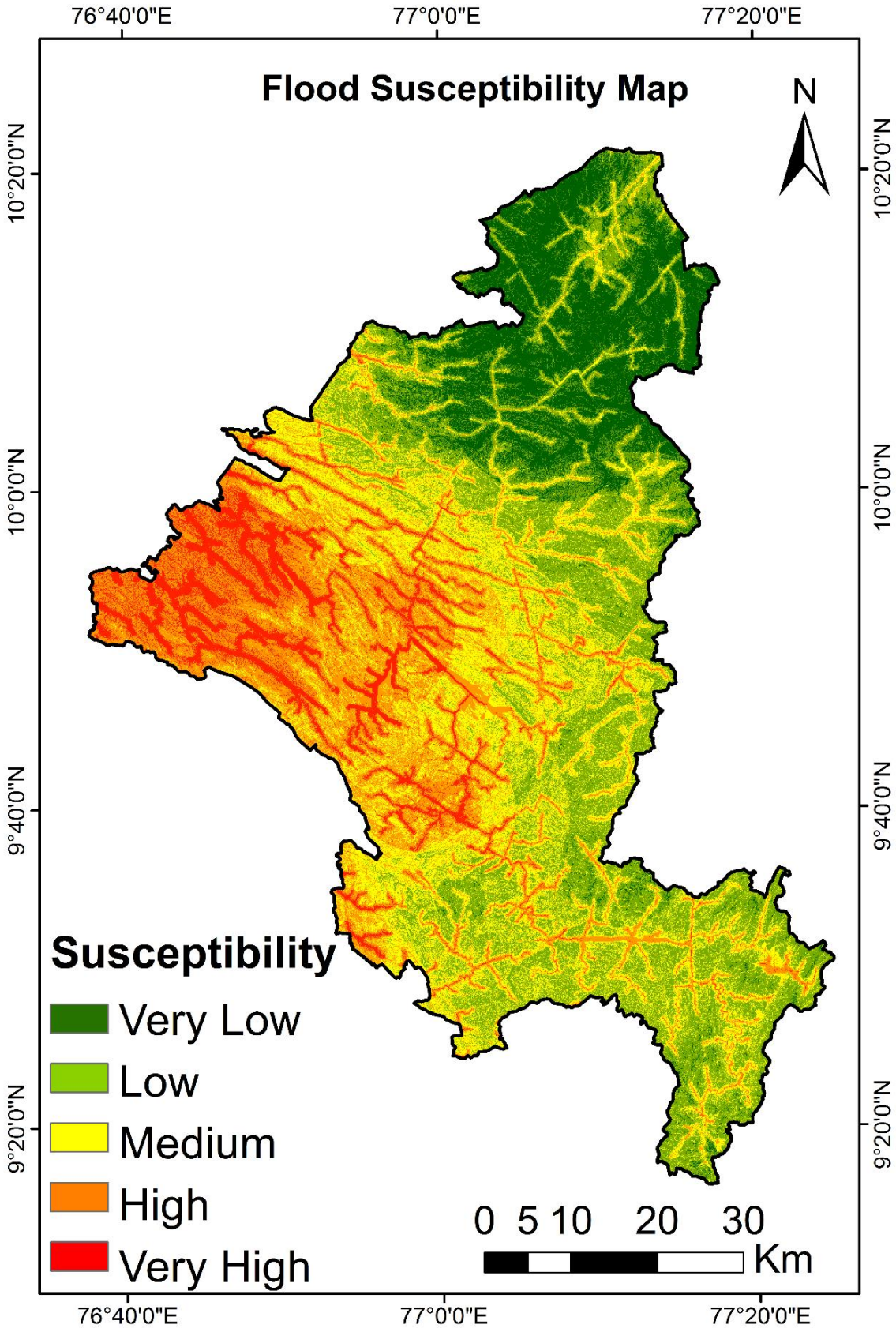

Figure 5.18 : Resultant Flood Susceptibility Map of Idukki District

From flood susceptibility map shown in Figure 5.18, it is worthwhile to note that more than 30% of the area (1346.4 km^2) falls in the category of very high to high flood prone zones (Table 5.3). Therefore, it becomes very important to assess the impact of these very high flood risk zones at subdivisional levels of Idukki.

Table 5.3 Area Distribution of Flood Prone Zones in the Idukki District

S.No.	Flood Prone Zones	Area (Km^2)
1.	Very Low	609.0417
2.	Low	1222.8336
3.	Moderate	1180.4571
4.	High	950.4855
5.	Very High	395.9487

5.2.2 Flood Susceptibility Across Idukki Subdivisions

There are five taluks or subdivision in Idukki namely Devikulam, Udumbanchola, Idukki, Peerumade and Thodupuzha as marked in Figure 5.19 which categorizes the flood prone zones for every taluk separately. The developed flood susceptible map indicates that majority of the Thodupuzha town falls under very high flood prone zones. This is due to the reason that Thodupuzha lies in areas of lower elevation, low slope and high rainfall as seen from Figure *5.1* (a), Figure *5.2* (a) and Figure *5.6* (b). The distance from river as shown in Figure *5.5* (a) also reveals that Thodupuzha and Idukki have dense stream networks and major river flow through these districts, which become the paramount reason for having high likelihood of flooding in these towns. During Kerala floods of 2018, among all the towns, Thodupuzha and Idukki were the worst affected. Seventeen villages constitute the Thodupuzha taluk or subdivision, which shows that people in these villages are at a very high risk of flooding and substantial damage due to floods in future could occur in these areas. Furthermore, majority of the Idukki subdivision falls under high to very high flood prone zones. It is due to the presence of Idukki dam and large number of tributaries of Periyar river. During the Kerala floods of August 2018, all the five gates of the dam were opened by the authorities after 26 years which caused massive outflow of six lakh litres per second along the Periyar river and its tributaries. Due to this reason, Periyar river and its tributaries flows under spate condition which leads to flooding of the river banks causing damage to the people residing in these areas. Nine villages constitute the

Idukki town and is home to a lot many people, therefore inhabitants residing in these villages are at very high risk of flood related natural hazards. Peermade subdivision which is situated in the south east region of Idukki falls under moderate to high flood prone regions as depicted in the developed flood susceptibility map Figure 5.18 and Figure 5.19. This region generally receives considerable amount of rainfall in the monsoon season.

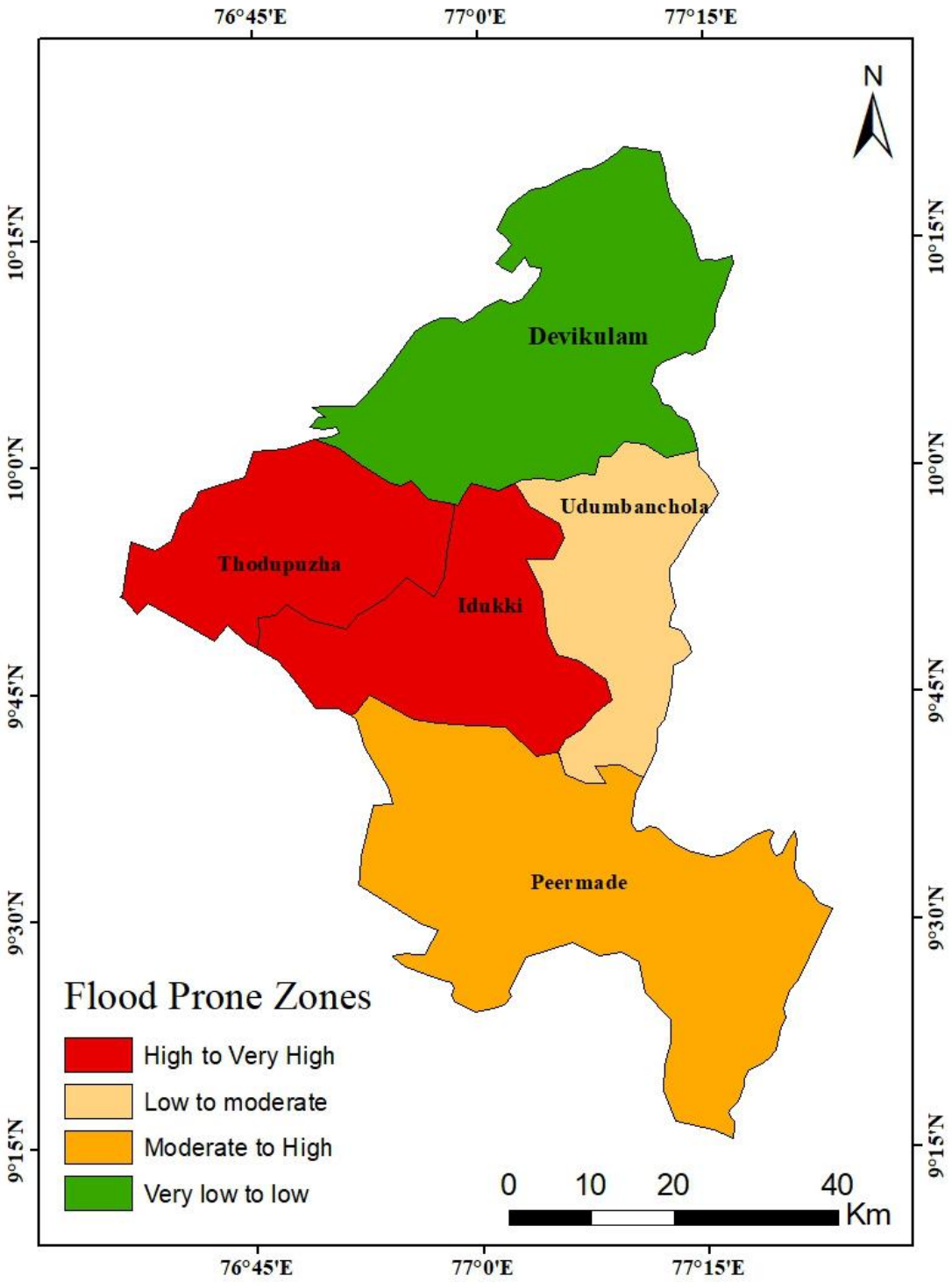

Figure 5.19 : Categories of Flood Prone Zones in Subdivisions of Idukki

During the Kerala floods of 2018 and 2021, this region has received rainfall in the range of 300 – 350 mm per day and some portion falls under low lying areas, therefore the majority of the region falls under moderate to high zones of flooding. Udumbanchola falls under low to moderate flood prone zones as the region has dense stream network, high TWI values and low rainfall. From flood susceptibility map, it is clearly depicted that Devikulam taluk falls under low to very low flood prone zones because of higher elevation values, smaller number of streams, low TWI values and comparatively less rainfall among other subdivisions. The flood prone zones in various subdivisions of Idukki, along with the taluks of maximum flood prone regions and least flood prone areas, are shown in Figure 5.19. The process involves partitioning the vast majority of susceptible areas into distinct subcategories based on Taluks. This measure is implemented with the aim of decreasing the affected population in that particular locality in the event of a disaster.

5.2.3 Parameter-Wise Impact Analysis on Flood Susceptibility

The detailed impact of all the twelve flood conditioning factors on flood susceptibility map are also discussed below:

Impact of Elevation: It largely influences floods in a region as low lying areas are most likely to get affected with floods. As shown in flood susceptibility map (Figure 5.18), it clearly indicates that subdivisions such as Thodupuzha, and Idukki are situated on comparatively lower elevation comes under high to very high-risk zones in flood susceptibility mapping (Xu et al., 2021).

Impact of Slope: Another factor which largely influences and controls the flood is slope. In regions of higher slope, runoff flows with a high velocity and chances of water infiltrating through soil becomes very less and hence water gets stagnated in areas with small or flat slopes. This is evident as western and central regions of Idukki has low slope and hence it is categorized in the areas of very high flood susceptibility (Figure 5.18). Though regions in the north of Idukki have comparatively higher slope, yet we still see medium flood risk in flood susceptibility map. This is due to the presence of large number of streams such as Pembar, Edamalaya and Muthirapuzha river which overflows in events of heavy rainfall and hence makes a region prone to flooding.

Impact of TRI: Higher TRI, indicates steep and rugged regions whereas lower TRI indicates flatter areas. As Idukki is situated in a mountainous areas factor such as TRI in conjunction with slope assists in accurate assessment of flood mapping.

Impact of TWI: Topographic Wetness Index is an indicator of depth of surface and subsoil layers. Higher TWI indicates the presence of higher order streams while lower values give an idea of ridge lines (Pourali et al., 2016). In the Flood Susceptibility map, higher values of TWI can be seen in the subdivision of Thodupuzha and Peerumade and hence these regions fall in the category of high to very high flood prone zones.

Impact of SPI: It is a measure of the erosive power of surface runoff. It is a measure of flowing water to perform geomorphic task. Geomorphic task in relation with flood susceptibility studies would involve occurrence of weathering, deposition, and erosion process over a land surface to assess their effects during events of heavy rainfall and flooding. Higher values of SPI can be seen in the Northern regions of Idukki which implies large erosion and heavy flowing water. This is because of mountainous regions, where water flows with a high velocity and causes erosion near the river bank. Resulting flood susceptibility map reveals that low to medium risk flood zones are present in this area.

Impact of STI: Sediment Transport Index indicates the process of erosion and deposition. It is indictive of the effect of topography on soil loss. Higher STI values represents the higher mobility of sediments while the lower values indicate the accumulation of sediments. It is employed to characterize the erosive potential of the terrain and responsible for the occurrence of changes in the channel bed geometry due to sediment deposition. Higher values of STI are found in the streams present in the Idukki district due to heavy flowing water which is helps in sediment deposition near the streams. Moreover, the flood susceptibility map also depicts very high risk of flooding in or near the streams. Therefore, STI develops a direct relation with the flood risk map. Lower STI values are present in the Idukki reservoir and Periyar lake, which is in sync with the flood susceptibility map. (Nones (2019); Siam et al., 2022).

Impact of LULC: LULC has identified 5 major classes to quantify the effect of land use and land cover on floods. The capability of land cover types to either absorb rainfall or facilitate its infiltration into the soil varies. The presence of natural vegetation, such as forests or grasslands, has the potential to intercept rainfall and promote infiltration, thereby mitigating the volume of surface runoff. Conversely,

urban regions or impermeable surfaces exhibit restricted infiltration potential, thereby leading to escalated surface runoff and expedited water flow towards streams and rivers, thereby augmenting the likelihood of inundation. Rough terrain, such as that found in wooded areas or open grasslands, can impede the velocity of water flow, thereby facilitating its infiltration or retention within the topography. Conversely, surfaces that are devoid of roughness such as roads tend to accelerate the flow of water, resulting in increased quantities of runoff and the possibility of inundation. The cutting down of forests or vegetation cover results in the disturbance of the natural equilibrium of water absorption and interception. The process of deforestation has been observed to have a negative impact on the hydrological cycle, as it leads to a reduction in the amount of rainfall that is intercepted by trees. Additionally, deforestation has been found to increase surface runoff and decrease infiltration capacity. In addition, in the absence of tree roots that provide soil anchorage, the likelihood of soil erosion is heightened. The erosion of soil has the potential to impede the flow of water in rivers, streams, and drainage systems, thereby intensifying the occurrence of flooding. Presence of barren and fallow lands, small streams of river and urbanization in the north of Idukki, increases the chances of floods in the region and the flood map suggests that the western region of Idukki which constitutes high settlements are under high flood prone areas.

Impact of Distance from River: This parameter plays an important role in assessing flood prone zones because Periyar river flows in Idukki district which is considered to have the largest discharge potential in Kerala. Because of very less distance from river and dense drainage networks western, central regions of Idukki are under very high flood risk categories in the final flood susceptibility map (Figure 5.18).

Impact of Soil: This parameter explains the reason of frequent floods in Idukki experienced in the past. As indicated in the soil map most of the study region is covered with clayey and loam soil, which has extremely low rates of permeability due to which water is unable to infiltrate into the ground and hence majority of the water flows as surface runoff which further increases the chances of flooding.

Impact of Geology: This parameter indirectly controls the water infiltration rates. Approximately 50% of the region is covered with Charnockite rock, while other major rocks in region are Biotite Gneiss and Granite Gneiss. Charnockite is a type of metamorphic rock which is an impermeable rock. Similarly, biotite gneiss and granite

gneiss rocks belong to the family of metamorphic rocks and hence are treated as impermeable rocks. Because these rocks are impervious, some parts of the Idukki district face high to very high flood risk.

Impact of Rainfall: Rainfall plays a major part in production of flood susceptibility maps. From the rainfall map, it is clearly depicted that Idukki and Thodupuzha received highest annual rainfalls and hence both regions are under very high flood prone zones. Higher magnitude of rainfall results in more surface runoff and hence increases the chances of flooding in a region.

Impact of Aspect: Factor such as aspect determines the path of floods in flood susceptibility mapping. Aspect map is created from the DEM and further classified into 10 classes. With this map, direction of flow of water is determined which further assists in production of flood susceptibility map accurately in the Idukki district.

5.2.4 Sensitivity Analysis

Sensitivity analysis was carried out to identify the parameters that exert the strongest influence on the generation of the flood susceptibility map. This approach examines how variations in individual input factors affect the model outputs, thereby providing insight into the responsiveness of the system to changes in its controlling variables. Such analyses are widely applied in decision-making frameworks to assess the robustness and reliability of modelling results. The primary objective of sensitivity analysis is to understand how interactions among input parameters influence the final output of a model or system. The results of this analysis help in recognizing the variables that play a dominant role in controlling model behaviour. Such insights support efficient allocation of resources during data collection, allow greater emphasis on influential parameters, and contribute to improved and informed decision making processes. Additionally, it has the potential to offer valuable perspectives on the hazards and unpredictability linked to the system under examination. The sensitivity analysis was performed based on the final weights generated through the AHP approach.

According to the sensitivity analysis as shown in Figure 5.20, parameters such as rainfall, elevation, distance from river, slope and TWI are the key contributing variables while aspect, geology, LULC and soil are least important variables among all the flood conditioning parameters.

Adjustments in the weights of these parameters produce noticeable variations in the susceptibility patterns, highlighting their dominant contribution to flood occurrence. At the same time, the overall spatial distribution of flood-prone zones remains reasonably consistent, suggesting that the model output is stable and that the selected variables adequately represent the controlling factors of flooding in the study region.

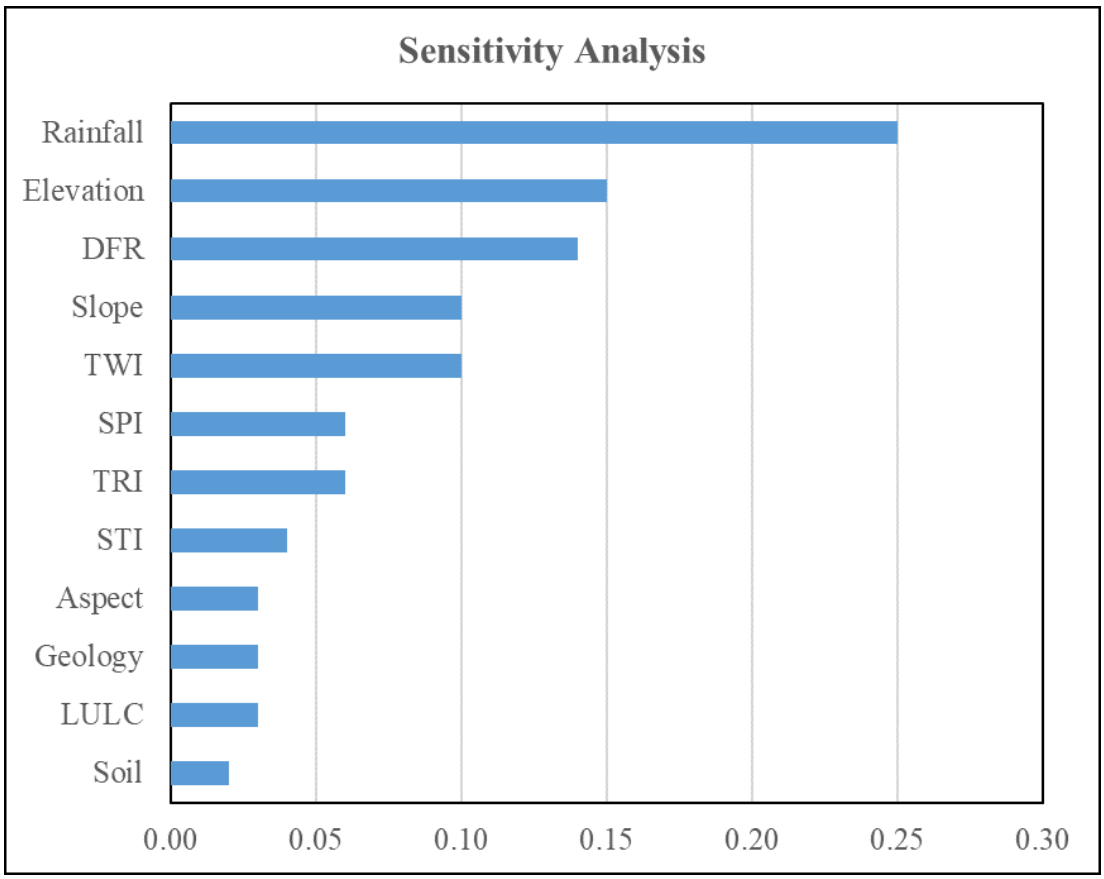

Figure 5.20 : Variable importance of conditioning factors showing the sensitivity of each parameter

For development of flood susceptibility, GIS based AHP approach was employed to assess the flood prone regions in Idukki district and the sensitive parameters that assisted in development of an accurate flood susceptibility map. The efficacy and usage of the AHP model have been confirmed with several works in the domain of flood hazards and risk assessment (Pathan et al., 2022, Liu et al., 2020). Twelve flood conditioning parameters are utilized including topo-hydrological aspects such as TWI, TRI, STI and SPI in the delineation of flood susceptibility map to perform detailed assessment on the different subdivisions or taluks of Idukki. Weighted parameters of different flood conditioning factors were used with the AHP model in GIS platform in a linear way using geo spatial technology. Sensitivity analysis shows

the most influencing parameters responsible for disastrous floods in the district. It is evident that rainfall is the primary factor contributing to flooding. The incidence of flooding can be attributed to the substantial rainfall, which is consistent with the sensitive parameter derived from the AHP model. Elevation is a highly significant parameter in the region, second only to rainfall. This is due to the presence of the Western Ghats, which influences the magnitude of floods by generating runoff from higher terrains. The distance from the stream is identified as a crucial parameter for flood susceptibility, alongside the elevation. The areas adjacent to the streams are typically the first to experience flooding, and these regions are inundated and significantly impacted by the floods, as evidenced in the Idukki region. The areas in close proximity to bodies of water such as streams, rivers, and reservoirs exhibited a higher degree of the susceptibility to flooding.

The slope of a land surface plays a significant role in worsening the inundation process by enhancing the velocity of the water flow. Areas with steep slopes tend to produce floods with high velocity, while areas with gentle slopes are more susceptible to severe flooding, which can have a significant impact on the inhabitants of such terrain. Furthermore, the runoff originating from higher slopes can trigger landslides and transport substantial quantities of sediment to low lying regions, exacerbating the socioeconomic conditions and normal livelihoods of affected communities. The development of TWI holds significant implications in the context of flooding, as it can impede the absorption of water into the ground in areas that have already been saturated with moisture due to precipitation, leading to surface runoff. This phenomenon will result in an amplification of the flood's magnitude. The SPI exhibits a direct correlation with flood events, as it serves as an indicator of the stream's potential energy where the flood velocity is expected to reach its peak during inundation. The TRI, STI, and Aspect parameters are utilized to assess the roughness of the terrain, transport of sediments, and slope direction, respectively, which are indicative of the severity of flooding. The Geology and LULC are subsequent factors in the analysis, as they provide insight into permeability of a rock and the rate of infiltration that induce surface runoff and the land cover that may be significantly impacted during flooding, respectively, and the soil's porosity and permeability, which play a crucial role. The primary factor contributing to the occurrence of floods is excessive rainfall. However, the severity of the flooding is significantly amplified by the topographical characteristics of the area. The relative importance of each sensitive

parameter should be considered by policymakers, as their contributions to flood mapping vary.

5.2.5 Validation of AHP Model

The paramount characteristic of any proposed model is to verify with the reality that can present expressive results and to validate the AHP flood susceptibility mapping, the success rate is required. Historical flood extents were delineated using data obtained from the Survey of India, and pre and post flood sentinel-1 images. For the validation procedure, one SAR image before the actual flood event (17th May 2018) and another SAR image during the flood event (21st August 2018) in VV polarization were acquired. The Sentinel-1 images are subject to erroneous noise, which includes rigorous geometric and radiometric corrections, thermal effects, and speckle. Prior to its application, any satellite data necessitates careful pre-processing. The pre-processing stage involves two key procedures: firstly, the correction of orbital file to eliminate orbital noise; and secondly, the correction of thermal noise to remove noise in the data acquired by sensors during the process of satellite's data collection. The degradation of data quality in regions with low mean signal response detected by the Synthetic Aperture Radar (SAR) system, such as lakes, standing water, and rivers, can be attributed to thermal noise. Radiometric calibration is applied to calibrate radar reflectivity values (DN) into physical backscattering coefficients and is mainly used for comparing SAR images acquired at different times. Terrain correction involves the conversion of Sentinel-1 SLC (Single Look Complex) data from slant range geometry to a map coordinate system and the correction of distortions such as foreshortening, layover, and shadowing effects. Following the pre-processing stage of Sentinel-1 VV SAR images, a speckle filter is implemented to achieve image smoothing for both before and during the flood event as shown in Figure 5.21 and Figure 5.22, respectively. To obtain the flooded region or points, both the SAR images are analysed using the image ratio technique with a threshold value of 1.2. The flooded SAR image is depicted in Figure 5.23, where white colour indicates flooded region and black indicates non flooded areas. The obtained results are in coherence with the previous studies (Jacinth Jennifer et al. 2020; Parthasarathy et al. 2021) and are validated using the maps published by Kerala State Disaster Management Authority (KSDMA 2022). This procedure assisted in acquiring actual historic flood locations of the Idukki district in a raster format. The data is then vectorised and transformed to a polygon, from which random points for both flooded locations and non flooded locations are created

using spatially balanced points in ArcGIS. As the current study also aims for validating the performance and efficiency of the AHP model through AUC-ROC technique (Figure 5.24). For validating the developed flood susceptibility map, the area under the curve-receiver operating characteristics was plotted to validate the flood mapping for AHP model with that of the flooded points. In the AUC-ROC curve, the False positive rate are plotted on the "X" axis and true positive rate are plotted on "Y" axis. Values of AUC-ROC varies from 0 to 1, where 0.50-0.60 indicates poor, 0.61 – 0.7 indicates average, 0.70 – 0.8 indicates good, 0.81 – 0.9 indicates very good and 0.91 – 1 indicates excellent agreement. AUC is useful as it assists in computing the performance of prediction accuracy and ROC is an effective method in assessing the accuracy of the model. The AUC value is evaluated as 0.91 or 91%, which is remarkably good accuracy for the employed spatial mapping model for flood susceptibility studies. This signifies that the adopted methodology approach for flood susceptibility can very well forecast the likelihood that a region will be flooded accurately. It seems that the proposed AHP approach can assist in developing flood susceptible maps for other study areas also as this approach is not dependent upon the scale of the study region.

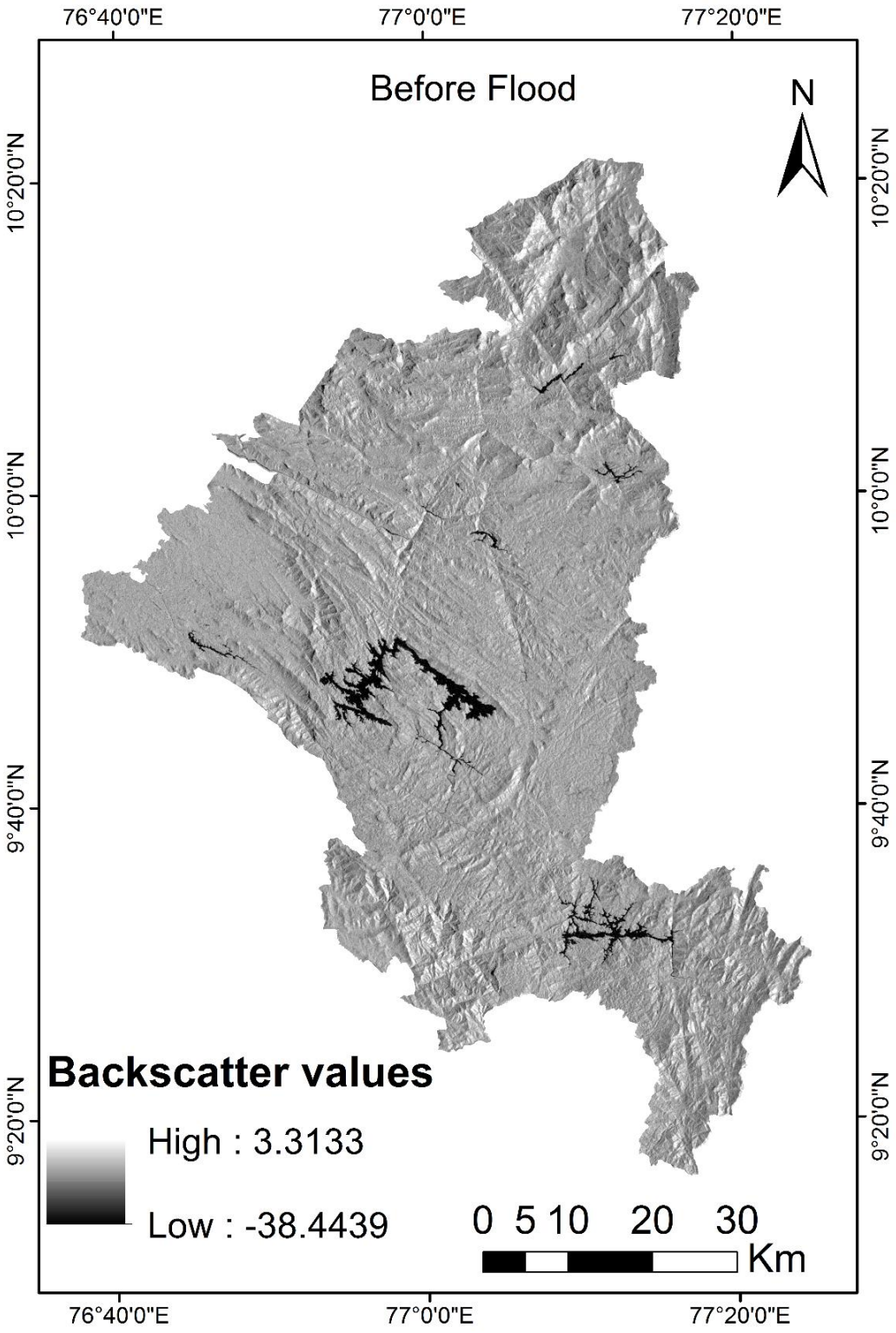

Figure 5.21 : SAR Image before flood event

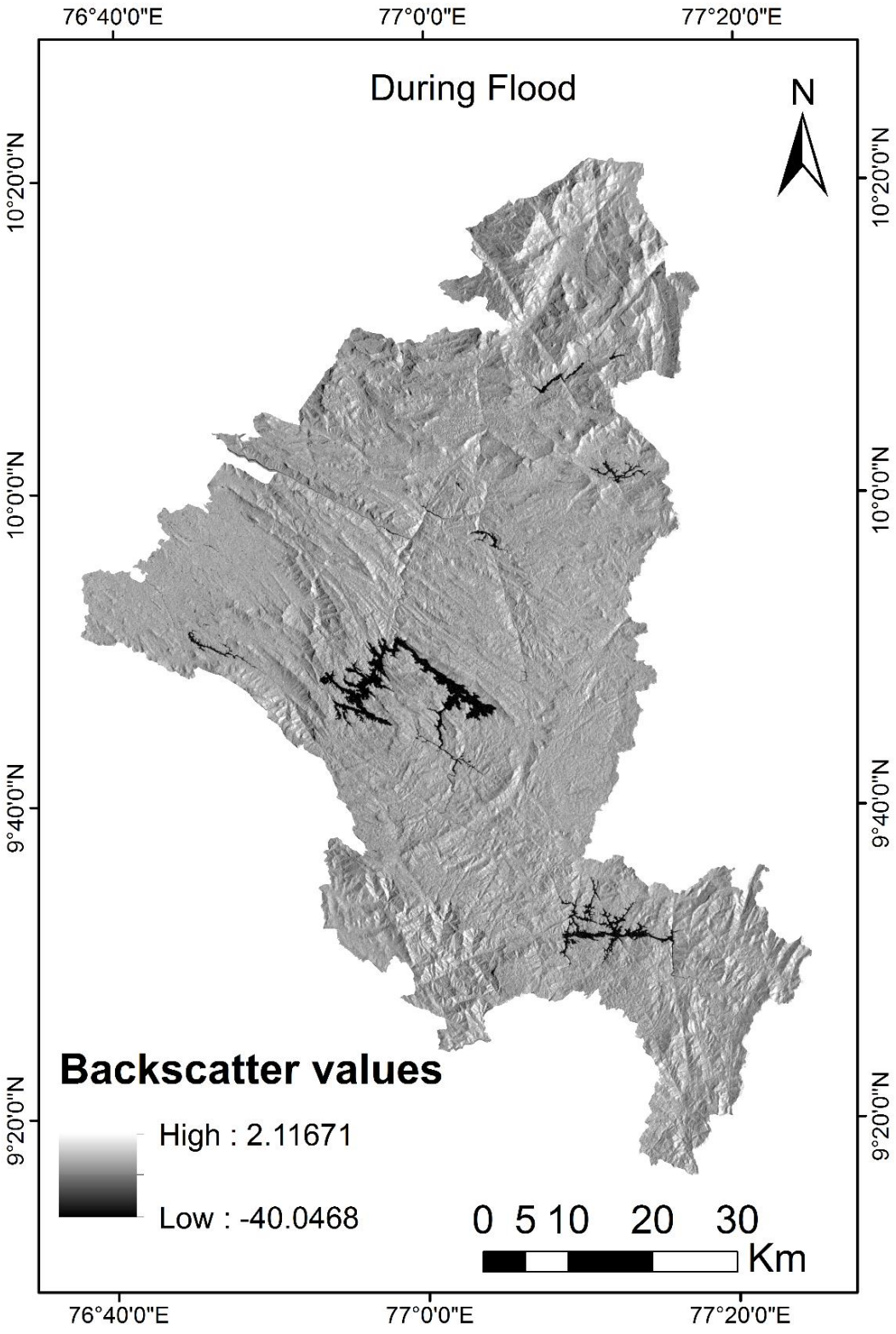

Figure 5.22 : SAR Image during the flood event

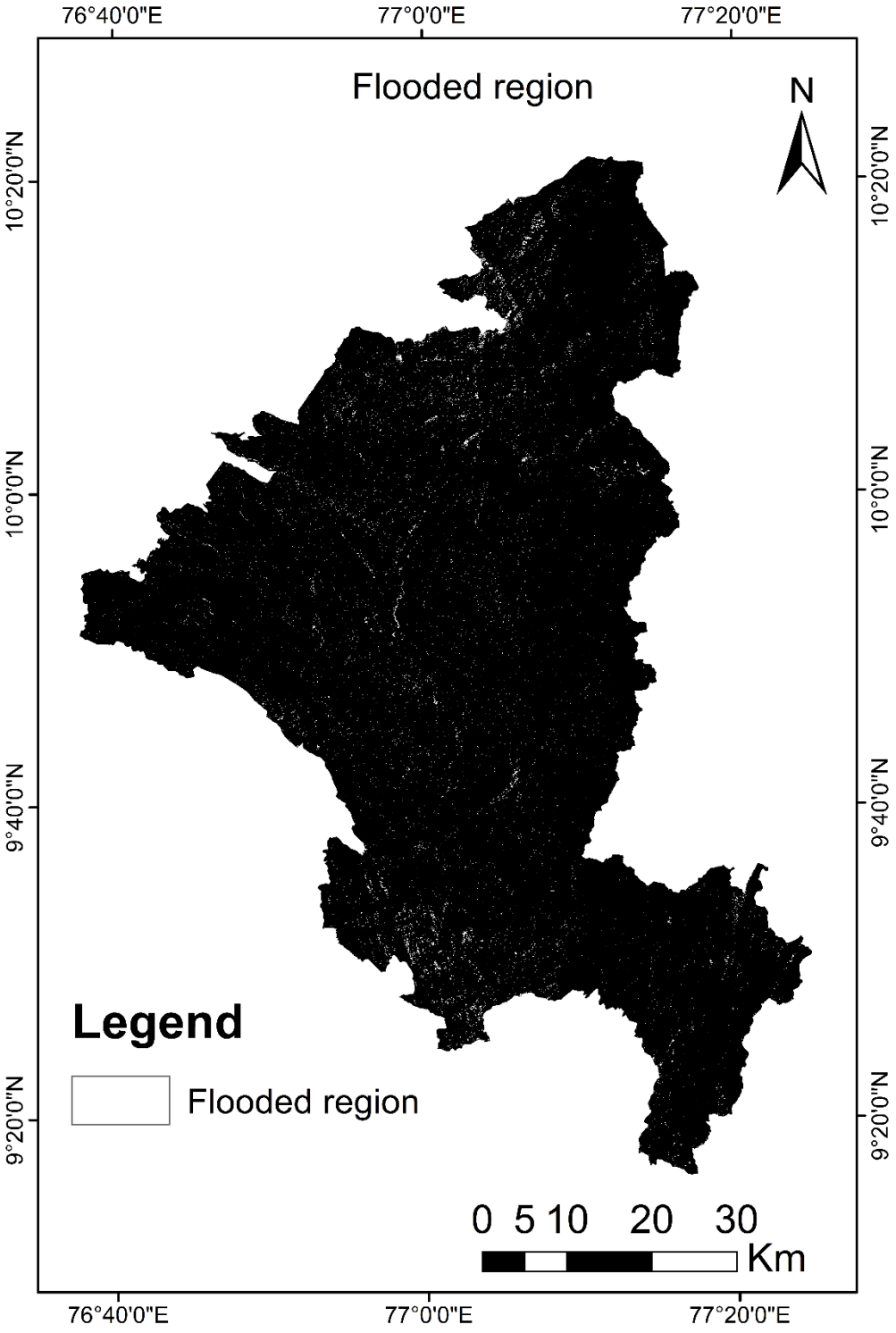

Figure 5.23 : SAR Image of Flooded Region of Idukki district

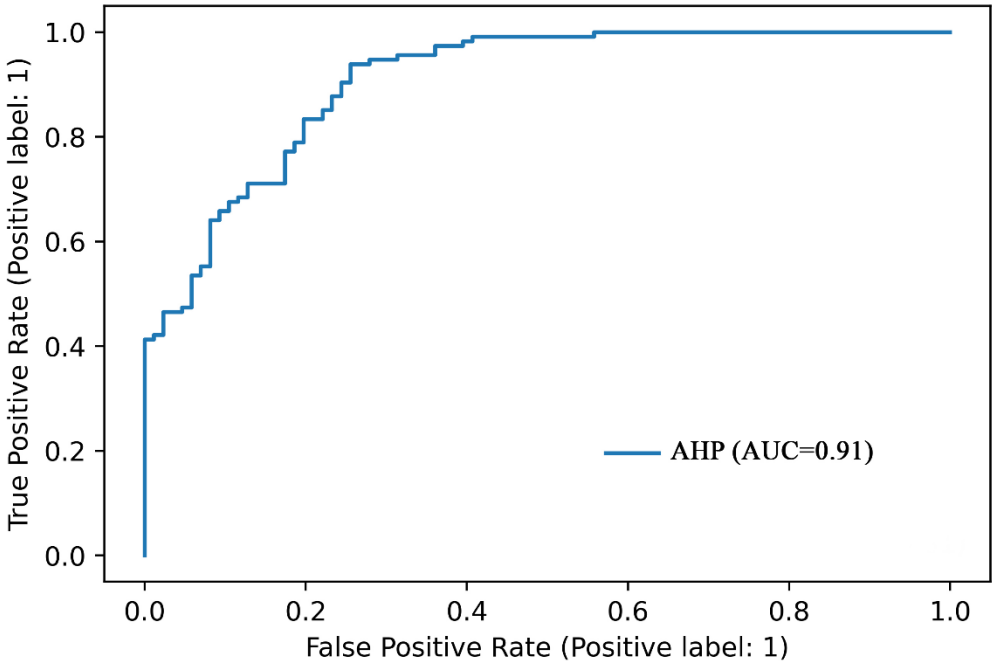

Figure 5.24 : Validation of the Flood susceptibility map using AUC-ROC curve

119 The AHP-based flood susceptibility model successfully delineated the spatial distribution of flood prone zones across the Idukki district. The developed flood susceptibility map reveals that about 1346.4 km^2 (~30% of the total area) was significantly susceptible to floods. These regions are mainly found in the Western, central and southern sections of the Idukki district, where abrupt variations in slope occur and several small tributaries converge with the main river. The accuracy of the AHP model is performed with the help of AUC-ROC approach which indicated an accuracy of 91%.

While the AHP framework provides a transparent and effective multi-criteria evaluation method, its reliance on fixed pairwise comparisons introduces certain limitations, particularly when dealing with large sets of parameters. Nonetheless, the approach proved robust for integrating diverse hydrological, geological, and topographic factors relevant to flood generation in Idukki. The methodology adopted for flood mapping for Idukki district can be effectively applied to formulate flood mitigation and management strategies.

With the spatial extent of flood prone areas now comprehensively identified, the next stage of this research focuses on examining how these flood-prone zones influence groundwater potential across the district using advanced GIS and machine learning

techniques. This transition enables an integrated assessment of surface and subsurface hydrological responses to extreme rainfall events in Idukki.

5.3 Effect of floods on Groundwater Zones in Idukki district

The delineation of Groundwater Potential Zones (GWPZ) using Machine Learning technique in Idukki marks a significant step toward interpreting the district's intricate hydrogeological behaviour. By integrating 14 diverse spatial variables, including elevation, slope, curvature, TRI, lineament density (LD), soil, drainage density (DD), geology, TWI, STI, rainfall, geomorphology, land use/land cover (LULC), and the normalized difference vegetation index (NDVI), the analysis captures the combined influence of terrain features, lithological controls, surface water dynamics, and climatic factors on groundwater availability within a highly varied landscape. Incorporating flood susceptibility layers further strengthens the assessment by revealing how repetitive flood events can reconfigure recharge mechanisms, alter surface flow routes, and, in certain cases, reduce the groundwater potential of areas that would otherwise appear favourable.

The following section will present the comprehensive results of the GWPZ delineation, illustrating how the integrated parameters and flood susceptibility inputs collectively shape the spatial variability of groundwater potential across Idukki.

5.3.1 Groundwater Potential Zones of Idukki District

It is crucial to evaluate the reliability and significance of the conditioning elements prior to begin the modelling process. To investigate the feature importance, the Recursive Feature Elimination (RFE) approach was used (Jesudasan 2022). The variable importance of the fourteen parameters included in this investigation is shown in Figure 5.25. Among all the other parameters, it has been identified that lineament density is the one with the most significance. This explains why the groundwater potential is thought to be greatly influenced by faults and fissures. It is also evident from the figure that the TWI, TRI, and rainfall play a significant role in influencing the groundwater potential. The fact that ordinary monsoon rainfall affects groundwater potential positively while floods have a negative impact on GWP due to the runoff phenomena which is crucial knowledge to comprehend at this point. This is what caused the Idukki district to experience drought following the 2018 floods.

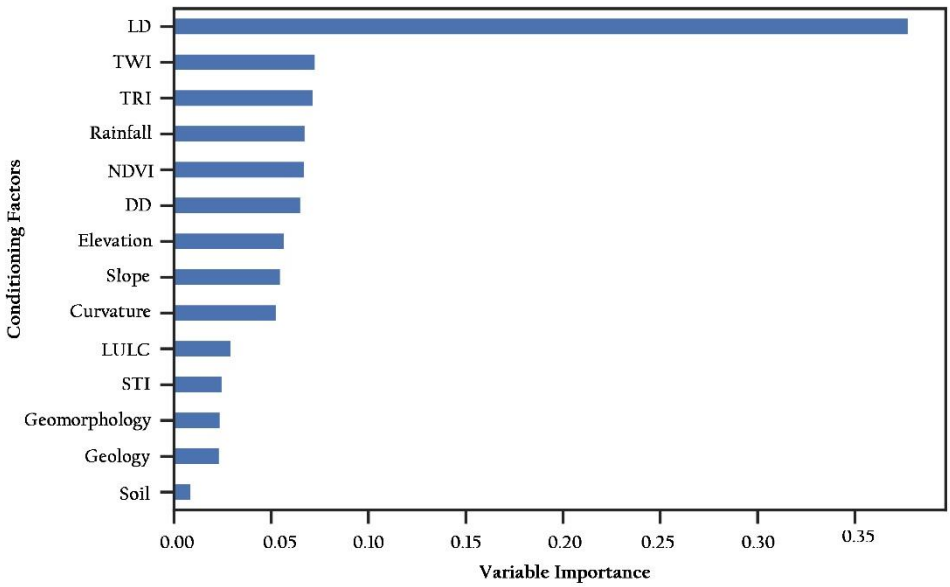

Figure 5.25 : Variable Importance of Conditioning Factors

It was found that the effects of geomorphology, geology, and soil were less significant than those of the other factors. Soil was identified as the least influential factor on the GWPM because more than 30% of the Western Ghats are made of hard rock, which has very little primary porosity. Although these factors are less significant, they are nonetheless not insignificant enough to be disregarded. In addition, it was discovered that all other factors aside from lineament density held lesser significance. To avoid omitting or neglecting any variable, it was also deduced from the RFE approach that all the conditioning factors considered possess important value.

5.3.2 Performance of ML Models for GWPZ

Before beginning the modelling procedures, the dataset underwent pre-processing process. The well locations with adequate groundwater were given the number 1, and those with inadequate groundwater were given the value 0. The machine learning models were trained using the training dataset, which had 177 rows (well locations) and 14 columns (conditioning factors). To achieve an optimal and improved accuracy, the three models used in this study are Random Forest, adaboost, and gradient boost were tweaked by changing the hyperparameters.

The obtained groundwater potential zonation maps were exported into the ArcGIS environment and were reclassified into five classes representing the potential of the groundwater level varying from very low to very high. Figure 5.26, Figure 5.27 and Figure 5.28 indicates the groundwater potential zonation maps of the Idukki district generated from the random forest, adaboost and gradient boosting models respectively.

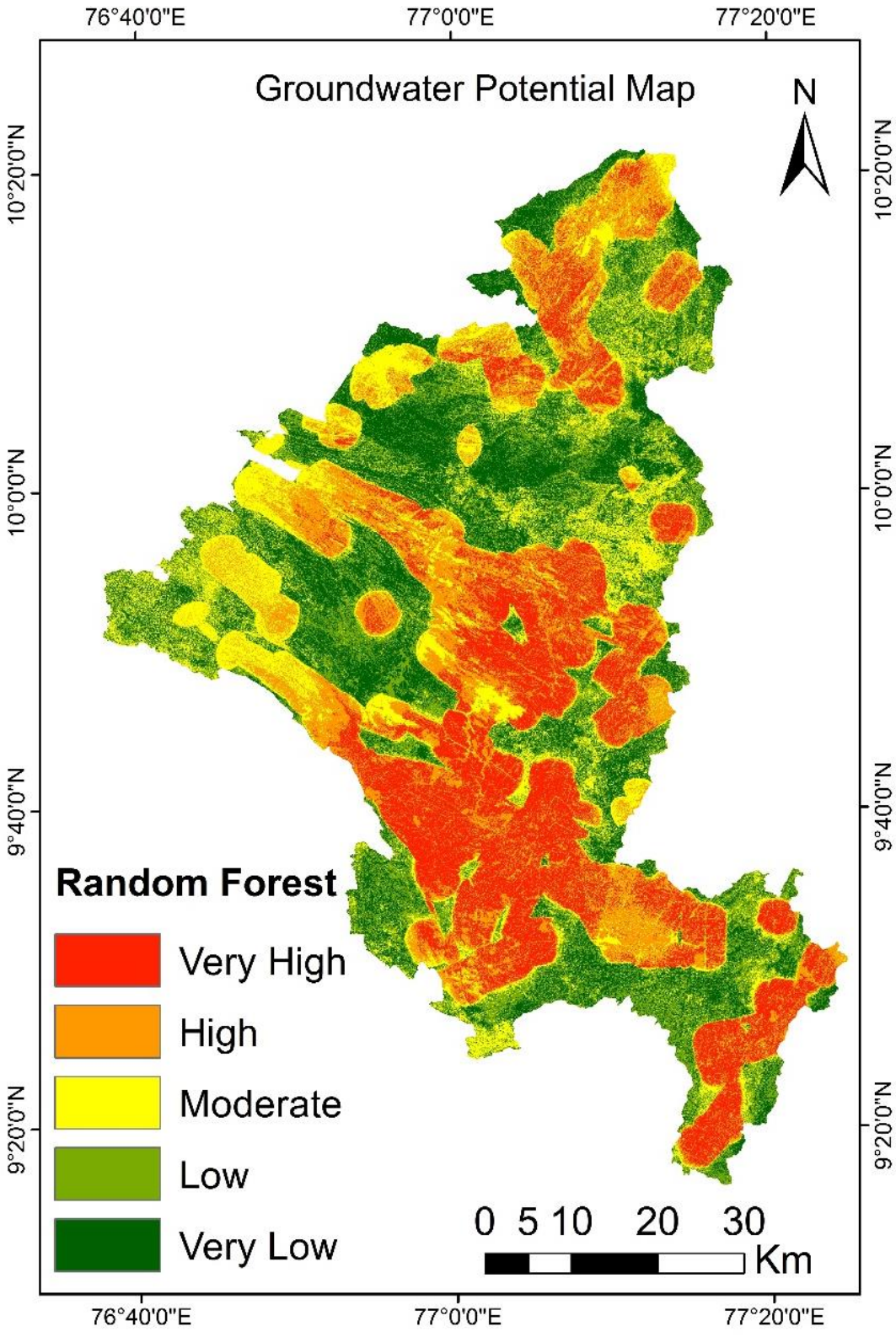

Figure 5.26 : Groundwater Potential Zonation map of the Idukki district from the Random Forest Model

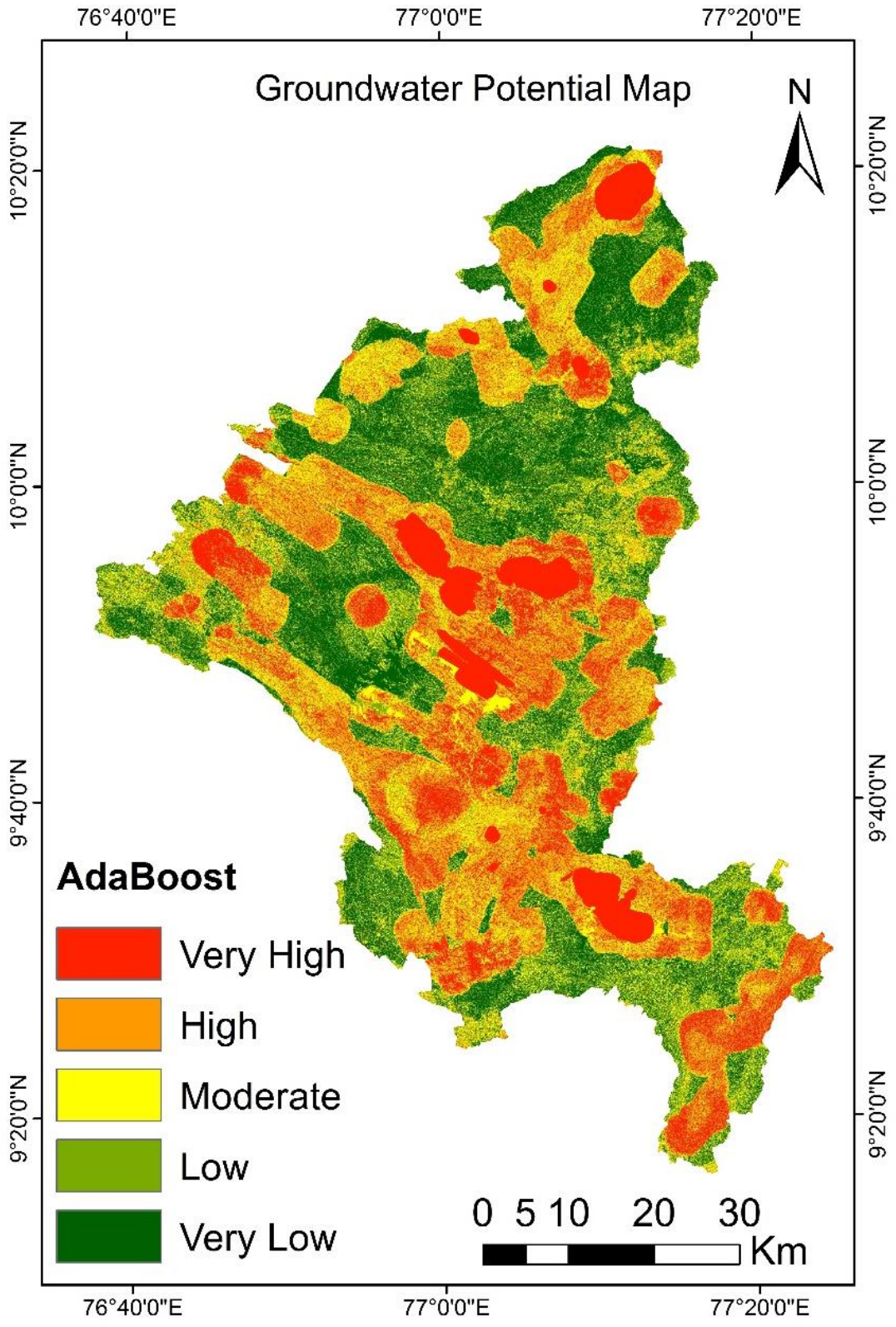

Figure 5.27 : Groundwater Potential Zonation map of the Idukki district from the AdaBoost Model

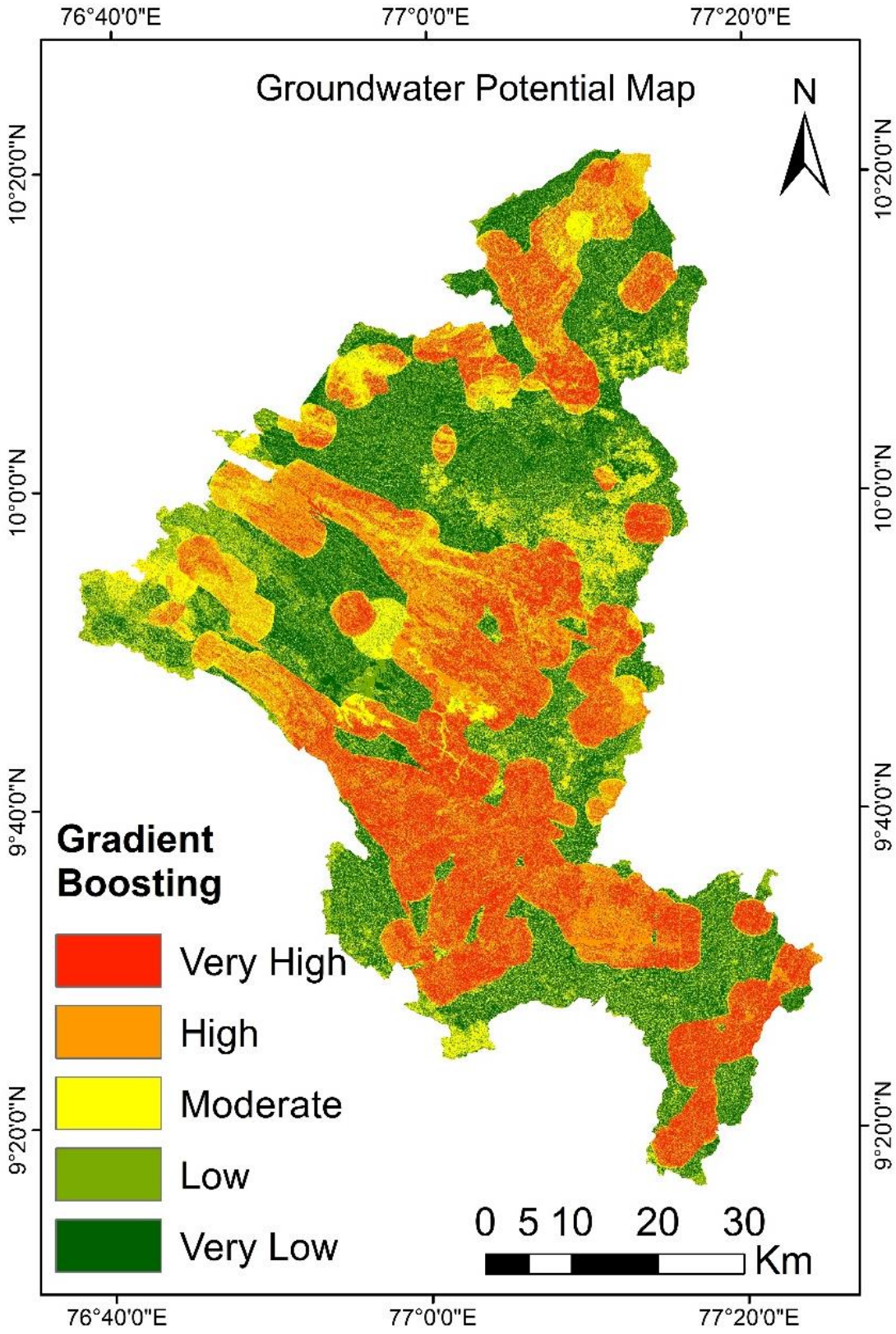

Figure 5.28 : Groundwater Potential Zonation map of the Idukki district from the Gradient Boosting Model

According to the results, more than half of the Idukki district is classified as being in "very high" or "high" zones. This explains the outcome of the district receiving sufficient rainfall. The "low" and "very low" classes, on the other hand, represent significant areas with poor groundwater levels. This is related to factors like land use, where concrete-built areas do not encourage infiltration, or slopes where runoff predominates and interferes with downward hydraulic conductivity. Even deforestation activities could be blamed as it causes soil erosion and hence reduced infiltration. Furthermore, lower elevation zones within the study area show greater groundwater potential due to the hydraulic gradient and existence of low water table, yet majority of the Idukki district falls on higher elevation.

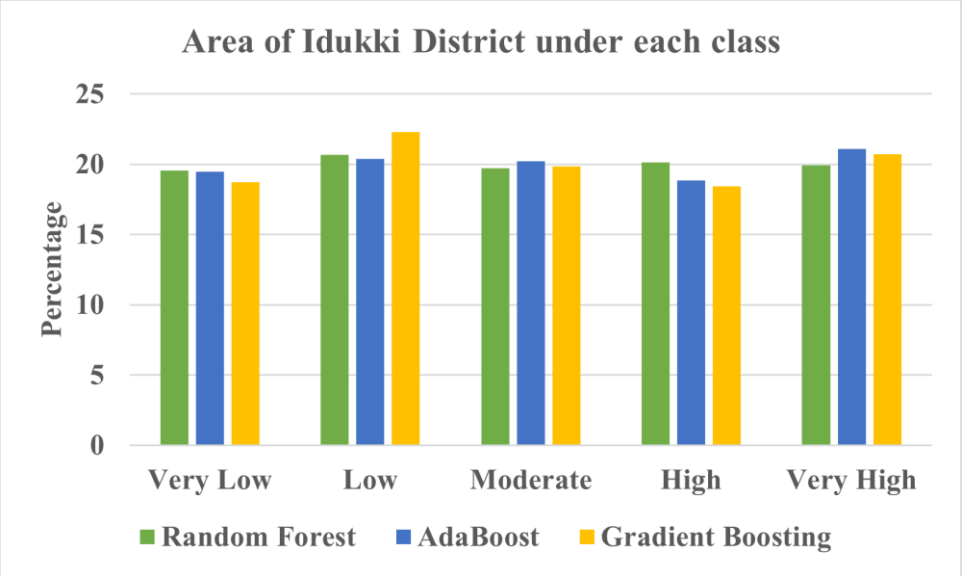

Figure 5.29 : Area of Idukki District under each class (in percentage)

Figure 5.29 displays the percentage of each class, viz., very low, low, moderate, high, and very high, for the area. The chart makes clear that all machine learning algorithms consistently classify the zones with potential for groundwater. Additionally, it can be inferred that all GWP zonation classes are evenly spread throughout the Idukki region, highlighting the fact that while some parts of the district have a high potential for groundwater, other parts have lower potential.

Another notable highlighted occurrence that shows the groundwater potential and the influence of external environmental elements over it is the aftermath of the flood disaster in 2018, where the entire Kerala state went under a drought condition. As long as the state got optimal rainfalls, the groundwater potential was relatively high however, with the emergence of devastating events like floods and landslides, the

region incurs topographical alterations that impact the hydraulic conductivity. Moreover, the augmentation of runoff activity with the onset of floods lowers the infiltration capacity, which substantially affects the groundwater potential of the region negatively.

5.3.3 Validation and Comparison on GWPM

The validation dataset, which had 76 rows and 14 columns indicating the well locations and the conditioning factors, was used to validate each ML model. The AUROC, accuracy, and kappa values were used to validate the three ML models for their dependability and accuracy. The confusion matrix and the AUROC curve of the models can be seen in Figure 5.30 and Figure 5.31 respectively. An AUC value of 0.92, an accuracy of 0.88, and a kappa value of 0.76 were obtained by the random forest model. The adaboost model's AUC, accuracy, and kappa scores are 0.88, 0.84, and 0.68, respectively. With AUC, accuracy, and kappa values of 0.90, 0.87, and 0.73, respectively, the gradient boost model also demonstrated its performance.

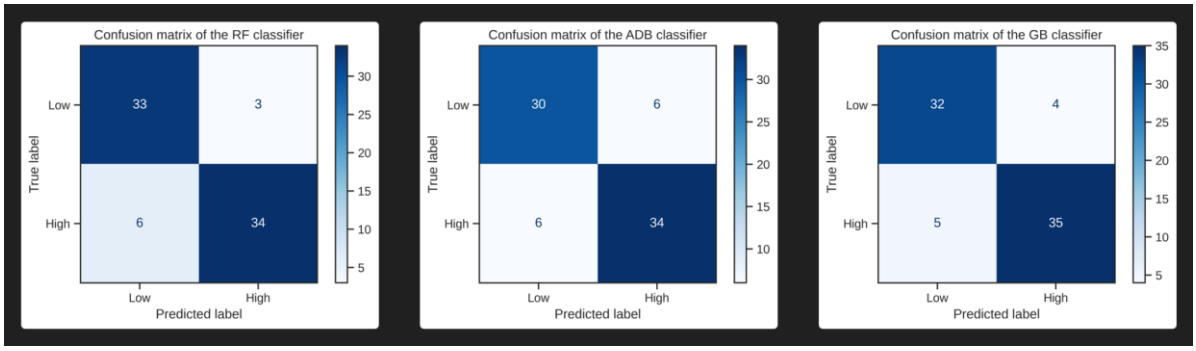

Figure 5.30 : Confusion Matrix of the Machine Learning Models

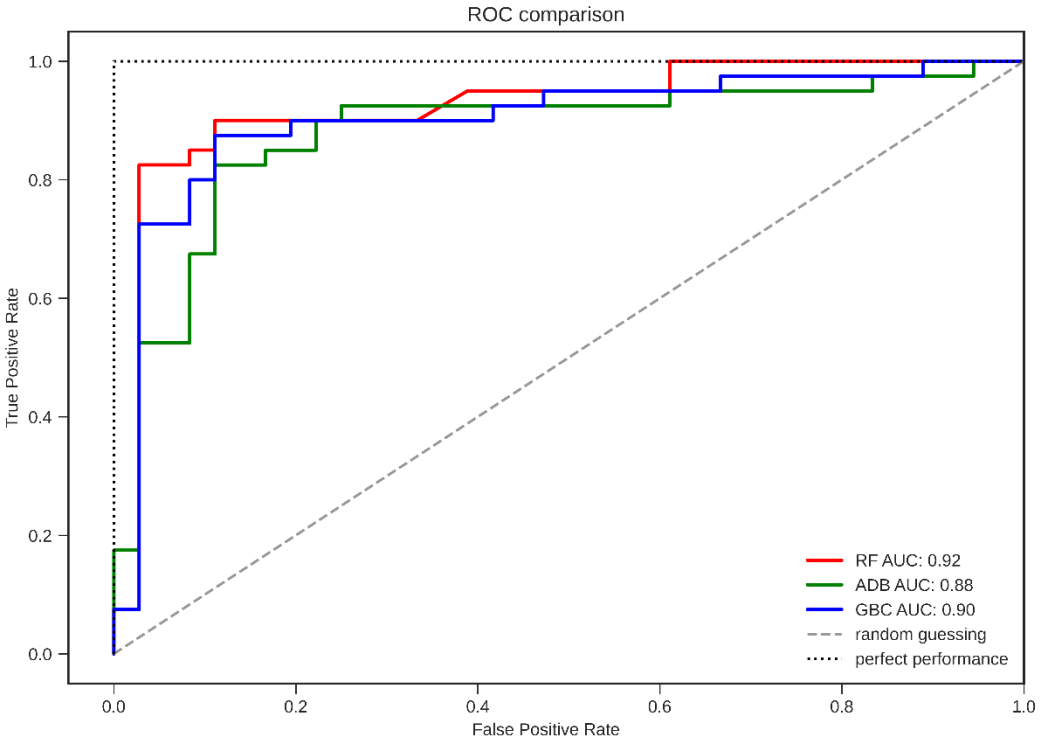

Figure 5.31 : AUROC Curve of the Machine Learning Models

Comparing the three models, the random forest model demonstrated greatest accuracy and AUROC values, with gradient boosting earning the second spot and the adaboost model performing inferior to the other two. With their measure of the inter/intra-rater reliability using the kappa values, all three models showed "substantial agreement." This demonstrates that the models have higher consistency when gauging a constant phenomenon.

The Machine learning based groundwater potential mapping in the Idukki district demonstrates that groundwater occurrence is governed by area's rugged, mountainous terrain and associated variations in slope, elevation, land cover, and soil characteristics. The RFE analysis highlights that all fourteen conditioning factors contribute to groundwater potential, with lineament density emerging as the most influential. This aligns with the district's fractured and faulted hard-rock terrain, where secondary porosity plays a major role in groundwater storage.

34

The analysis further shows that drainage density, NDVI, land use/land cover, and topographic roughness markedly influence infiltration and recharge. These parameters capture the interplay between surface flow, vegetation cover, terrain irregularity, and human activity factors that collectively determine the spatial variability of groundwater potential in steep, monsoon-dominated landscapes. The Random Forest

model produced the highest predictive performance (AUC = 0.92), confirming its suitability for complex, nonlinear hydrogeological settings such as Idukki.

The final groundwater potential zonation map reveals a balanced distribution of very low to very high potential zones, indicating both opportunities and vulnerabilities in groundwater availability.

5.3.4 Flood Influence on Groundwater Recharge

- Areas exposed to **very low flood hazard** generally coincide with strong groundwater potential and display the safest conditions for long term aquifer storage.
- **Low flood prone zones** show favourable hydrological behaviour, where limited surface runoff supports gradual seepage into the subsurface.
- **Medium flood exposure** marks the most significant interface between flood dynamics and aquifer recharge, offering potential for enhanced groundwater replenishment if supported by suitable landscape features.
- Regions classified as **high flood prone** demonstrate restricted infiltration and greater surface flow, making recharge uncertain and spatially inconsistent.
- **Very high flood prone zones** present the least conducive setting for groundwater storage, dominated by rapid runoff, erosion, and limited water retention, resulting in heightened sensitivity of underlying aquifers.

5.3.4.1 Groundwater Susceptibility

The combined analysis of flood exposure and groundwater potential illustrates a clear pattern: **groundwater susceptibility rises with increasing flood intensity**.

To further assess the effect of floods on groundwater potential in Idukki district, a groundwater susceptibility map was made. The developed groundwater susceptibility map as shown in Figure 5.32 was generated by integrating the groundwater potential zonation with the flood susceptibility raster to identify areas where groundwater conditions are likely to be adversely affected during extreme rainfall events. Both input raster were first standardized and reclassified into discrete classes representing groundwater potential levels and flood severity. These layers were then combined within a GIS environment using a cell by cell overlay operation, which assigned each pixel a unique paired value representing its corresponding flood class and groundwater

potential class. The resulting integrated raster was further analysed to determine zones where high flood exposure coincides with low groundwater potential, thereby delineating regions that are more vulnerable to reduced recharge and groundwater stress. This combined analysis provides a spatial representation of groundwater susceptibility driven by the interaction between flood behaviour and groundwater response.

While controlled or moderate flooding may provide opportunities for replenishing aquifers, areas that frequently experience severe flood events tend to lose water rapidly as overland flow rather than allowing it to enter the subsurface (Tackley et al., 2023). These landscapes often possess physical constraints such as gradient, thin soil cover, or impermeable geology that restrict percolation, preventing effective recharge (Zhang et al., 2017). As a result, the most flood affected regions are also the most vulnerable from a groundwater perspective, facing reduced storage capacity and greater uncertainty in sustaining water availability during dry periods. This reinforces that the magnitude of flooding alone does not determine recharge benefits; the capacity of the terrain to retain and transmit water is equally decisive.

The integrated spatial interpretation map shown in Figure 5.32 demonstrates that the impact of flooding on groundwater conditions in the Idukki district is distinctly spatial and strongly influenced by local terrain and hydrogeological factors. The developed Groundwater Susceptibility Map has six zones namely, Favourable Recharge zones, high to critical susceptibility, mixed response zone, moderate susceptibility, recharge opportunity zone and stable recharge zone, which are crucial to understand the behaviour of groundwater under extreme flood event such as the one that happened in 2018.

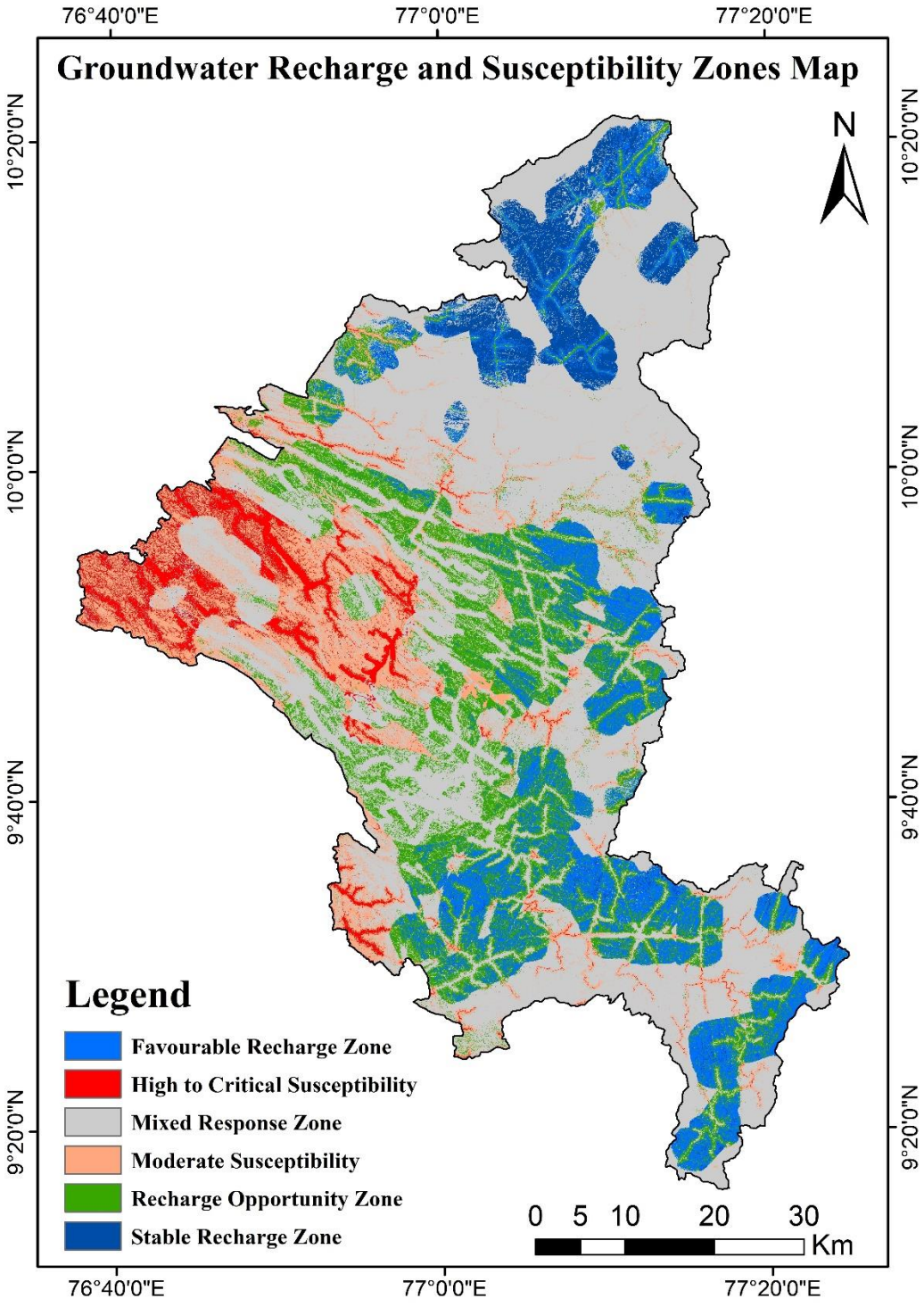

Figure 5.32 : Groundwater Recharge and Susceptibility Zones

While low and medium flood prone areas align with favourable recharge and higher groundwater potential, the very high flood-prone zones exhibit high to critical groundwater susceptibility, where rapid runoff and limited infiltration capacity result in reduced groundwater potential and weak recharge response (Mirlas et al., 2022). The Mixed response zones denote regions where the combined influence of flood

susceptibility and groundwater potential leads to variable groundwater behaviour rather than a consistent outcome. In such areas, flood events may support limited recharge under favourable conditions, while in other instances they may predominantly generate surface runoff. This variability is controlled by factors such as rainfall magnitude, event duration, and site specific terrain characteristics, making the groundwater response in these zones dynamic and dependent on individual flood events.

In the context of Idukki, this pattern indicates that intense flooding has a predominantly negative influence on groundwater potential, making aquifers more vulnerable and less capable of retaining recharge during extreme rainfall events. These findings underscore that the presence of floodwater does not inherently translate into groundwater gains and, in fact, may aggravate groundwater stress where the landscape inhibits infiltration, reiterating the importance of localized flood–groundwater management strategies.

Table 5.4 indicates that the flooding exerts a measurable influence on groundwater recharge behaviour in Idukki, but the effect varies significantly with flood severity. In very low and low flood prone areas, where flood intensity is minimal, groundwater potential remains generally moderate to high. This suggests that limited inundation allows rainfall driven infiltration to dominate, enabling stable recharge conditions even during flood periods.

In contrast, medium to high flood prone regions reveal a shift in groundwater behaviour, where increased runoff, soil saturation, and sediment transport begin to interfere with infiltration. These zones exhibit a mixed groundwater response, reflecting the competing influences of enhanced surface water availability and reduced percolation opportunities during flood events.

The most pronounced impact occurs in the high and very-high flood-susceptible zones. Here, intense flooding leads to rapid overland flow, reduced infiltration windows, and frequent surface destabilization, resulting in a predominance of low groundwater potential and increased groundwater susceptibility. Instead of enhancing recharge, extreme flood conditions in these areas restrict effective infiltration, indicating that floods can negatively influence groundwater replenishment in steep and hydrologically sensitive terrains.

Table 5.4 Influence of Floods on GW Recharge and Susceptibility

Flood Prone Category	Groundwater Potential Response	Hydrological Significance	Groundwater Recharge Interpretation	Groundwater Susceptibility
Very Low Flood Prone (Class 1)	Medium to Very High GW Potential	Hydrology dominated by rainfall percolation rather than flood pulses	Steady recharge possible through natural infiltration	**Low** susceptibility: Aquifer remains stable and resilient
Low Flood Prone (Class 2)	High to Very High GW Potential	Seasonal overland flow supports distributed infiltration	Favourable recharge; floodwater retained without major runoff	**Low to Moderate** Susceptibility: Recharge supportive zones
Medium Flood Prone (Class 3)	Medium to High GW Potential	Balanced runoff–infiltration dynamics; floodwater can contribute meaningfully	Recharge opportunity zones; intervention improves recharge efficiency	**Moderate** Susceptibility: depends on LULC, slope, and soil permeability
High Flood Prone (Class 4)	Low to Medium GW Potential	Floodwater surges with limited retention due to slope & sediment	Recharge occurs only where geomorphology supports infiltration	**Moderate to High Susceptibility:** GW Recharge uncertain and runoff more dominant
Very High Flood Prone (Class 5)	Very Low to Low GW Potential	Flashy, rapid runoff; poor infiltration and high erosion	Floodwater largely lost; very less aquifer contribution	**High to Critical Susceptibility:** Most vulnerable to groundwater depletion

5.3.4.2 Zonal Statistical Assessment

The zonal statistical assessment reveals that groundwater potential does not consistently increase with flood intensity. The highest mean groundwater potential occurs in moderately flood-prone areas (Class 3), after which a notable decline is observed as flood severity reaches the high and very high categories. The zonal statistical analysis further demonstrates that areas experiencing higher levels of flooding correspond to zones with lower groundwater potential, indicating reduced

infiltration and greater vulnerability in terms of groundwater recharge. This relationship reinforces the link between flood severity and groundwater susceptibility as shown in Figure 5.33.

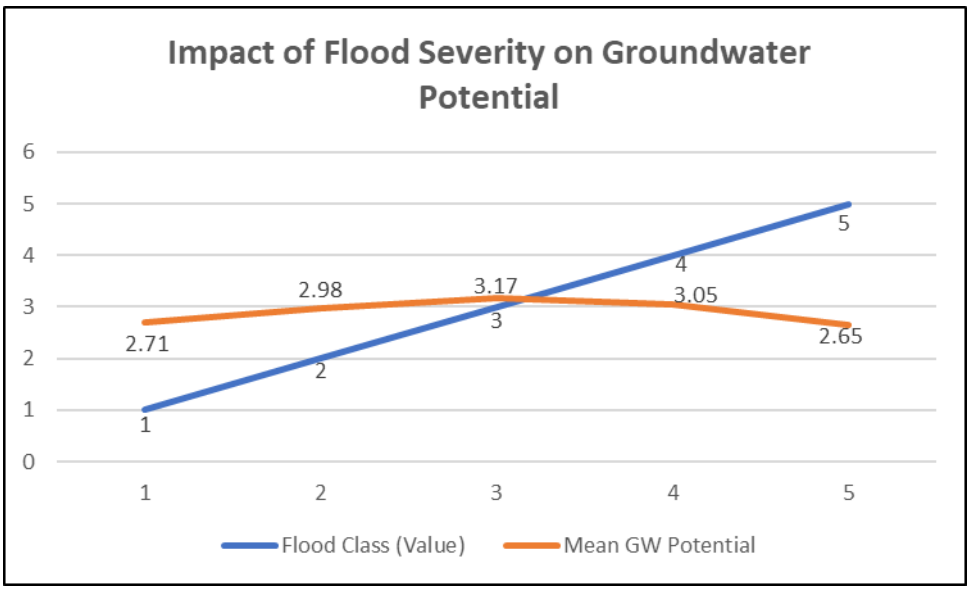

Figure 5.33 : Statistical Assessment of Floods on GW Potential

In particular, the very high flood prone zone records one of the lowest groundwater potential means, indicating that extreme flooding adversely influences recharge. This suggests that intensive flood events in the Idukki district are associated with increased runoff and reduced infiltration capacity, resulting in greater groundwater susceptibility and diminished recharge potential.

The trend increases toward the moderate flood zone (Class 3) and subsequently declines as flood severity reaches the high and very high categories, indicating that excessive flooding negatively impacts groundwater recharge and contributes to groundwater susceptibility.

The graphical representation of flood severity against mean groundwater potential demonstrates a trend consistent with the spatial overlay analysis. Groundwater potential shows a gradual increase from very low to moderate flood prone zones, indicating that moderate flooding may facilitate short-term infiltration and localized recharge. However, beyond this threshold, the trend reverses, with mean groundwater potential declining sharply across high and very high flood severity classes. This pattern suggests that intense or prolonged flooding in the Idukki district does not translate into enhanced aquifer recharge. Instead, excessive runoff, steep terrain, and reduced infiltration opportunities appear to limit groundwater replenishment, making

these landscapes hydrologically susceptible (Zhang et al., 2022). The graphical trend therefore reinforces the spatial interpretation map by confirming that while moderate flood events may support recharge, extreme floods contribute to groundwater vulnerability and reduced groundwater potential.

The research delineates groundwater potential zones in the Idukki district, a critical undertaking in light of Kerala's increasing water scarcity and the lack of prior spatial assessments for the region. Using three machine learning models (RF, AdaBoost, GB) and fourteen conditioning parameters, the results indicate that a substantial portion of the district falls within high to very high groundwater potential categories. Notably, areas heavily impacted during the 2018 floods align with zones of lower groundwater potential, demonstrating that intense flooding can exacerbate groundwater susceptibility by reducing infiltration opportunities and altering recharge conditions (Ren et al., 2020). This integrated analysis underscores the close relationship between flood dynamics and groundwater vulnerability in a mountainous district such as Idukki.

5.4 Effect of Floods on Land use and Land Cover

Land Use/Land Cover (LULC) information was derived using the Random Forest machine learning algorithm through the Google Earth Engine (GEE) platform. GEE is a cloud-based geospatial analysis environment that hosts a massive archive of multi-petabyte Earth observation data and provides high performance, parallel computing capabilities. The platform enables rapid visualization, processing, and analysis of geospatial datasets via an online application programming interface (API). Its data repository includes extensive publicly available satellite imagery acquired across optical, thermal, and microwave spectra, notably from the complete Landsat archive and Sentinel missions. A key advantage of GEE is access to a wide range of pre-processed datasets related to land cover, environmental variables, meteorology, and climate, allowing efficient and seamless data retrieval and analysis.

5.4.1 Effect of Floods on LULC 2018

To analyse the impact of floods on LULC, satellite imagery of LANDSAT 8 is utilized for the year 2018 and 2021. Land use and land cover maps were generated for the years 2018 and 2021. The imagery was trained using a classification model that grouped the data into five distinct classes namely built up, barren, water, agriculture and forest. Every class was trained using 60 Region of Interests (ROIs) and verified using 50 ROI

points, following a widely accepted guideline (Lillesand and Kiefer 1979). The accuracy of the map is assessed after satisfactory results have been achieved. Flood extent mapping was performed in the Google Earth Engine (GEE) environment using the image ratio technique, consistent with the methodology adopted in Objective 1 for identifying flood prone zones. The extracted flood extent was then overlaid on the corresponding LULC maps to generate land use information under flood conditions. Subsequently, GIS tools were employed to quantify the area of each LULC class impacted by flooding.

1 The Random Forest technique is employed to train the ROIs in which the ntrees of 55 per-formed better for the classification. The result of LULC 2018 shown in Figure 5.34 and showed an accuracy of 88.32%. Accordingly, the pre flood land use and land cover is illustrated through the classified maps presented in Figure 5.34. Flood extents extracted from SAR imagery were overlaid on the corresponding annual LULC map to generate the land use/land cover scenario during the 2018 flood event, as shown in Figure 5.35.

126 Analysis of the LULC under flooded conditions enabled identification of the inundated areas and assessment of flood induced impacts across different land cover categories. Land use and land cover (LULC) change after floods is important because flood events often alter surface characteristics, drainage patterns, and land stability. Post flood LULC analysis helps identify damaged agricultural land, expansion of water bodies, and changes in built-up areas, which influence future flood behaviour. Understanding these changes supports effective recovery planning, risk reduction, and sustainable land management. It also provides critical inputs for updating flood susceptibility and hazard models.

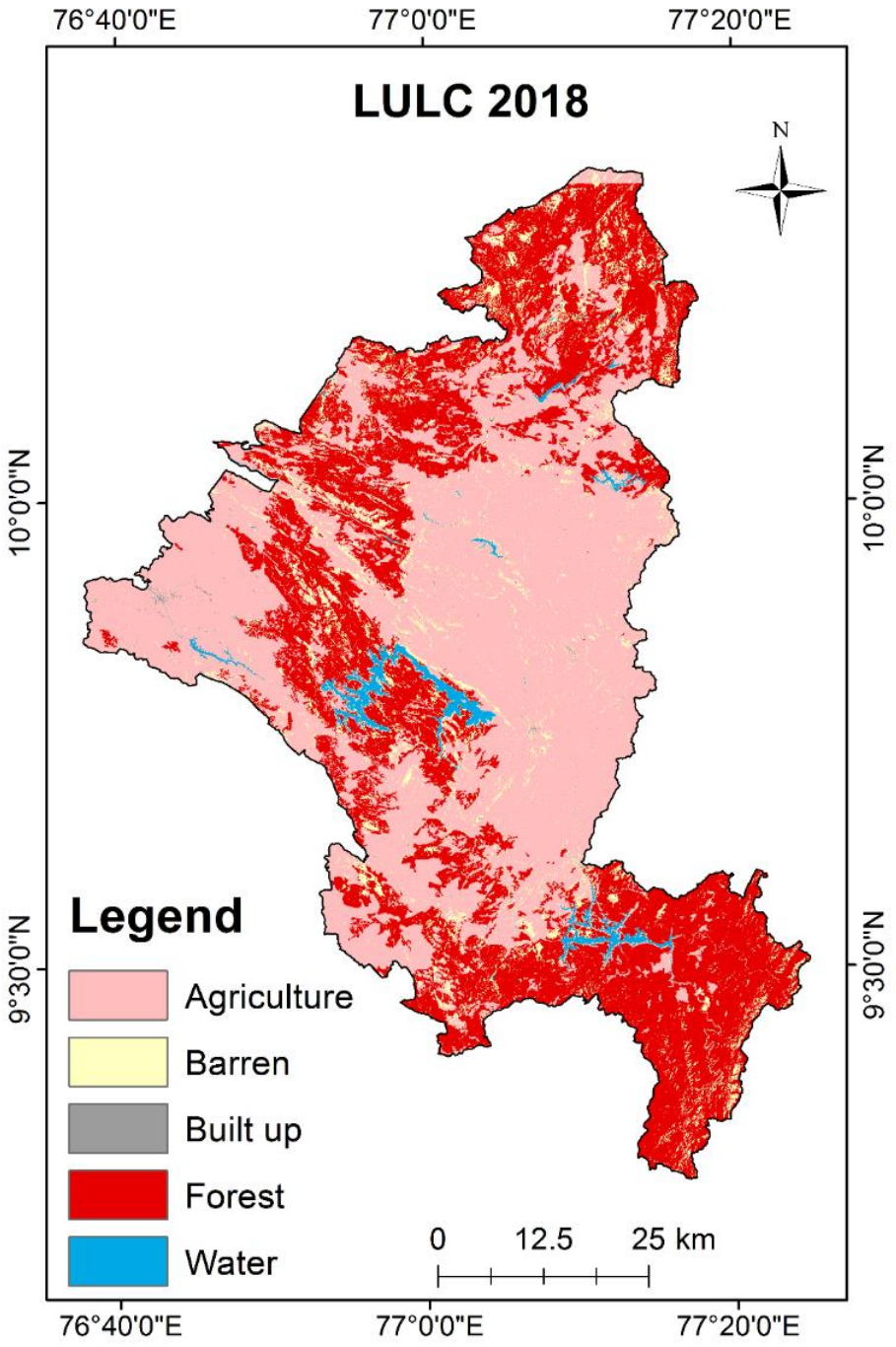

Figure 5.34 : LULC for August 2018 (Before Flood)

Table 5.5 Area Distribution of LULC Classes

S.No.	LULC Class	Area (Km^2)
1	Built up	13.3101
2	Agriculture	2230.223
3	Barren	365.7465
4	Forest	1680.337
5	Water	74.5524

From Table 5.5, it is seen that the land use and land cover analysis indicates that agriculture is the most dominant category in the Idukki district, covering approximately 2230 km², which reflects the extensive cultivation and plantation based land use in the region. Forests form the next major class with about 1680 km², highlighting the district's substantial natural vegetation and hilly terrain. Barren land accounts for around 366 km², representing areas with minimal vegetation or limited land use activity. Water bodies occupy roughly 75 km², corresponding to rivers, reservoirs, and other surface water features. Built-up areas constitute the smallest share at about 13 km², indicating that the district remains largely rural with concentrated settlements.

After superimposing the flood maps derived from SAR images over the LULC classes, the flooded area of each LULC class is obtained. The table below shows the Flooded area for each LULC class.

Table 5.6 Flooded area for Each LULC Class (2018)

S.No.	LULC Class	Flooded Area (Km^2)
1	Built up	0.4797
2	Agriculture	5.1138
3	Barren	4.6701
4	Forest	10.5957

The LULC analysis indicates that nearly 20.85 km² of total land in the Idukki district was inundated during the 2018 flood event. Within this, built-up areas were particularly vulnerable, with about 0.47 km² of the total 13.3 km² of settlements becoming submerged, reflecting the substantial loss to housing and infrastructure. Agricultural areas, which form the largest land use category, recorded around 5.1 km² of flooding, affecting cultivation and plantation landscapes. Both barren and forested regions were also impacted, with approximately 4.67 km² and 10.6 km² inundated, demonstrating the extent of disturbance across the terrain.

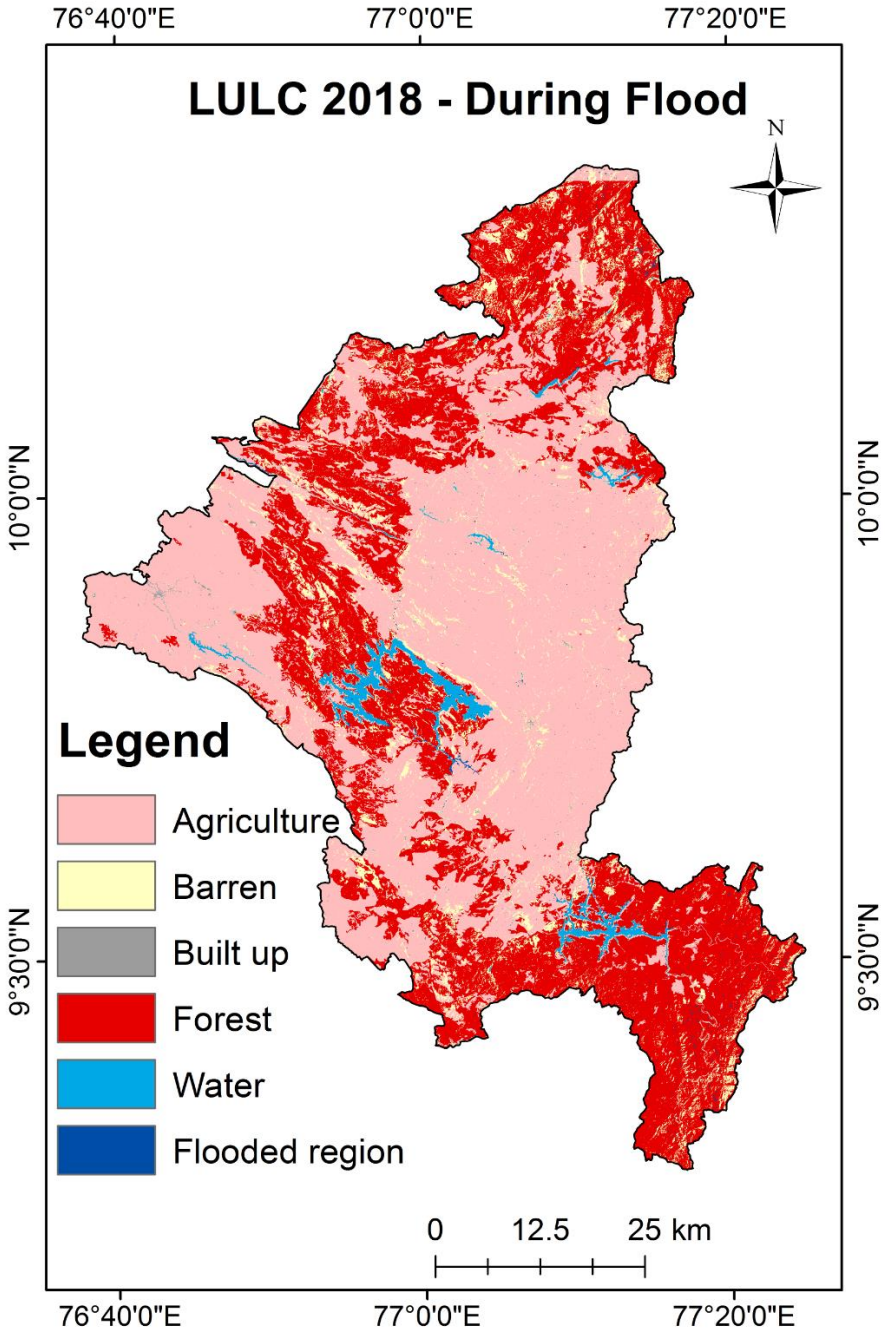

Figure 5.35 : LULC for August 2018 (During Flood)

5.4.2 Effect of Floods on LULC 2021

92

To assess the impact of subsequent flood events on land use and land cover, the 2021 LULC classification was generated using the same methodological approach adopted for the 2018 analysis. Each LULC category was trained with 60 Regions of Interest (ROIs) and validated using 50 additional ROIs, following established remote sensing practices (Lillesand and Kiefer, 1979). The Random Forest classifier was employed for supervised classification, with an optimal configuration of 55 trees yielding the

highest accuracy. The resulting 2021 LULC map, shown in Figure 5.36, achieved an overall accuracy of 89.94%. The inclusion of the 2021 LULC assessment is important as it allows for the evaluation of landscape response to consecutive flood events, enabling a clearer understanding of how repeated hydrological extremes continue to alter land cover patterns in the Idukki district. The flood extent extracted from SAR imagery was overlaid onto the corresponding year's LULC map to generate the land use/land cover distribution under flood conditions for 2021, as illustrated in Figure 5.37.

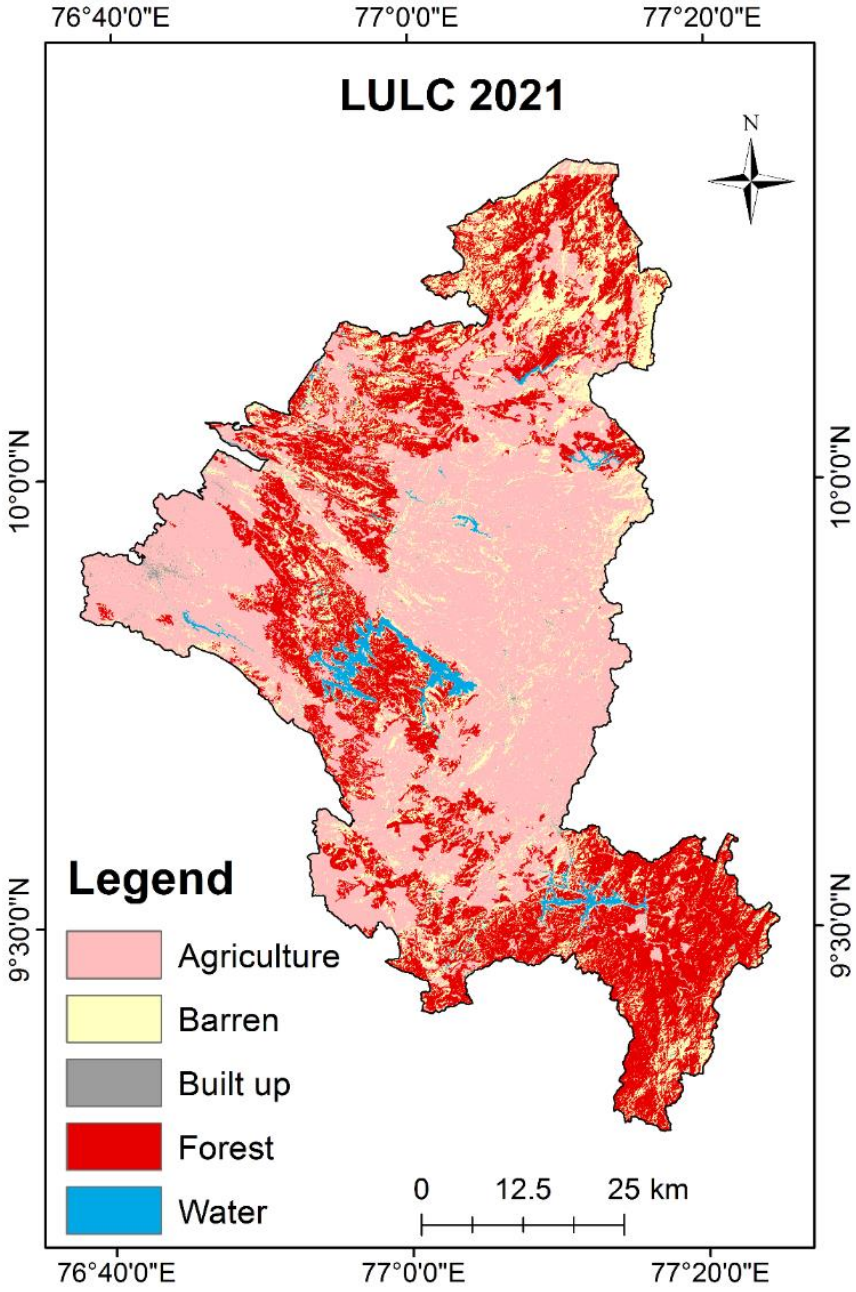

Figure 5.36 : LULC for October 2021 (Before Flood)

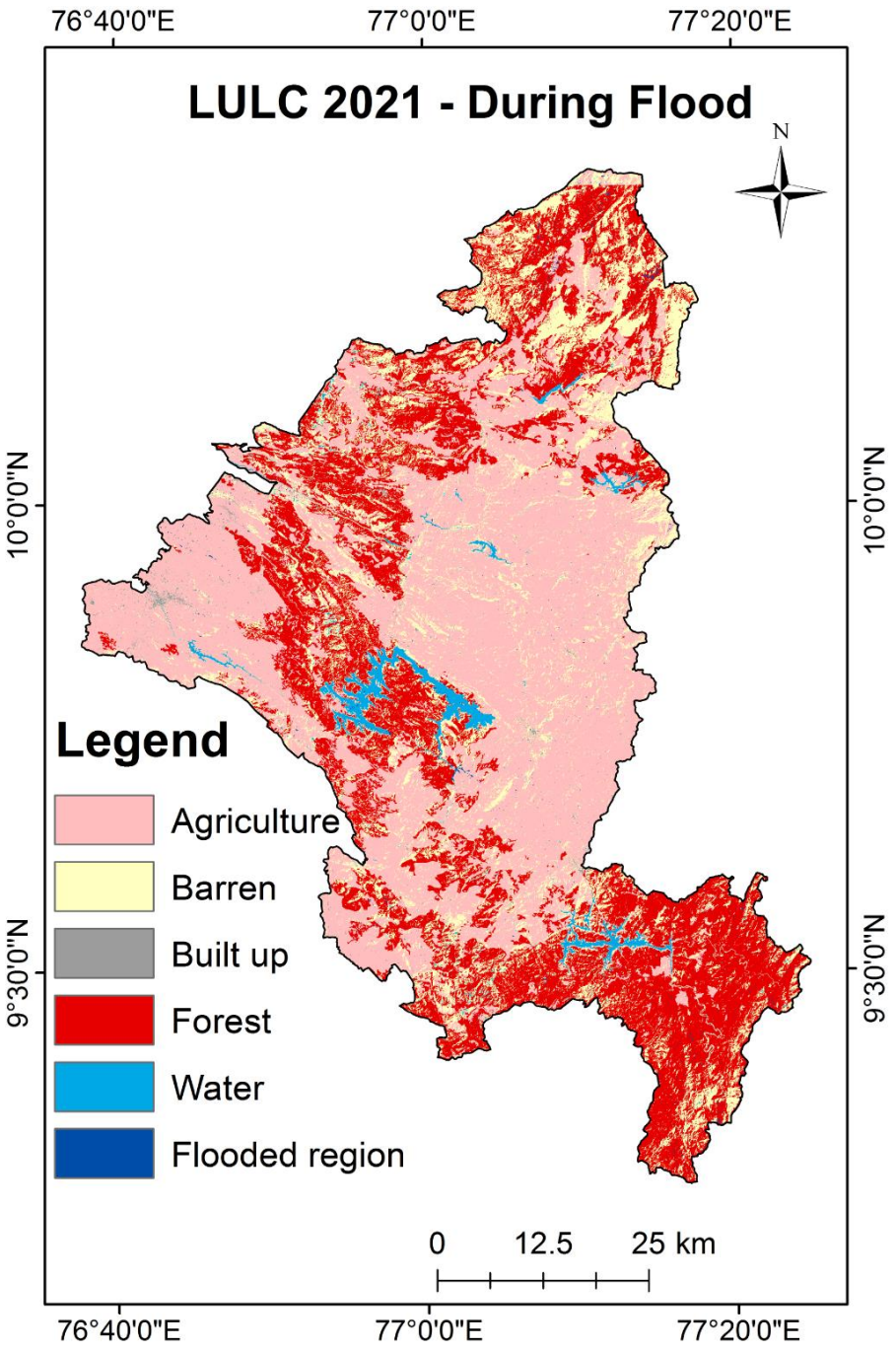

Figure 5.37 : LULC for October 2021 (During Flood)

Table 5.7 Flooded Area for Each LULC Class (2021)

S.No.	LULC Class	Flooded Area (Km^2)
1	Built up	0.2466
2	Agriculture	6.2289
3	Barren	2.817
4	Forest	9.9495

The flooded LULC assessment for 2021 as illustrated in Table 5.7 indicates that approximately 19.24 km² of land in the Idukki district was inundated during the 2021 flood event. Built-up areas experienced around 0.25 km² of flooding, reflecting localised impacts on settlements. Agricultural land recorded about 6.23 km² of inundation, suggesting notable disruption to cultivated regions. Barren areas and forests were affected by 2.82 km² and 9.95 km² of flooding, respectively, indicating the spread of floodwaters across both open and vegetated terrain. These patterns illustrate the continued sensitivity of Idukki's landscape to recurring flood events.

5.4.3 Comparison of LULC Changes Between 2018 and 2021

Comparing the LULC of 2018 and 2021 enables an assessment of how repeated flood events have altered land-use patterns in the Idukki district. When examined alongside the flood inundation maps, these changes help clarify which LULC categories are consistently exposed to flooding and how their spatial extent has shifted over time. This comparison provides insight into the cumulative landscape response to successive floods and identifies zones that are becoming increasingly vulnerable.

Table 5.8 depicts the alteration in area of each LULC from the year 2018 to 2021. It is established that there is a 15%, and 57% increase in water, and built-up areas respectively. In contrast, agricultural land and forest cover declined substantially by 9% and 18%, respectively. Conversely, barren land increased by 132%, primarily due to the intensification of landslide activity, which led to the conversion of forested and agricultural areas into barren terrain. Consequently, under these changing landscape conditions, floods triggered by torrential rainfall are likely to exert a pronounced impact on the regional landscape.

Table 5.8 Change in area of LULC (in Sq Km)

LULC	Area in 2018 (in Sq. Km)	Area in 2021 (in Sq. Km)
Water	74.55	85.79
Built up	13.31	20.93
Agriculture	2230.22	2030.57
Barren	365.75	849.47
Forest	1680.34	1377.41

5.4.4 Comparison of Flooded areas

In 2018, the floods affected about 20.85 sq. km of area, with the built-up area accounting for 0.48 sq. km. The forests, agriculture and barren area cover around 10.60, 5.11, 4.67 Sq. km, respectively. The floods of 2021 impacted a total area of 19.24 sq. km comprising of 0.24 sq. km of built up, 6.23 sq. km of agriculture, 2.82 sq. km of barren and 9.95 sq. km of forest areas. Hence, Figure 5.38 displays the magnitude of flooding in 2018 and 2021 for each LULC class.

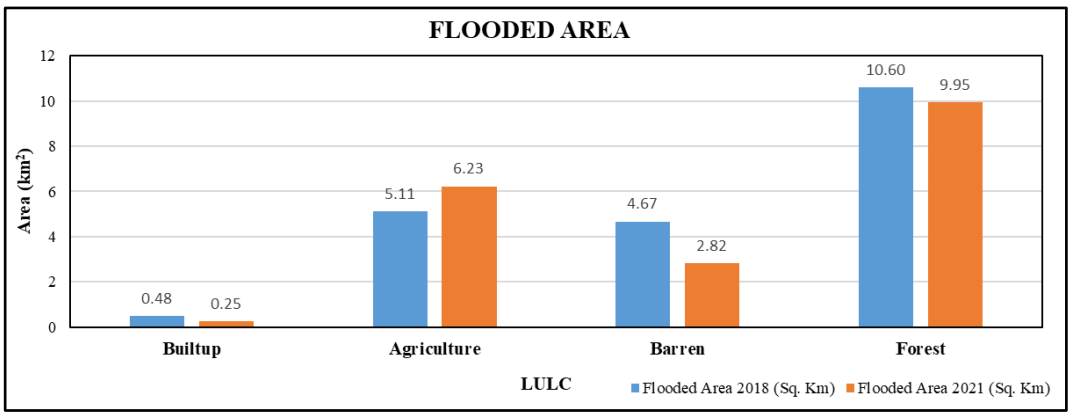

Figure 5.38 : LULC affected by the floods

LULC map indicates a marked expansion of built-up, water, and barren land classes, accompanied by a substantial decline in agricultural and forested areas, largely attributable to their conversion into barren land. It is found those regions converted from forest into barren areas are majorly due to the landslides occurred in those regions during the time of heavy rainfall between the years 2018 and 2021. The floods had created havoc in these regions during 2018 and 2021, resulting in submerging 20.86 and 19.24 sq. km of the LULC. The impact of floods on land use and land cover is substantial, as repeated inundation alters the extent and distribution of agricultural areas, forests, settlements, and water bodies. These flood driven transformations disrupt existing land-use patterns and increase the sensitivity of affected landscapes to further environmental stress. Recognising how successive flood events modify LULC is essential for understanding the evolving dynamics of the region and for identifying areas that are becoming increasingly vulnerable to future hydrological extremes.

5.5 Effect of Floods on Surface Runoff

To assess how extreme rainfall episodes altered runoff generation within the Periyar River Basin, the SWAT hydrological modelling framework was applied using DEM, land-use, soil, and climatic inputs. For the streamflow analysis, the Periyar River Basin

was selected because it is the largest basin within the Idukki district and encompasses the majority of its geographic area. The model successfully delineated sub basins and Hydrological Response Units (HRUs), enabling a spatially explicit analysis of runoff behaviour under flood and non-flood conditions.

5.5.1 SWAT Modelling for Periyar River Basin

SWAT modelling for the Periyar River Basin involved a series of steps designed to represent the basin's landscape and hydrological processes. The model setup began with watershed delineation using a Digital Elevation Model, which defined the basin boundary, drainage network, and sub basins. Land use, soil, and slope layers were then combined to generate Hydrological Response Units (HRUs), each reflecting unique surface and subsurface conditions that govern runoff and infiltration. Daily climatic data such as rainfall, temperature, solar radiation, wind speed, and humidity were incorporated to drive the model's water balance components.

After establishing the input datasets, SWAT simulates streamflow, surface runoff, evapotranspiration, and groundwater contributions across the basin. The delineated Periyar River basin using ArcSWAT below shows the delineated Periyar basins and outlet points for various sub basins. It shows various outlet points, river reach and longest flow path obtained after delineation in ArcSWAT environment. The various outlets are created as per the various sub basins for computation of surface runoff at different points.

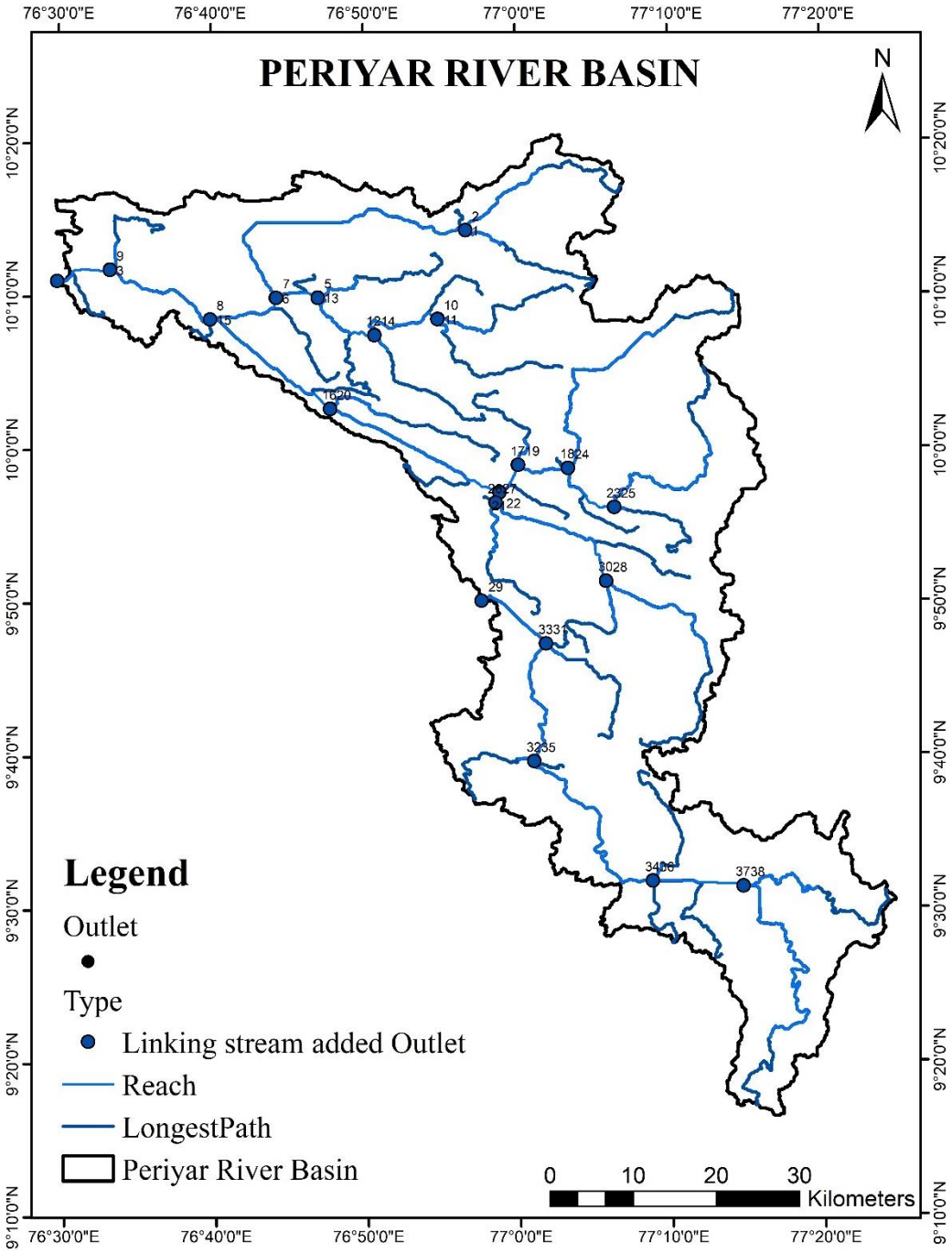

Figure 5.39 : River Reach Outlet Points for Flow calculations

5.5.2 Calibration and Validation

Before analysing the discharge results, the SWAT model was calibrated and validated to ensure that simulated streamflow adequately reflected the basin's hydrological response. Calibration involved adjusting key parameters to improve the match between observed and simulated flows, followed by validation on a separate time period to confirm model performance. During the process of identifying sensitive parameters for the Periyar River Basin, the parameter ranges within the SWAT model were

systematically adjusted using a trial-and-error approach to determine values that best represent the hydrological behaviour of the basin. This procedure involved iteratively modifying parameter values and observing their influence on the simulated runoff and discharge patterns until a satisfactory agreement between simulated and observed conditions was achieved. Through this sensitivity analysis, certain parameters were found to exert a stronger influence on the model outputs compared to others. In particular, **r_CN2.mgt (SCS runoff curve number)**, which controls surface runoff generation; **v_ALPHA_BNK.rte (baseflow alpha factor for bank storage)**, which regulates the rate of groundwater contribution from bank storage; and **r_GW_REVAP.gw (groundwater revap coefficient)**, which governs the movement of water from shallow aquifers back to the root zone, were identified as the most sensitive parameters affecting the hydrological response of the basin. These parameters therefore played a critical role in accurately simulating runoff and streamflow dynamics within the Periyar River Basin.

For the Periyar River Basin, model calibration was carried out for the period 2010–2013, followed by validation for 2016–2018 to assess the model's predictive reliability under independent conditions. Observed discharge data from the Neeleeswaram gauging station, located at the outlet of the basin, were used as reference measurements. The simulated runoff generated by SWAT was compared against these observations, and model performance was assessed using the coefficient of determination (R^2) and the Nash–Sutcliffe Efficiency (NSE).

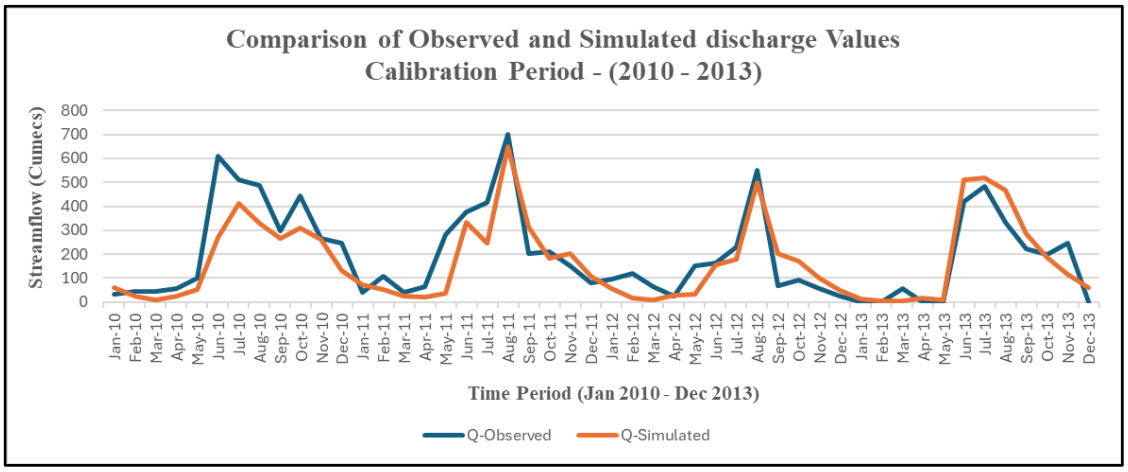

Figure 5.40 : Comparison of Observed and Simulated Discharge values for Calibration

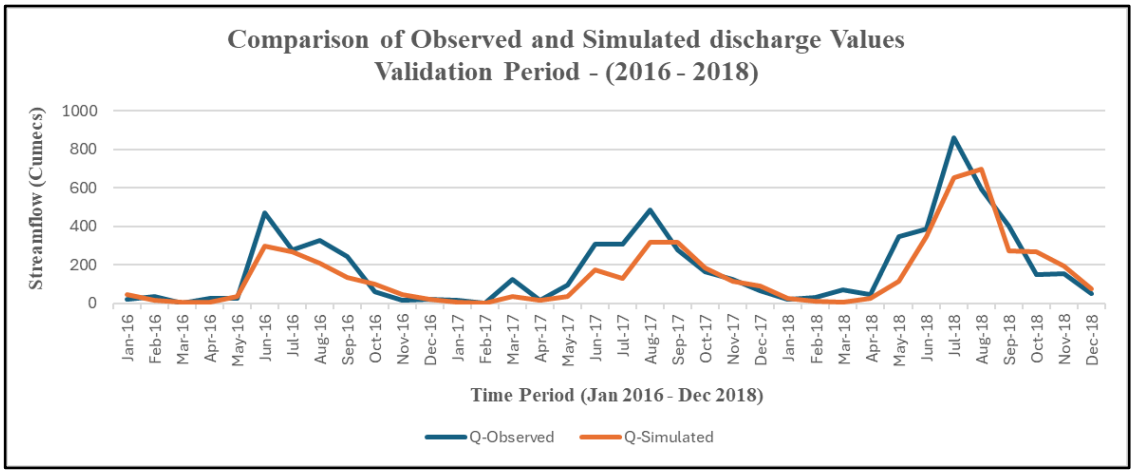

Figure 5.41 : Comparison of Observed and Simulated Discharge values for Validation

Coefficient of Determination (R^2)

In SWAT modelling, the coefficient of determination (R^2) is a commonly employed statistical metric used to quantify how well the simulated streamflow matches the observed streamflow. It indicates the proportion of the variance in the observed data that is explained by the model. R^2 values range from 0 to 1, where values closer to 1 represent a stronger agreement between observed and simulated flows. Higher R^2 values imply that the model effectively captures the variability and overall trend of the hydrological response.

$$R^2 = \left(\frac{\sum (Q_{obs} - \overline{Q_{obs}})(Q_{sim} - \overline{Q_{sim}})}{\sqrt{\sum (Q_{obs} - \overline{Q_{obs}})^2 \sum (Q_{sim} - \overline{Q_{sim}})^2}} \right)^2$$

Where:

- Q_{obs} = observed discharge
- Q_{sim} = simulated discharge
- $\bar{Q}_{obs}$ = mean of observed discharge
- $\bar{Q}_{sim}$ = mean of simulated discharge

Coefficient of Determination was calculated for the Periyar river basin which came out to be 0.76. Value of R^2 as **0.76** indicates a strong and reliable agreement between the simulated and the observed streamflow.

Nash–Sutcliffe Efficiency (NSE)

The Nash–Sutcliffe Efficiency (NSE) is a popularly used statistical measure in hydrological modelling that evaluates how well the simulated streamflow reproduces the observed streamflow. NSE assesses the predictive skill of the model by comparing the magnitude of residual errors to the natural variability of the observed data. Its values range from 1 to −∞, where 1 indicates perfect agreement, 0 means the model is no better than using the mean of observations, and negative values reflect poor model performance.

$$NSE = 1 - \frac{\sum(Q_{sim} - Q_{obs})^2}{\sum(Q_{obs} - \overline{Q_{obs}})^2}$$

Where:

- Q_{obs}= observed discharge
- Q_{sim}= simulated discharge
- $\bar{Q}_{obs}$= mean of observed discharge

NSE was calculated for the Periyar river basin which works out to be **0.74**. Value of 0.74 signifies good model efficiency, meaning that the SWAT simulated discharge captures the timing and magnitude of observed flows with reasonable accuracy.

5.5.3 Water Balance Components & Runoff

The basin-scale water balance as shown in Figure *5.42* revealed that surface runoff constituted the largest share of total water availability, contributing approximately 48%. Percolation to shallow aquifers accounted for about 32%, while evapotranspiration contributed 26%. The dominance of surface runoff reflects the basin's steep topographic gradients, high rainfall intensity, and the presence of land-cover categories with limited infiltration capacity. The magnitude of the runoff component also highlights the basin's susceptibility to rapid hydrological response during extreme rainfall events.

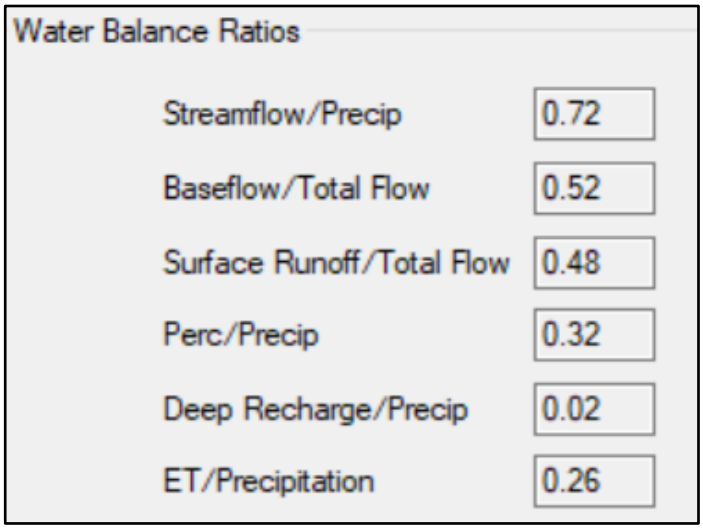

Figure 5.42 : Water Balance ratios obtained from SWAT Output

5.5.4 Runoff Intensification During Flood Events

A substantial amplification in surface runoff was evident during major flood years, particularly the Kerala floods of August 2018. At outlet (O4) shown in Figure 5.43 and Figure *5.45*, located within the central portion of the Idukki subdivision, the simulated discharge increased by more than 128% during the 2018 event compared to pre-flood years. This dramatic rise in flow volumes clearly reflects the basin's sensitivity to extreme rainfall, where short-duration, high intensity storms generate rapid overland flow before significant infiltration can occur. The spatial correspondence between this outlet and earlier flood susceptibility mapping where the region was categorized as very highly prone to flooding further corroborates the relationship between physiographic conditions and hydrological response. This further validates the flood susceptibility map, in the region where outlet 4 is located falls in very high flood prone zones, which implied that increase in runoff due to floods makes the region prone to flooding and hydrologically sensitive.

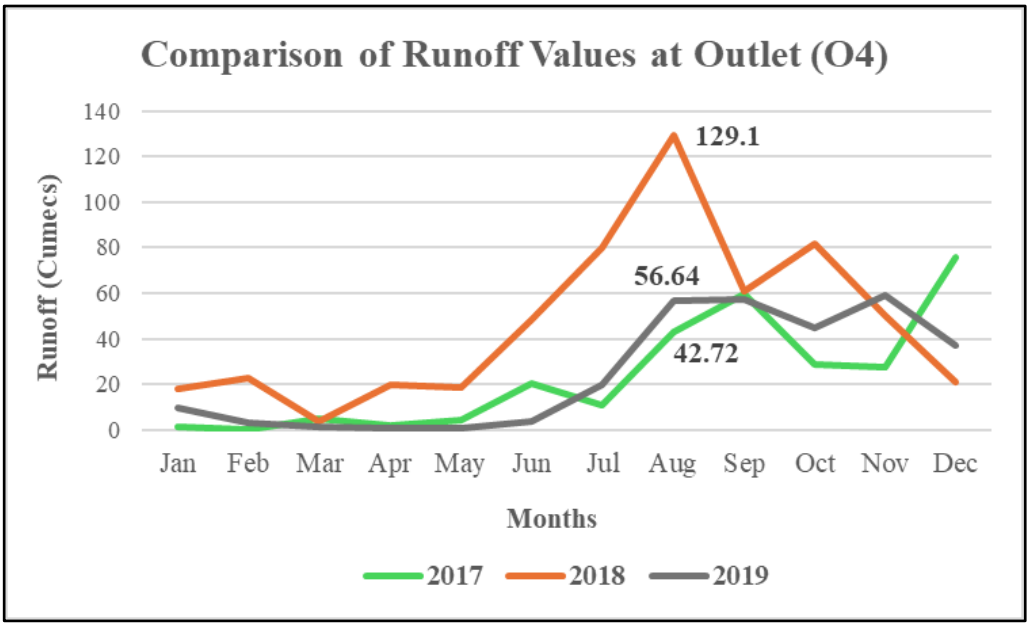

Figure 5.43: Comparison of discharge values at outlet of basin (O4)

A similar pattern was observed at outlet (O2) in the Thodupuzha region as shown in Figure 5.44 and Figure *5.45*. Here, discharge levels increased by nearly 126% during the 2018 flood relative to 2017. The severity of this increase signifies the high runoff potential of the sub-basin and validates earlier spatial analyses that classified Thodupuzha as a hydrologically sensitive and flood-prone zone. The steep terrain, combined with intensive rainfall accumulation, supported rapid saturation and generated substantial overland flow, contributing to the extreme flooding witnessed in the region.

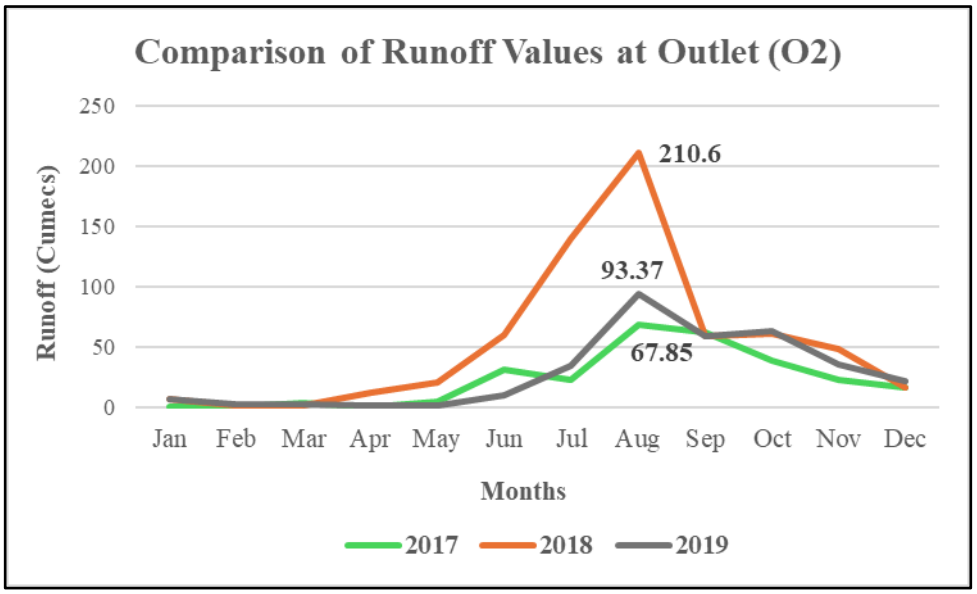

Figure 5.44 : Comparison of Discharge values at outlet of basin (O2)

5.5.5 Assessing the impact of floods on Surface Runoff

The evaluation of flood effects on surface runoff was done by estimating first on the runoff properties in the Periyar River Basin which is the largest and hydrologically important basin in the Idukki district. In order to determine the spatial connection between flooding and the response to runoff, the delineated basin and the selected outlet points were superimposed on the flood prone map as shown in Figure 5.45. To measure the spatial variation in runoff behaviour when the basin was under flood conditions, surface runoff was measured at several outlet points such as O1, O2, O3, O4 and O5 and these were spread around the basin shown in Figure *5.45*. The combined analysis will make it possible to examine the impact of flood prone regions on the generation and distribution of the runoff in detail, which will help identify the hydrologically sensitive areas of the Periyar Basin.

Variability in rainfall patterns, particularly the occurrence of high intensity precipitation over short durations, can strongly influence both flood susceptibility and surface runoff dynamics in mountainous terrains. When rainfall intensity exceeds the infiltration capacity of the soil, excess water rapidly converts into surface runoff, which is then quickly routed through the drainage network. Such conditions often lead to rapid soil saturation, increased stream discharge, and a quicker hydrological response of the watershed. In regions like the Idukki district, characterized by steep slopes, highly dissected terrain, and dense drainage systems, intense rainfall events can significantly amplify runoff generation. Consequently, large volumes of water are conveyed toward basin outlets in a relatively short time, resulting in higher discharge levels and increased potential for flooding in downstream and low-lying areas.

A combined map of flood susceptibility and Periyar river basin indicated different watershed outlets is shown below:

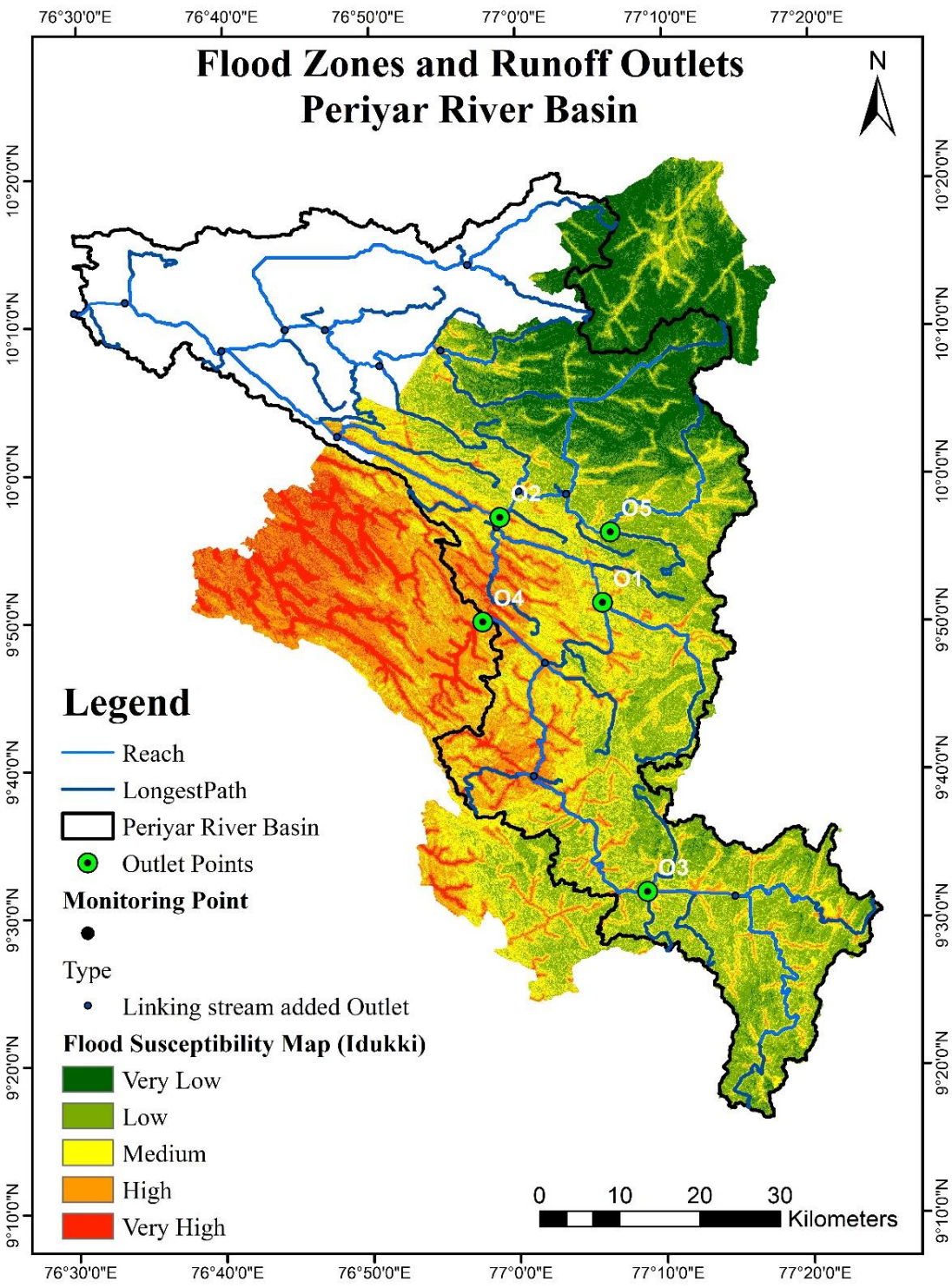

Figure 5.45 : Flood Zones of Idukki district and Periyar River Basin Map

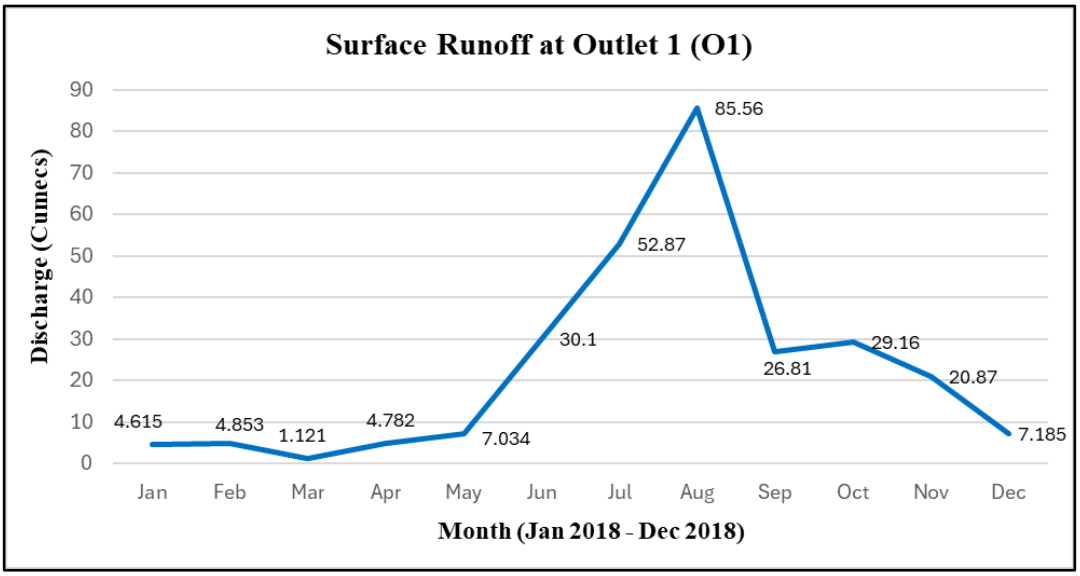

Figure 5.46 : Surface Runoff at Outlet 1 (O1)

- The discharge at Outlet 1 (O1) reaches approximately 85 m^3/s, representing an increase of nearly 40% compared to the preceding month, indicating a pronounced runoff response during the flood period. When examined alongside the flood susceptibility map, this outlet is positioned within a catchment predominantly classified as medium flood prone, suggesting that the elevated surface runoff generated within this zone directly contributes to localized flooding conditions.
- The spatial alignment of the increased discharge with areas designated as medium flood prone indicates that runoff generated within this part of the basin accumulates and channels toward the outlet, amplifying flow volumes during peak rainfall months. This pattern demonstrates that even zones categorized under moderate flood susceptibility are capable of producing considerable runoff when subjected to intense precipitation.

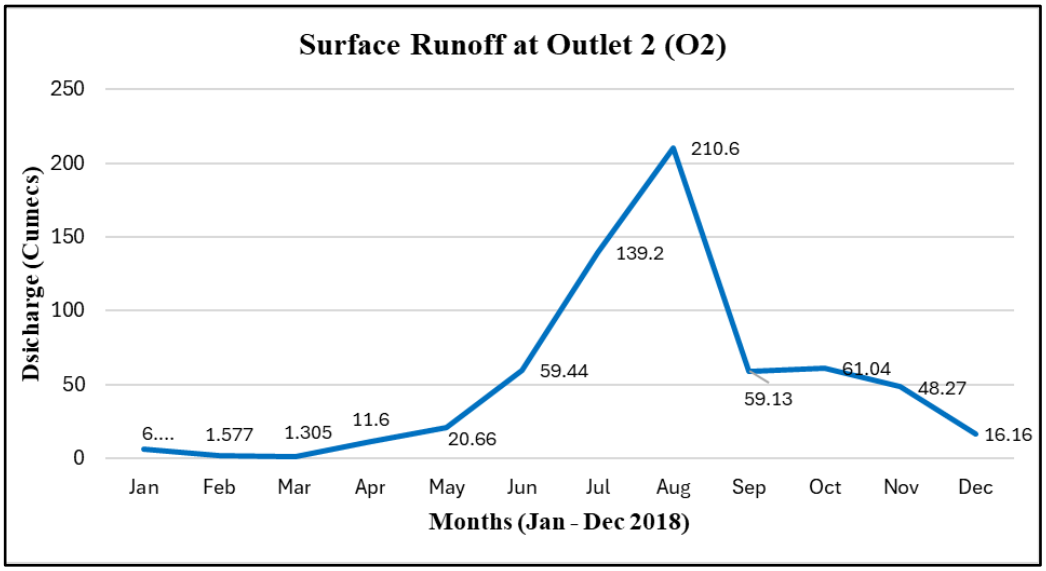

Figure 5.47 : Surface Runoff at Outlet 2 (O2)

- At Outlet 2, located directly along the Periyar River, the SWAT simulation indicates a substantial rise in surface runoff, resulting in high river discharge during the flood period. The flood susceptibility map classifies this river corridor as a very high risk zone, with adjacent areas falling within medium to high susceptibility classes. The concurrence of elevated runoff and mapped flood risk demonstrates how peak flows within the main channel can inundate adjoining low lying areas, highlighting the hydrological sensitivity of settlements and land uses situated along the Periyar floodplain.
- This outlet also falls in the west Thodupuzha block, which shows that this heavy runoff further makes this region more susceptible to flooding which is seen from the flood map also as shown in Figure 5.18 and Figure 5.19.

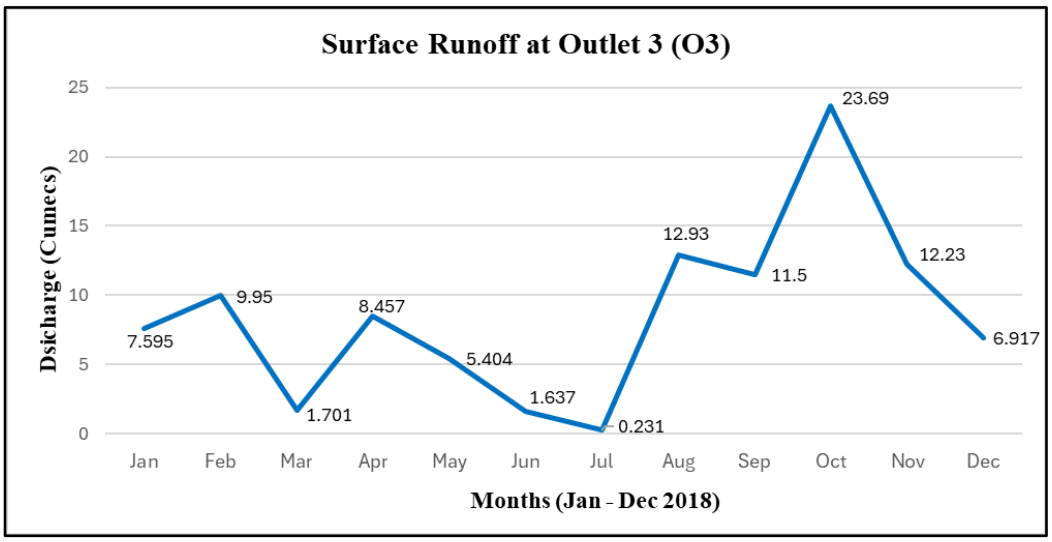

Figure 5.48 : Surface Runoff at Outlet 3 (O3)

- The Runoff at Outlet 3 (O3) corresponds to the location of the Mullaperiyar Dam, where the flood susceptibility classification indicates predominantly low risk zones in the surrounding area as shown in Figure 5.48. The discharge values recorded here remain relatively modest during the main flood month of August 2018, despite intense regional rainfall. The delayed rise in runoff observed later, in October, suggests that the reservoir upstream temporarily retains inflows, slowing the downstream response. In this instance, the presence of the Mullaperiyar dam functions as a regulating barrier, limiting immediate surface runoff and thereby reducing potential flood impacts in nearby areas that are mapped as less susceptible.
- With dam working as a flood control structure, this region lies in mostly low flood prone zones as indicated in Figure 5.45. This further validates that reduced discharge values and flood control structure makes a region less prone to floods which can be seen in this case.

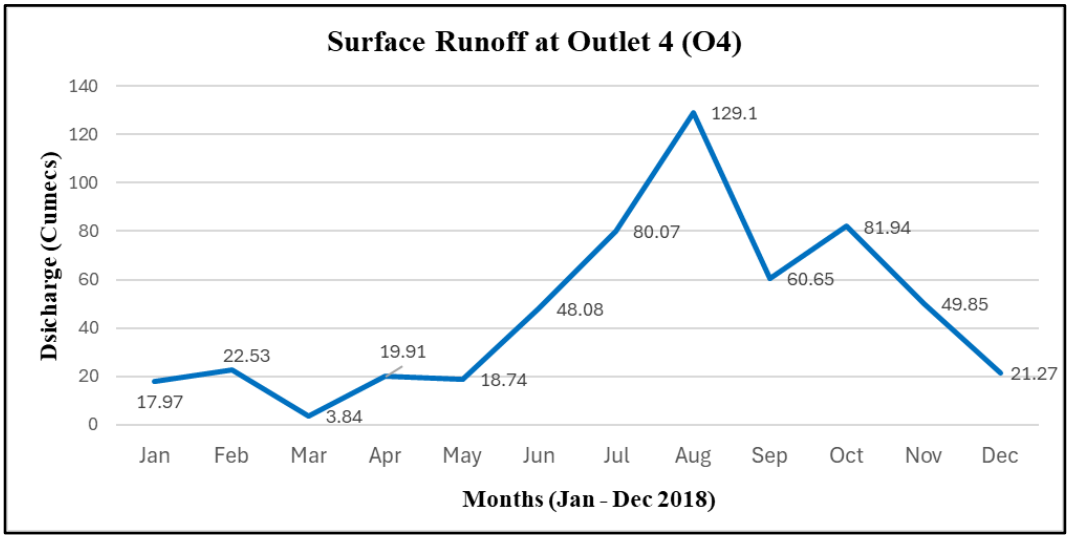

Figure 5.49 : Surface Runoff at Outlet 4 (O4)

- At Outlet 4, situated at the Idukki–Kulamavu reservoir system, the SWAT simulation indicates noticeably elevated surface runoff during the August 2018 flood event. This outlet lies within a zone classified as high to very high flood susceptibility, and the observed rise in reservoir water levels during the event corresponds with the modelled increase in runoff. The alignment between the susceptibility classification and the runoff response suggests that this segment of the basin is highly responsive to peak rainfall, and the spatial overlap reinforces the validity of both the flood mapping and the hydrological simulation outputs.

- The runoff at outlet O4 is found at the Kulamavu Reservoir which is a component of the Idukki Dam system. The high discharge that this outlet represents indicates that in the event of the 2018 flood, water levels in the reservoir will increase rapidly as the large inflows push the water levels to or closer to the Full Reservoir Level. These conditions reflect that water runoff was excessive and added overflow and hydrological stress to the surrounding areas. The Thodupuzha subdivision, located on the north-western of the Idukki district and being a highly flood prone area as shown in Figure *5.19*, recorded a considerable amount of runoff during this period. The evidence of these two in combination with high discharge and flood prone areas indicate that it is indeed a hydrologically sensitive area under extreme rainfall conditions.
- The markedly high runoff observed at this outlet suggests that intense surface flow dominates the hydrological response of the region, limiting effective infiltration and thereby increasing groundwater susceptibility. This relationship is clearly reflected in the Figure 5.45 which shows reduced groundwater potential in this region where the outlet point is located.

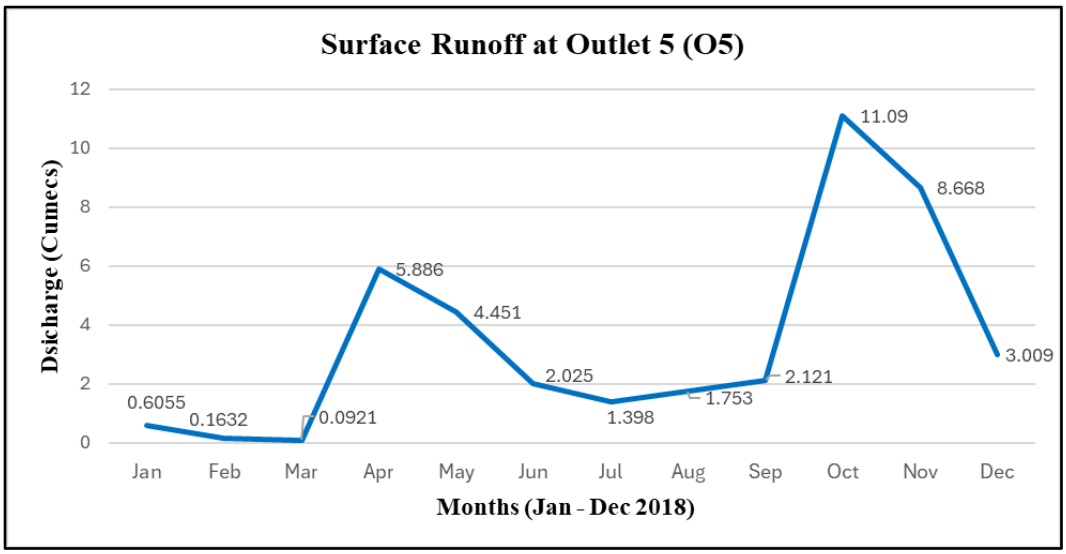

Figure 5.50 : Surface Runoff at Outlet 5 (O5)

- At Runoff Outlet 5 (O5), runoff during August 2018 remains comparatively low, which corresponds well with the flood susceptibility map that classifies the surrounding area as low to medium flood-prone as shown in Figure 5.45. The limited runoff response during the major flood month can be attributed to lower rainfall intensity. However, a noticeable increase in discharge is observed in October 2018, likely reflecting delayed catchment response and higher localized

precipitation later in the monsoon season. Furthermore, this outlet is located within the Udumbanchola region, which is predominantly categorised as a low to medium flood-prone zone as shown in Figure *5.19*. This spatial association indicates that the comparatively lower surface runoff observed at this outlet corresponds well with the reduced flood susceptibility of the surrounding area, thereby reinforcing the relationship between runoff behaviour and flood prone classifications. This pattern highlights the spatial variability of runoff generation in relation to flood susceptibility and rainfall distribution across the district.

Table 5.9 presents the classification of hydrologically sensitive regions in relation to areas identified as high to very high flood-prone zones. Hydrological sensitivity was assessed indirectly by examining peak surface runoff responses in conjunction with upstream catchment characteristics and rainfall intensity. This integrated evaluation allows for the identification of zones where flood susceptibility and runoff dynamics interact most strongly, thereby highlighting regions that exhibit heightened sensitivity to extreme hydrological events.

Table 5.9 Assessment of Hydrological Sensitivity in relation with FPZ

Outlet	**Flood Susceptibility Class**	**Peak Runoff Range (m^3/s)**	**Catchment Characteristics**	**Hydrological Sensitivity**
O1	Medium–High	80–90 m^3/s	Moderate basin size with steeper slopes that promote rapid runoff	Moderately High
O2	Very High	200–230 m^3/s	Large contributing catchment with intense rainfall and steep gradients leading to extreme runoff concentration	Very High / Critical Sensitivity
O3	Low	10–15 m^3/s	Small catchment area with strong reservoir buffering that reduces immediate runoff	Low Sensitivity
O4	High–Very High	>100 m^3/s	Large upstream area with steep terrain and reservoir influence contributing to pronounced runoff peaks	High Sensitivity

O5	Low–Medium	10–20 m^3/s	Smaller basin with lower rainfall inputs, producing subdued runoff response	Low Sensitivity

When expressed in discharge ranges, the runoff behaviour across the outlets continues to reflect the spatial pattern of flood susceptibility within the basin. Outlets positioned within high and very high susceptibility zones display markedly elevated runoff ranges, indicating rapid hydrological response to extreme rainfall events. In contrast, outlets located in low or low to medium susceptibility regions fall within substantially lower runoff ranges, demonstrating reduced flood response potential. Moderate ranges at Outlet 2 highlight the combined influence of high rainfall and gentle slopes, while the limited upstream catchment area restricts the overall discharge magnitude. This range based assessment further reinforces the designation of hydrologically sensitive zones and demonstrates how surface runoff dynamics correspond closely with flood susceptibility mapping.

CHAPTER 6

CONCLUSIONS AND SCOPE FOR FUTURE WORK

6.1 Conclusions

This research was undertaken to comprehensively examine the impacts of flooding on surface and subsurface hydrological processes in the Idukki district of Kerala by integrating flood susceptibility assessment, groundwater potential evaluation, land use and land cover (LULC) change analysis, and hydrological modelling. The study addresses a critical research gap by moving beyond isolated hazard assessment and instead adopting an integrated geospatial–hydrological framework to understand how floods influence multiple environmental components simultaneously in a complex mountainous terrain.

The first objective of the study established a robust flood susceptibility framework for the Idukki district using a GIS-based Analytical Hierarchy Process (AHP). By systematically evaluating important flood conditioning parameters such as slope, rainfall, drainage density, elevation, LULC, soil characteristics, and proximity to river networks, the region was categorised into five flood susceptibility classes spanning from very low to very high. The developed flood susceptibility map was classified into five susceptibility categories namely very low, low, moderate, high, and very high and these classes occupied the areas of 609.0417 km^2, 1222.83 km^2, 1180.45 km^2, 950.48 km^2 and 395.9487 km^2 respectively. The results reveal that more than 30% of the Idukki region is covered with high and very high flood prone zones. The developed flood susceptible map indicates that among all the subdivisions, Thodupuzha and Idukki subdivision falls under very high flood prone zones. Validation using historical flood records and satellite derived flood extents confirmed the reliability of the flood susceptibility map. The AUC value for the flood susceptibility mapping is evaluated as 0.91 or 91%, indicating a high level of predictive accuracy for the employed spatial mapping model. This spatial layer forms the foundation of the study, as it not only identifies flood prone regions but also serves as a critical reference for analysing the cascading impacts of floods on groundwater systems, land use patterns, and surface runoff behaviour.

Building upon this flood susceptibility framework, the second objective focused on delineating groundwater potential zones (GWPZs) using advanced machine learning techniques. By employing Random Forest, AdaBoost, and Gradient Boosting

algorithms with fourteen groundwater conditioning factors, the study demonstrated that groundwater potential in Idukki is spatially heterogeneous and strongly influenced by terrain and structural controls. The RFE analysis highlights that all fourteen conditioning factors contribute to groundwater potential, with lineament density emerging as the most influential. This aligns with the district's fractured and faulted hard-rock terrain, where secondary porosity plays a major role in groundwater storage. While a substantial portion of the district was classified under high to very high groundwater potential zones primarily found in areas of lower elevation regions and in the northern parts of the district, particularly Devikulam taluk, were dominated by low to very low groundwater potential zones. Notably, these areas coincide with regions severely affected by the 2018 flood and landslide events. This spatial correspondence highlights that extreme flooding in mountainous terrains does not necessarily enhance groundwater recharge; instead, it can increase groundwater susceptibility by promoting rapid runoff, erosion, and disruption of recharge pathways. An AUC value of 0.92, an accuracy of 0.88, and a kappa value of 0.76 were obtained by the RF model which is better among the other ML models. The superior performance of the Random Forest model further underscores the reliability of machine learning approaches in groundwater assessment within data-scarce, complex terrains.

The third objective extended the analysis to evaluate flood induced alterations in land use and land cover using satellite imagery. The comparison of pre and post flood LULC scenarios for both 2018 and 2021 floods revealed noticeable transformations in forested and agricultural areas, particularly within zones identified as moderate to very high flood susceptible. The 2018 floods affected approximately 20.86 km^2, influencing built-up (0.48 km^2), forest (10.60 km^2), agricultural (5.11 km^2), and barren (4.67 km^2) areas, whereas the 2021 flood event impacted about 19.24 (km^2) across built-up (0.24 km^2), agricultural (6.23 km^2), barren (2.82 km^2), and forest (9.95 km^2) classes. Several sub-basins exhibited reductions in forest cover and shifts from cultivated land to barren or degraded classes following major flood events. These changes reflect not only the immediate physical impacts of flooding, such as erosion and landslides, but also the longer term influence of repeated flood disturbances combined with human interventions. The close spatial alignment between flood prone zones and LULC changes demonstrates that flooding acts as a key driver of landscape transformation in

Idukki, with direct implications for hydrological response, ecosystem stability, and resource sustainability.

The fourth objective addressed the hydrological consequences of these combined factors by simulating surface runoff and discharge patterns using the SWAT. The calibrated and validated SWAT model successfully captured spatial variations in runoff across the Periyar River Basin, the largest and most hydrologically significant basin in the district. The analysis revealed that sub watersheds located within high to very high flood susceptibility zones consistently exhibited elevated runoff and discharge peaks, particularly during extreme rainfall events. These hydrologically sensitive zones correspond closely with areas experiencing land cover degradation and reduced groundwater potential, reinforcing the interconnected nature of flooding, land use change, and runoff dynamics. The SWAT outputs provide quantitative evidence that alterations in land cover especially deforestation and land degradation which amplify surface runoff and intensify flood risks in mountainous basins.

When viewed collectively, the outcomes of all four objectives highlight a clear and consistent pattern: flood susceptibility, groundwater vulnerability, land use transformation, and surface runoff are tightly interlinked processes in the Idukki district. Flood prone areas are not only more susceptible to surface inundation but also tend to experience reduced groundwater recharge efficiency, increased land degradation, and heightened runoff response. The integration of flood susceptibility mapping with groundwater potential assessment enabled the identification of groundwater susceptibility zones, including favourable recharge areas, mixed response zones, and high to critical susceptibility zones. This integrated interpretation demonstrates that in steep, hard-rock terrains like Idukki, extreme floods often exacerbate groundwater stress rather than alleviating it, contrary to common assumptions in alluvial settings.

Overall, this research demonstrates the effectiveness of combining multi-criteria decision analysis, machine learning models, remote sensing-based LULC assessment, and physically based hydrological modelling within a unified GIS framework. The integrated methodology developed in this study provides a comprehensive understanding of flood driven hydrological processes and their spatial variability in a mountainous environment. Beyond its scientific contributions, the study offers practical insights that can support flood mitigation planning, groundwater

management, land use regulation, and watershed scale interventions aimed at enhancing resilience and long-term water security in flood-prone regions such as Idukki.

6.2 Future Scope of Work

The possible extension of this study would be:

- Future studies may integrate climate change projections to evaluate how changes in rainfall intensity and frequency could influence flood susceptibility, groundwater recharge, and surface runoff dynamics.
- Integration of socio-economic and infrastructure vulnerability indicators may support comprehensive flood risk and resilience assessments for effective disaster management.
- Use of high-resolution and multi-temporal remote sensing datasets can enhance detection of short-term and cumulative land use changes following successive flood events.
- Coupling surface hydrological models with groundwater flow models would allow detailed simulation of surface–subsurface interactions during extreme flood events.

REFERENCES

Abdel Hamid, H.T., 2020. Environmental sensitivity of flash flood hazard using geospatial techniques. *Global Journal of Environmental Science and Management*, 6 (1), 31–46.

Abraham, A. and Kundapura, S. (2022) Spatio-temporal dynamics of land use land cover changes and future prediction using geospatial techniques, *Journal of the Indian Society of Remote Sensing*, 50(11), pp. 2175–2191.

Aggarwal, M., Subbarayan, S., Jeyaseelan, J.J. and Devanantham, A. (2019) Delineation of groundwater potential zones for hard rock region in Karnataka using AHP and GIS, in *IEREK Interdisciplinary Series for Sustainable Development*. Cham: Springer, pp. 315–317.

Ahern, M., Kovats, R.S., Wilkinson, P., Few, R. and Matthies, F. (2005) Global health impacts of floods: epidemiologic evidence, *Epidemiologic Reviews*, 27(1), pp. 36–46.

Ahmad, F., Rashid, I. and Romshoo, S.A. (2017) Impact of floods on land use land cover and water quality of Wular Lake, Kashmir Valley, India, *Environmental Monitoring and Assessment*, 189, 475.

Aladejana, O.A., Kalra, A., Ahmad, S. and Ajayi, V.O. (2020) Assessment of the impact of basin geology and best management practices on streamflow using SWAT model in the Owena River Basin, Nigeria, *Hydrological Sciences Journal*, 65(8), pp. 1351–1366.

Akay, H. and Baduna, M. (2020) Comparison of traditional and multi-criteria decision-making methods for flash flood susceptibility assessment, *Environmental Earth Sciences*, 79, 405.

Anil, S. and Das, S. (2021) Identification of soil erosion-prone sub-watersheds using fuzzy AHP and GIS: a case study of the Agrani watershed, India, *Environmental Monitoring and Assessment*, 193, 411.

Ashfaq, S., Tufail, M., Niaz, A., Muhammad, T., Alzahrani, H. and Tariq, A. (2025) Flood susceptibility assessment and mapping using GIS-based analytical hierarchy process and frequency ratio models: a case study of District Nowshera, Pakistan, *Global and Planetary Change*, 251, 104831.

Arabameri, A., Saha, S., Chen, W., Roy, J., Pradhan, B. and Bui, D.T. (2020). Flash flood susceptibility modelling using functional tree and hybrid ensemble techniques. Journal of Hydrology, 587, 125007.

Arthur, J.D., Wood, H.A.R., Baker, A.E., Cichon, J.R. and Raines, G.L. (2007) Development and implementation of a Bayesian-based aquifer vulnerability assessment in Florida, *Natural Resources Research*, 16(2), pp. 93–107.

Arfasa, G.F., Owusu-Sekyere, E., Doke, D.A. and Aygei Ampofo, J. (2024) Impacts of climate and land use/cover changes on the sustainability of irrigation water in West Africa: a systematic review, *All Earth*, 36(1), pp. 1–13.

Aslam, M., Ye, D., Tariq, A., Asad, M., Hanif, M., Ndzi, D., Chelloug, S. A., Elaziz, M. A., Al-Qaness, M. A. A., and Jilani, S. F. (2022). "Adaptive Machine Learning Based Distributed Denial-of-Services Attacks Detection and Mitigation System for SDN-Enabled IoT." *Sensors, 22(7),* 2697.

Asrade, B. (2024) Groundwater potential zone mapping using GIS-based analytical hierarchy process and frequency ratio models in the Jedeb watershed, Ethiopia, *Arabian Journal of Geosciences*, 17, 214.

Aydin, M., Uysal, M. and Aksoy, B. (2021) Flood hazard zoning using GIS-based analytical hierarchy process: a case study of Bitlis Province, Turkey, *Arabian Journal of Geosciences*, 14, 2147.

Ayadi, Y., Zghibi, A., Mirchi, A., Bouri, S. and Zairi, M. (2024) Integrating geospatial artificial intelligence and GIS for groundwater potential mapping in the Majerda transboundary basin (Tunisia–Algeria), *Environmental Earth Sciences*, 83, 112.

Band, S.S., Janizadeh, S., Pal, S.C., Saha, A., Chakrabortty, R., Melesse, A.M. and Mosavi, A. (2020). Flash flood susceptibility modeling using new approaches of hybrid and ensemble tree-based machine learning algorithms. *Remote Sensing*, 12(21), 3568.

Benito, G., Rico, M., Sánchez-Moya, Y., Sopeña, A., Thorndycraft, V.R., Barriendos, M., 2010. The impact of late Holocene climatic variability and land use change on the flood hydrology of the Guadalentín River, southeast Spain. Glob. Planet. Chang. 70 (1–4), 53–63.

Bera, A., Mukhopadhyay, B.P. and Ghosh, A. (2020) Groundwater potential zone mapping using remote sensing, GIS and analytical hierarchy process in Karha River Basin, Maharashtra, India, *Applied Water Science*, 10, 140.

Bhuyan, M., Jayaram, C., Menon, N.N. and Joseph, K.A. (2020) Satellite-based study of seasonal variability in water quality parameters in a tropical estuary along the southwest coast of India, *Journal of the Indian Society of Remote Sensing*, 48, pp. 1265–1276.

Biswas, S., Das, B., Pal, S.C. and Saha, A. (2020) Groundwater potential zone mapping using GIS, remote sensing and analytical hierarchy process in Uttar Dinajpur district, West Bengal, India, *Sustainable Water Resources Management*, 6, 92.

Bradshaw, C.J.A., Sodhi, N.S., Peh, K.S.-H. and Brook, B.W. (2007). Global evidence that deforestation amplifies flood risk and severity in the developing world. *Global Change Biology*, 13(11), pp. 2379–2395

Breiman, L. (2001) Random Forests, *Machine Learning*, 45(1), pp. 5–32.

Bronstert, A., 2003. Floods and climate change: interactions and impacts. *Risk Analysis*, 23 (3), pp. 545 – 557.

Bui, D. T., Ngo, P. T. T., Pham, T. D., Jaafari, A., Minh, N. Q., Hoa, P. V., and Samui, P. (2019). "A novel hybrid approach based on a swarm intelligence optimized extreme learning machine for flash flood susceptibility mapping." *CATENA, 179,* 184–196.

Catani, F., Lagomarsino, D., Segoni, S. and Tofani, V. (2013) Landslide susceptibility estimation by random forests technique: sensitivity and scaling issues, *Natural Hazards and Earth System Sciences*, 13(11), pp. 2815–2831.

Central Water Commission (CWC) (2018) Study report: Kerala floods of August 2018, Trivandrum: Central Water Commission.

Chakraborty, S., and Mukhopadhyay, S. (2019). "Assessing flood risk using analytical hierarchy process (AHP) and geographical information system (GIS): application in Coochbehar district of West Bengal, India." *Natural Hazards, 99(1),* 247–274.

Chakraborty, S., Mukhopadhyay, S. and Das, S. (2018) Groundwater potential mapping using GIS-based analytical hierarchy process: a case study of Raniganj Block, West Bengal, India, *Arabian Journal of Geosciences*, 11, 117.

Charlton, R., Fealy, R., Moore, S., Sweeney, J. and Murphy, C. (2006). Assessing the impact of climate change on water supply and flood hazard in Ireland using statistical downscaling and hydrological modelling techniques. *Climatic Change*, 74.

Chen, J., Li, Q., Wang, H. and Deng, M. (2020). A machine learning ensemble approach based on random forest and radial basis function neural network for risk evaluation of regional flood disaster: a case study of the Yangtze River Delta, China. *International Journal of Environmental Research and Public Health*, 17(1), 49.

Chen, Y.-R., Yeh, C.-H. and Yu, B. (2011) 'Integrated application of the analytic hierarchy process and the geographic information system for flood risk assessment and flood plain management in Taiwan', *Natural Hazards*, 59, pp. 1261–1276.

Chen, W., Li, H., Hou, E. et al. (2018a) GIS-based groundwater potential analysis using novel ensemble weights-of-evidence with logistic regression and functional tree models, *Science of the Total Environment*, 634, pp. 853–867.

Chen, W., Li, X., Wang, Y. et al. (2014) Forested landslide detection using LiDAR data and the random forest algorithm: a case study of the Three Gorges, China, *Remote Sensing of Environment*, 152, pp. 291–301.

Chen, W., Panahi, M., Khosravi, K. et al. (2019) Spatial prediction of groundwater potentiality using ANFIS ensembled with teaching–learning-based and biogeography-based optimization, *Journal of Hydrology*, 572, pp. 435–448.

Chen, W., Peng, J., Hong, H. et al. (2018b) Landslide susceptibility modelling using GIS-based machine learning techniques for Chongren County, Jiangxi Province, China, *Science of the Total Environment*, 626, pp. 1121–1135.

Chenini, I., Mammou, A.B. and May, M.E. (2010) Groundwater recharge zone mapping using GIS-based multi-criteria analysis: a case study in Central Tunisia (Maknassy Basin), *Water Resources Management*, 24, pp. 921–939.

Chung, J.W. and Rogers, J.D. (2012). Interpolations of groundwater table elevation in dissected uplands, *Groundwater*, 50(4), pp. 598–607.

Chu, H., Wu, W., Wang, Q.J., Nathan, R. and Wei, J. (2020) 'An ANN-based emulation modelling framework for flood inundation modelling: Application, challenges and future directions', *Environmental Modelling & Software*, 124, 104587.

Conforti, M., Pascale, S., Robustelli, G. and Sdao, F. (2014) Evaluation of prediction capability of artificial neural networks for mapping landslide susceptibility in the Turbolo River catchment (northern Calabria, Italy), *Catena*, 113, pp. 236–250.

Danandeh Mehr, A. and Kahya, E. (2017) 'A Pareto-optimal moving average multigene genetic programming model for daily streamflow prediction', *Journal of Hydrology*, 549, pp. 603–615.

Danumah, J.H., Odai, S.N., Saley, B.M., Szarzynski, J., Thiel, M., Kwaku, A., Kouame, F.K. and Akpa, L.Y. (2016) 'Flood risk assessment and mapping in Abidjan district using multi-criteria analysis (AHP) model and geoinformation techniques (Côte d'Ivoire)', *Geoenvironmental Disasters*, 3(1), p. 10.

Das, S. (2019) Flood risk mapping and vulnerability assessment of the western coastal region of India using analytical hierarchy process and geospatial techniques, *Natural Hazards*, 98(2), pp. 617–642.

Das, S. and Gupta, A. (2021) Multi-criteria decision-based geospatial mapping of flood susceptibility and temporal hydro-geomorphic changes in the Subarnarekha River basin, India, *Geoscience Frontiers*, 12(6), 101206.

Das, S. and Pardeshi, S.D. (2018) 'Comparative analysis of lineaments extracted from Cartosat, SRTM and ASTER DEM: a study based on four watersheds in Konkan region, India', *Spatial Information Research*, 26(1), pp. 47–57.

Das, S. (2018) 'Geographic information system and AHP-based flood hazard zonation of Vaitarna basin, Maharashtra, India', *Arabian Journal of Geosciences*, 11(19), p. 576.

Das, S. (2019) 'Geospatial mapping of flood susceptibility and hydro-geomorphic response to the floods in Ulhas basin, India', *Remote Sensing Applications: Society and Environment*, 14, pp. 60–74.

Das, S. and Pal, S.C. (2020) Groundwater vulnerability assessment using AHP and fuzzy logic: a case study of Ghoghat-I and II Blocks, West Bengal, India, *Environmental Monitoring and Assessment*, 192, 602.

Desalegn, H. and Mulu, A. (2020) Flood inundation mapping using HEC-RAS and GIS: a case study of the Fetam River, Ethiopia, *SN Applied Sciences*, 2, 1778.

Department of Mining and Geology (2016) District survey report of minor minerals (except river sand), Thiruvananthapuram, Government of Kerala.

Devanantham, A. and Subbarayan, S. (2021). Assessment of land use and land cover change detection and prediction using remote sensing and CA–Markov in the northern coastal districts of Tamil Nadu, India. *Environmental Science and Pollution Research*, 29.

Devanantham, A., Subbarayan, S., Singh, L. et al. (2020) GIS-based multi-criteria analysis for identification of potential groundwater recharge zones: a case study from Ponnaniyaru watershed, Tamil Nadu, India, *HydroResearch*, 3(1), pp. 1–14.

Devanantham, A., Subbarayan, S., Singh, L., Jennifer, J.J., Saranya, T. and Parthasarathy, K.S.S. (2020). GIS-based multi-criteria analysis for identification of potential groundwater recharge zones: a case study from the Ponnaniyaru watershed, Tamil Nadu, India. *HydroResearch*, 3, pp. 1–14.

Dodangeh, E., Choubin, B., Eigdir, A.N., Nabipour, N., Panahi, M., Shamshirband, S. and Mosavi, A. (2020) 'Integrated machine learning methods with resampling algorithms for flood susceptibility prediction', *Science of the Total Environment*, 705, 135983.

Doke, A., Zolekar, R.B., Patel, H. et al. (2021) Groundwater potential zone mapping using GIS-based analytical hierarchy process in the Ulhas Basin, Maharashtra, India, *Environmental Earth Sciences*, 80, 423.

Dottori, F, Szewczyk, W, Ciscar, JC, Zhao, F, Alfieri, L, Hirabayashi, Y, Bianchi, A, Mongelli, I, Frieler, K, Betts, RA & Feyen, L 2018, 'Increased human and economic losses from river flooding with anthropogenic warming', *Nature Climate Change*, vol. 8, no. 9, pp. 781-786.

Dou, X., Song, J., Wang, L., Tang, B., Xu, S., Kong, F. and Jiang, X. (2018) 'Flood risk assessment and mapping based on a modified multi-parameter flood hazard index model in the Guanzhong Urban Area, China', *Stochastic Environmental Research and Risk Assessment*, 32(4), pp. 1131–1146

E.E. Koks, B. Jongman, T.G. Husby, W.J.W. Botzen, combining hazard, exposure and social vulnerability to provide lessons for flood risk management, *Environmental Science & Policy*, Volume 47, 2015, pp. 42-52.

Elmahdy, S. I. and Mohamed, M. M. (2014) 'Groundwater potential modelling using remote sensing and GIS: a case study of the Al Dhaid area, United Arab Emirates', *Geocarto International*, 29(4), pp. 433–450. doi: 10.1080/10106049.2013.784366.

El Jazouli, A., Barakat, A. and Khellouk, R. (2019) 'GIS-multicriteria evaluation using AHP for landslide susceptibility mapping in Oum Er Rbia high basin (Morocco)', *Geoenvironmental Disasters*, 6(1), p. 3.

Freund, Y. and Schapire, R.E. (1997) A decision-theoretic generalization of on-line learning and an application to boosting, Journal of Computer and System Sciences, 55(1), pp. 119–139.

Freund, Y. and Schapire, R.E. (1995) A decision-theoretic generalization of on-line learning and an application to boosting, in Proceedings of the Second European Conference on Computational Learning Theory, pp. 23–37.

Friedman, J.H. (2002) Stochastic gradient boosting, Computational Statistics and Data Analysis, 38(4), pp. 367–378.

Gabriels, K., Willems, P. and Van Orshoven, J. (2022) 'A comparative flood damage and risk impact assessment of land use changes', *Natural Hazards and Earth System Sciences*, 22(2), pp. 395–410.

Gebrechorkos, S.H., Bernhofer, C. and Hülsmann, S. (2020) Climate change impact assessment on the hydrology of a large river basin in Ethiopia using a local-scale climate modelling approach, *Science of the Total Environment*, 742, 140504.

George, S.L., Kantamaneni, K., Rasme, A.V., Prasad, K.A., Shekhar, S., Panneer, S., Rice, L. and Balasubramani, K. (2022) 'A multi-data geospatial approach for understanding flood risk in the coastal plains of Tamil Nadu, India', *Earth*, 3(1), pp. 383–400.

Gidey, E., Dikinya, O., Sebego, R., Segosebe, E. and Zenebe, A. (2017) Cellular automata and Markov chain (CA–Markov) model-based predictions of future land use and land cover scenarios (2015–2033) in Raya, northern Ethiopia, *Modeling Earth Systems and Environment*, 3, pp. 1245–1262.

Giovannettone, J., Sangameswaran, S., Maderia, C. and Batten, B. (2020) 'Spatial analysis of flood susceptibility throughout Currituck County, North Carolina', *Journal of Hydrologic Engineering*, 25(8), 05020021.

Ghazavi, R., Vali, A. and Eslamian, S. (2012) Impact of flood spreading on groundwater level variation and groundwater quality in an arid environment, *Water Resources Management*, 26(6), pp. 1651–1665.

Ghoraba, S.M. (2015) Hydrological modelling of Simly Dam watershed using ArcSWAT, *Alexandria Engineering Journal*, 54(3), pp. 583–594.

GSI (2006) Geological Survey of India: District Resource Map of Kerala. https://www.gsi.gov.in/webcenter/portal/OCBIS

Golkarian, A., Naghibi, S.A., Kalantar, B. and Pradhan, B. (2018) Groundwater potential mapping using C5.0, random forest and multivariate adaptive regression spline models in GIS, *Environmental Monitoring and Assessment*, 190(3), 149.

Gupta, L. and Dixit, J. (2022) 'A GIS-based flood risk mapping of Assam, India, using the MCDA-AHP approach at the regional and administrative level', *Geocarto International*, 37(26), pp. 11867–11899.

Gupta, M. and Srivastava, P.K. (2010) Integrating GIS and remote sensing for identification of groundwater potential zones in the hilly terrain of Pavagarh, Gujarat, India, *Water International*, 35(2), pp. 233–245.

Hadipour, V., Vafaie, F. and Deilami, K. (2020) 'Coastal flooding risk assessment using a GIS-based spatial multi-criteria decision analysis approach', *Water*, 12(9), 2379.

Hamlat, A., Kadri, C.B., Guidoum, A. and Bekkaye, H. (2021). Flood hazard areas assessment at a regional scale in M'zi Wadi Basin, Algeria. Journal of African Earth Sciences, 182, 104281.

Hamdani, M. and Baali, A. (2020) Groundwater potential mapping using GIS-based analytical hierarchy process in the Central Middle Atlas, Morocco, *Arabian Journal of Geosciences*, 13, 1095.

Hallouz, F., Meddi, M. and Zeroual, A. (2018) Application of SWAT model for runoff and sediment yield simulation in the Harraza basin, northwestern Algeria, *Arabian Journal of Geosciences*, 11, 407

Hasan, M.M. and Wyseure, G. (2018) Hydrological modelling using SWAT to assess climate change impacts on hydropower generation in the Jubones River Basin, Ecuador, *Hydrological Sciences Journal*, 63(8), pp. 1125–1143.

Haq, M., Akhtar, M., Muhammad, S. et al. (2013) Techniques of remote sensing and GIS for flood monitoring and damage assessment: a case study of Sindh Province, Pakistan, *Egyptian Journal of Remote Sensing and Space Science*, 16(2), pp. 135–141.

Herman, E., Abdallah, A., Abdelaziz, R. and El-Mahdy, M. (2021) Assessment and mitigation of flash floods using optical and radar remote sensing in Ras Gharib, Egypt, *Remote Sensing Applications: Society and Environment*, 22, 100493.

Himanshu, S., Pandey, A. and Shrestha, P. (2016) Application of SWAT in an Indian river basin for modeling runoff, sediment and water balance, *Environmental Earth Sciences*, 76(1), p. 3.

Houze, R.A., McMurdie, L.A., Rasmussen, K.L., Kumar, A. and Chaplin, M.M. (2017) 'Multiscale aspects of the storm producing the June 2013 flooding in Uttarakhand, India', *Monthly Weather Review*, 145(11), pp. 4447–4466

Hsu, T.-W., Shih, D.-S., Li, C.-Y., Lan, Y.-J. and Lin, Y.-C. (2017). 'A study on coastal flooding and risk assessment under climate change in the mid-western coast of Taiwan', *Water*, 9(6), 390

Hunt, K.M.R. and Menon, A. (2020). 'The 2018 Kerala floods: a climate change perspective', *Climate Dynamics*, 54, pp. 2433–2446.

Hunt, C.E. (2007) Thirsty planet: strategies for sustainable water development, Academic Foundation, New Delhi.

Islam, A.R.M.T., Rahman, M.M., Siddique, M.A.B. and Dewan, A. (2021) Flood susceptibility mapping using machine learning models in the Teesta River basin, Bangladesh, *Sustainable Water Resources Management*, 7, 48.

Jacinth Jennifer, J. and Saravanan, S. (2022). 'Artificial neural network and sensitivity analysis in the landslide susceptibility mapping of Idukki district, India', *Geocarto International*, 37(19), pp. 5693–5715

Jesudasan, J.J. (2022) Feature elimination and comparison of machine learning algorithms in landslide susceptibility mapping, *Environmental Earth Sciences*, 81(11), 320.

Jena, S.K., Mishra, P. and Sahoo, S. (2020) Groundwater recharge and storage potential mapping using GIS, remote sensing and AHP, *Journal of Hydrology: Regional Studies*, 28, 100673.

Jia, Y., Zhang, J., Guo, E. et al. (2019) Integrated flood risk assessment based on fuzzy variable set theory and analytical hierarchy process in Henan Province, China, *Natural Hazards*, 95(3), pp. 999–1021.

Jha, A.K., Bloch, R. and Lamond, J. (2012) Cities and flooding: A guide to integrated urban flood risk management for the 21st century, World Bank Publications, Washington, DC.

Joseph, J.K., Anand, D., Prajeesh, P., Zacharias, A., Varghese, A.G., Pradeepkumar, A.P. and Baiju, K.R. (2020) Community resilience mechanism in an unexpected extreme weather event: an analysis of the Kerala floods of 2018, India, *International Journal of Disaster Risk Reduction*, 49, 101741.

Kader, Z., Islam, M.R., Aziz, M.T., Hossain, M.M., Islam, R., Miah, M. and Wan Jaafar, W.Z. (2024) GIS and AHP-based flood susceptibility mapping: a case study of Bangladesh, *Sustainable Water Resources Management*, 10(5), 170.

Kazakis, N., Kougias, I. and Patsialis, T. (2015) Assessment of flood hazard areas at a regional scale using an index-based approach and analytical hierarchy process: Application in the Rhodope–Evros region, Greece, *Science of the Total Environment*, 538, pp. 555–563.

Kearns, M. and Valiant, L. (1994) Cryptographic limitations on learning Boolean formulae and finite automata, *Journal of the ACM*, 41(1), pp. 67–95.

Kerala State Disaster Management Authority (KSDMA) (2022) *Annual report*. Thiruvananthapuram: Government of Kerala.

Koç, G., Özdemir, A. and Şen, Z. (2020) Flood risk prioritisation of Istanbul districts using fuzzy AHP, *Natural Hazards*, 104(3), pp. 2871–2896.

Kraus, C.N., Bonnet, M.P., Nogueira, I.S., Lobo, M.T.M.P.S., Marques, D.M., Garnier, J. and Vieira, L.C.G. (2019) Unraveling flooding dynamics and nutrients' controls upon phytoplankton functional dynamics in Amazonian floodplain lakes, *Water*, 11(1), 154.

Kron, W. (2002) Keynote lecture: flood risk = hazard × exposure × vulnerability, in *Proceedings of the Flood Defence Conference*, Science Press, New York, pp. 1–9.

Kron, W. (2005) 'Flood Risk = Hazard • Values • Vulnerability', *Water International*, 30(1), pp. 58–68.

Kuhn, M. (2015) caret: classification and regression training, *Astrophysics Source Code Library*, ascl:1505.003.

Landis, J.R. and Koch, G.G. (1977) The measurement of observer agreement for categorical data, *Biometrics*, 33(1), pp. 159–174.

Lei, X., Chen, W., Avand, M., Janizadeh, S., Kariminejad, N., Shahabi, H., Costache, R., Shirzadi, A. and Mosavi, A. (2020) GIS-based machine learning algorithms for gully erosion susceptibility mapping in a semi-arid region of Iran, *Remote Sensing*, 12(15), 2478.

Li, J., Heap, A.D., Potter, A. and Daniell, J.J. (2011) Application of machine learning methods to spatial interpolation of environmental variables, *Environmental Modelling and Software*, 26(12), pp. 1647–1659.

Lillesand, T.M. and Kiefer, R.W. (1979) *Remote sensing and image interpretation*. New York: John Wiley & Sons.

Lim, J. and Lee, K. (2017) Investigating flood susceptible areas in inaccessible regions using remote sensing and geographic information system, *Environmental Monitoring and Assessment*, 189, 96.

Liu, Y., Lu, C., Yang, X., Wang, Z. and Liu, B. (2020) Fine-scale coastal storm surge disaster vulnerability and risk assessment model: A case study of Laizhou Bay, China, *Remote Sensing*, 12, 1301.

Lyubimova, T., Lepikhin, A., Parshakova, Y. and Tiunov, A. (2016) The risk of river pollution due to washout from contaminated floodplain water bodies during periods of high magnitude floods, *Journal of Hydrology*, 534, pp. 579–589.

Mahato, S., Pal, S., Talukdar, S., Saha, T.K. and Mandal, P. (2021) Field-based index of flood vulnerability (IFV): A new validation technique for flood susceptible models, *Geoscience Frontiers*, 12(5), 101175.

Mahmoud, S.H. and Gan, T.Y. (2018) Multi-criteria approach to develop flood susceptibility maps in arid regions of the Middle East, *Journal of Cleaner Production*, 196, pp. 216–229

Mahmood, S., Sajjad, A. and Atta-ur Rahman (2021) Cause and damage analysis of 2010 flood disaster in district Muzaffar Garh, Pakistan, *Natural Hazards: Journal of the International Society for the Prevention and Mitigation of Natural Hazards*, 107(2), pp. 1681–1692.

Mandal, B. and Mandal, S. (2018) Analytical hierarchy process (AHP) based landslide susceptibility mapping of Lish River basin of Eastern Darjeeling Himalaya, India, *Advances in Space Research*, 62, pp. 3114–3132.

Meles, M.B., Younger, S.E., Jackson, C.R., Du, E. and Drover, D. (2020) Wetness index based on landscape position and topography (WILT): Modifying TWI to reflect landscape position, *Journal of Environmental Management*, 255, 109863.

Meyer, V., Kuhlicke, C., Luther, J., Fuchs, S., Priest, S., Dorner, W., Serrhini, K., Pardoe, J., McCarthy, S., Seidel, J., Palka, G., Unnerstall, H., Viavattene, C. and Scheuer, S. (2012) Recommendations for the user-specific enhancement of flood maps, *Natural Hazards and Earth System Sciences*, 12(5), pp. 1701–1716

Moghaddam, D.D., Pourghasemi, H.R. and Rahmati, O. (2019) Assessment of the contribution of geo-environmental factors to flood inundation in a semi-arid region of SW Iran, in *GIS-Based Spatial Modeling Using Data Mining Techniques*, Springer, Cham, pp. 59–78.

Moghaddam, D.D., Rezaei, M., Pourghasemi, H.R. et al. (2015) Groundwater spring potential mapping using bivariate statistical model and GIS in the Taleghan Watershed, Iran, *Arabian Journal of Geosciences*, 8(2), pp. 913–929.

Mohebzadeh, H., Biswas, A., Rudra, R. and Daggupati, P. (2022) Machine learning techniques for gully erosion susceptibility mapping: a review, *Geosciences*, 12(12), 429.

Msabi, M.M. and Makonya, S. (2020) Flood susceptibility mapping using GIS-based analytical hierarchy process: a case study of Dodoma Region, Tanzania, *Physics and Chemistry of the Earth*, 118, 102900.

Mukherjee, I. and Singh, U.K. (2020) Delineation of groundwater potential zones using GIS and analytical hierarchy process in Birbhum District, eastern India, *Sustainable Water Resources Management*, 6, 67.

Muthu, R. and Sadalaimuthu, R. (2021) Groundwater potential zone mapping using remote sensing, GIS and analytical hierarchy process in Pattukottai Taluk, Tamil Nadu, India, *Arabian Journal of Geosciences*, 14, 1924.

Murthy, K.S.R. and Mamo, A.G. (2009) multi-criteria decision evaluation in groundwater zones identification in Moyale–Teltele sub-basin, South Ethiopia, *International Journal of Remote Sensing*, 30(11), pp. 2729–2740.

Mirlas, V., Kulagina, N. and Hadas, A. (2022) Field experimental study on infiltration and soil clogging processes in river basin soils, *Sustainability*, 14(23), pp. 15645–15658.

Mishra, V., Aadhar, S., Shah, H., Kumar, R., Pattanai, D.R. and Tiwari, A.D. (2018) The Kerala flood of 2018: combined impact of extreme rainfall and reservoir storage, *Hydrology and Earth System Sciences*.

Naghibi, S.A., Ahmadi, K. and Daneshi, A. (2017) Application of support vector machine, random forest and genetic algorithm optimized random forest models in groundwater potential mapping, *Water Resources Management*, 31(9), pp. 2761–2775.

Naghibi, S.A., Pourghasemi, H.R. and Dixon, B. (2016) GIS-based groundwater potential mapping using boosted regression tree, classification and regression tree and random forest models in Iran, *Environmental Monitoring and Assessment*, 188(1), 44.

Nampak, H., Pradhan, B. and Manap, M.A. (2014) Application of GIS-based evidential belief function model to predict groundwater potential zonation, *Journal of Hydrology*, 513, pp. 283–300.

NBSS, (1996). Soil Map of Kerala. National Bureau of Soil Science and Land Use Planning. https://nbsslup.icar.gov.in/

Neumann, B., Vafeidis, A.T., Zimmermann, J. and Nicholls, R.J. (2015) Future coastal population growth and exposure to sea-level rise and coastal flooding – a global assessment, *PLoS ONE*, 10(3), e0118571.

Nones, M. (2019) Dealing with sediment transport in flood risk management, *Acta Geophysica*, 67, pp. 677–685. https://doi.org/10.1007/s11600-019-00273-7

Natarajan, M., Kumar, A. and Kumar, S. (2021) Flood susceptibility mapping using frequency ratio model: a case study of Chennai Corporation, India, *Natural Hazards*, 106(1), pp. 1–25.

Nigussie, T., Yilma, S. and Moges, M.A. (2019) Groundwater potential zone mapping using GIS-based analytical hierarchy process in the Ketar watershed, Main Ethiopian Rift, *Hydrogeology Journal*, 27(6), pp. 2135–2152.

Nugroho, H., Sudaryanto, S., Hidayat, R. and Pradhan, B. (2024) Groundwater potential mapping using random forest, support vector machine and artificial neural networks in West Java, Indonesia, *Hydrogeology Journal*, 32(2), pp. 421–439.

Nsangou, D., Kpoumié, A., Mfonka, Z., Ndzié, J.P. and Ndzié, E. (2021) Flood susceptibility assessment using the analytical hierarchy process in the Mfoundi catchment, Cameroon, *Natural Hazards*, 108(3), pp. 2607–2631.

Odewole, O.O., Ojo, O.I. and Akinluyi, F.O. (2020) Assessment of pre- and post-flood land cover changes along Hadejia–Tiga floodplain using Sentinel-2 data, *Remote Sensing Applications: Society and Environment*, 19, 100349

Olabanji Aladejana et al. (2021) Flood investigation and adaptation strategies through best management practices in an ungauged basin in Southwest Nigeria, *African Geographical Review*, 40(2), pp. 141–162

Oh, H.J., Kim, Y.S., Choi, J.K. et al. (2011) GIS mapping of regional probabilistic groundwater potential in the area of Pohang City, Korea, *Journal of Hydrology*, 399(3–4), pp. 158–172.

Olden, J.D., Lawler, J.J. and Poff, N.L. (2008) Machine learning methods without tears: a primer for ecologists, *Quarterly Review of Biology*, 83(2), pp. 171–193.

Osei, B.K., Ahenkorah, I., Ewusi, A. and Forkuo, E.K. (2021) Flood susceptibility mapping using GIS techniques in the Tarkwa mining area, Ghana, *Arabian Journal of Geosciences*, 14, 1832.

Osei, M.A., Amekudzi, L.K., Wemegah, D.D. and Preko, K. (2019) Hydrological modelling of land use land cover change impacts on streamflow and water balance using SWAT: a case study of the Owabi catchment, Ghana, *Modeling Earth Systems and Environment*, 5, pp. 1031–1046.

Ozdemir, A. (2011) Using a binary logistic regression method and GIS for evaluating groundwater spring potential in the Sultan Mountains (Aksehir, Turkey), *Journal of Hydrology*, 405(1–2), pp. 123–136.

Pascale, S., Parisi, S., Mancini, A. et al. (2013) Landslide susceptibility mapping using artificial neural network in urban areas of southern Italy, in *Computational Science and Its Applications – ICCSA 2013*, Springer, Berlin, Heidelberg, pp. 473–488.

Pavelic, P., Brindha, K., Amarnath, G. et al. (2012) Controlling floods and droughts through managed aquifer recharge: evidence from the Chao Phraya River Basin, Thailand, *Journal of Hydrology*, 468–469, pp. 188–201.

Patra, S., Mishra, P. and Mahapatra, S.C. (2017) Delineation of groundwater potential zones using analytical hierarchy process and GIS in Hooghly District, West Bengal, India, *Hydrological Sciences Journal*, 62(3), pp. 486–501.

Pourghasemi, H.R. and Kerle, N. (2016) Random forests and evidential belief function-based landslide susceptibility assessment in western Mazandaran Province, Iran, *Environmental Earth Sciences*, 75(3), 185.

Pal, S. and Ziaul, S. (2017) Detection of land use and land cover change and land surface temperature in English Bazar urban centre, *Egyptian Journal of Remote Sensing and Space Science*, 20(1), pp. 125–145.

Paranunzio, R., Guerrini, M., Dwyer, E., Alexander, P.J. and O'Dwyer, B. (2022) Assessing coastal flood risk in a changing climate for Dublin, Ireland, *Journal of Marine Science and Engineering*, 10(11), 1715.

Parthasarathy, K.S.S., Deka, P.C., Saravanan, S., Abijith, D. and Jacinth Jennifer, J. (2021) Assessing the impact of 2018 tropical rainfall and the consecutive flood-related damages for the state of Kerala, India, *Disaster Resilience and Sustainability*, Elsevier, pp. 379–395.

Pathan, A.I., Agnihotri, P.G., Said, S. et al. (2022) AHP and TOPSIS based flood risk assessment: a case study of the Navsari City, Gujarat, India, *Environmental Monitoring and Assessment*, 194, 509.

Paul, G.C., Saha, S. and Hembram, T.K. (2019) Application of the GIS-based probabilistic models for mapping the flood susceptibility in Bansloi sub-basin of Ganga–Bhagirathi River and their comparison, *Remote Sensing of Earth Systems Sciences*, 2(2–3), pp. 120–146.

Pourali, S.H., Arrowsmith, C. and Chrisman, N. et al. (2016) Topographic wetness index application in flood-risk-based land use planning, *Applied Spatial Analysis and Policy*, 9, pp. 39–54.

Pradhan, B. and Youssef, A.M. (2011) A 100-year maximum flood susceptibility mapping using integrated hydrological and hydrodynamic models: Kelantan River Corridor, Malaysia, *Journal of Flood Risk Management*, 4(3), pp. 189–202.

Pramanick, N., Acharyya, R., Mukherjee, S., Pal, I., Mitra, D. and Mukhopadhyay, A. (2022) SAR based flood risk analysis: a case study Kerala flood 2018, *Advances in Space Research*, 69(4), pp. 1915–1929.

Pourtaghi, Z.S. and Pourghasemi, H.R. (2014) GIS-based groundwater spring potential assessment and mapping in the Birjand Township, Iran, *Hydrogeology Journal*, 22(3), pp. 643–662.

Pradhan, A.M.S., Kim, Y.T., Shrestha, S. et al. (2021) Application of deep neural network to capture groundwater potential zones in mountainous terrain, Nepal Himalaya, *Environmental Science and Pollution Research*, 28(14), pp. 18501–18517.

Prasad, P., Loveson, V.J., Kotha, M. and Yadav, R. (2020) Application of machine learning techniques in groundwater potential mapping along the west coast of India, *GIScience and Remote Sensing*, 57(6), pp. 735–752.

Pulvirenti, L., Pierdicca, N., Chini, M. and Guerriero, L. (2011) An algorithm for operational flood mapping from synthetic aperture radar (SAR) data using fuzzy logic, *Natural Hazards and Earth System Sciences*, 11(2), pp. 529–540

Rehman, S., Kazmi, J.H. and Khan, M.M. (2016) Flood impact assessment using Landsat-8 OLI imagery in Upper Sindh, Pakistan, *Natural Hazards*, 84(3), pp. 1537–1558.

Rahman, M., Chen, N., Mahmud, G.I., Islam, M.M., Pourghasemi, H.R., Ahmad, H., Habumugisha, J.M., Washakh, R.M.A., Alam, M., Liu, E., Han, Z., Ni, H., Shufeng, T. and Dewan, A. (2021) Flooding and its relationship with land cover change, population growth, and road density, *Geoscience Frontiers*, 12(6), 101224.

Rajasekhar, M., Raju, G.S. and Reddy, B. (2019) Identification of groundwater potential zones using remote sensing and GIS techniques, *Journal of the Geological Society of India*, 94(3), pp. 287–296.

Rajesh, J., Prasad, R. and Kumar, A. (2021) Groundwater potential zone delineation using GIS-based analytical hierarchy process in the Godavari River Basin, India, *Environmental Monitoring and Assessment*, 193, 534.

Ramasamy, S., Gunasekaran, S., Saravanavel, J. et al. (2020) Geomorphology and landslide proneness of Kerala, India: a geospatial study, *Landslides*, 17(11), pp. 2579–2596.

Rebouh, R., Benhamouche, S., Khellouk, R. and Barakat, A. (2024) Flood susceptibility mapping using GIS-AHP, remote sensing and Google Earth Engine: a case study of Ain Smara, Algeria, *Journal of African Earth Sciences*, 206, 104982.

Ren, X., Zhang, S., Li, Y. and Wang, Q. (2020) Influence of infiltration rate changes on runoff generation processes, *Geoderma*, 370, pp. 114347–114358.

Resmi, R., Krishnakumar, A. and Anoop Krishnan, K. (2025) Groundwater chemistry and quality of the Lower Chalakudy River Basin, India during extreme climatic events: lessons to understand for evolving future mitigation measures in the Western Ghats, India, *Cleaner Water*, 100196.

Riley, S.J., DeGloria, S.D. and Elliot, R. (1999) A terrain ruggedness index that quantifies topographic heterogeneity, *Intermountain Journal of Sciences*, 5(1–4), pp. 23–27.

Rodrigues, M. and de la Riva, J. (2014) An insight into machine-learning algorithms to model human-caused wildfire occurrence, *Environmental Modelling and Software*, 57, pp. 192–201.

Saha, A.K. and Agrawal, S. (2020) Mapping and assessment of flood risk in Prayagraj district, India using GIS and AHP, Nanotechnology for Environmental Engineering, 5, 11.

Saranya, T. and Saravanan, S. (2020) Groundwater potential zoning using GIS-AHP approach in Kancheepuram District, Tamil Nadu, India, *Sustainable Water Resources Management*, 6, 56.

Shadmaan, M. and Hassan, K. (2024) Assessment of flood susceptibility in Sylhet using analytical hierarchy process and geospatial technique, *Geomatica*, 76, 100003.

Sharker, R. (2025) Assessment and zonation of flood susceptibility in Sylhet Division using GIS and analytical hierarchy process, *Journal of Flood Risk Management*.

Shaji, E., Kunhambu, V. and Pradeepkumar, A.P. (2021) Post flood groundwater Kerala 2018, *Water Resources of Kerala: Status and Management* , pp. 48–51.

Singh, L. and Saravanan, S. (2020) Simulation of monthly streamflow using the SWAT model of the Ib River watershed, India, *HydroResearch*, 3, pp. 95–105.

Suthirat, K., Athit, P., Patchapun, R. and Brundiers, K. (2020) GIS-AHP-based flood hazard assessment for Ayutthaya World Heritage Site, Thailand, *International Journal of Disaster Risk Reduction*, 46, 101612.

Suthirat, K., Athit, P., Patchapun, R., Brundiers, K., Buizer, J.L. and Melnick, R. (2020) AHP-GIS analysis for flood hazard assessment of the communities nearby the world heritage site on Ayutthaya Island, Thailand, *International Journal of Disaster Risk Reduction*, 48, 101612.

Surwase, T., Pardeshi, S.D. and Kulkarni, P. (2019) Flood hazard mapping using spatial flood frequency maps and AHP: a case study of the Mahanadi River, Odisha, India, *SN Applied Sciences*, 1, 1527.

Tackley, H.A., Smith, J.D. and Brown, L.R. (2023) Impacts of repeated flooding on soil and groundwater processes, *Science of the Total Environment*, 873, pp. 162346–162356.

Thomas, J. and Raghunath, R. (2020) Delineation of groundwater potential zones using GIS and AHP in Manimala River Basin, Kerala, India, *Arabian Journal of Geosciences*, 13, 1128.

Saaty, R.W. (1987) The analytic hierarchy process—what it is and how it is used, *Mathematical Modelling*, 9(3–5), pp. 161–176.

Shrestha, S., Dahal, D., Poudel, B., Banjara, M. and Kalra, A. (2025) Flood susceptibility analysis with integrated geographic information system and analytical hierarchy process: a multi-criteria framework for risk assessment and mitigation, *Water*, **17**(7), 937.

Surwase, T., Sree, P.M., Nagamani, P. and Jaisankar, G. (2019) Novel technique for developing flood hazard map by using AHP: a study on part of Mahanadi River in Odisha, *SN Applied Sciences*, 1, 1233

Saaty, T.L. (1980) The analytic hierarchy process: planning, priority setting, resources allocation, McGraw-Hill, New York.

Saha, A., Pal, S.C., Arabameri, A., Blaschke, T., Panahi, S., Chowdhuri, I., Chakrabortty, R., Costache, R. and Arora, A. (2021) Flood susceptibility assessment using novel ensemble of hyperpipes and support vector regression algorithms, *Water*, 13(2), 241.

Saha, A.K. and Agrawal, S. (2020) Mapping and assessment of flood risk in Prayagraj district, India: a GIS and remote sensing study, *Nanotechnology for Environmental Engineering*, 5, 11.

Samanta, S., Pal, D.K. and Palsamanta, B. (2018) Flood susceptibility analysis through remote sensing, GIS and frequency ratio model, *Applied Water Science*, 8, 66.

Sampson, C.C., Smith, A.M., Bates, P.D., Neal, J.C., Alfieri, L. and Freer, J.E. (2015) A high-resolution global flood hazard model, *Water Resources Research*, 51, pp. 7358–7381.

Saravanan, S. and Abijith, D. (2022) Flood susceptibility mapping of northeast coastal districts of Tamil Nadu, India using multi-source geospatial data and machine learning techniques, *Geocarto International*, pp. 1–30.

Siam, Z. S. *et al.* (2022) 'National-scale flood risk assessment using GIS and remote sensing-based hybridized deep neural network and fuzzy analytic hierarchy process models: a case of Bangladesh', *Geocarto International*, 37(26), pp. 12119–12148.

Singh, S. (2019) Analytical study of Kerala floods, *International Journal for Research in Applied Science and Engineering Technology*, 7(6), pp. 1796–1802.

Mahmoud, S.H. and Gan, T.Y. (2018) Multi-criteria approach to develop flood susceptibility maps in arid regions of Middle East, *Journal of Cleaner Production*, 196, pp. 216–229.

Stevaux, J.C., de Azevedo Macedo, H., Assine, M.L. and Silva, A. (2020) Changing fluvial styles and backwater flooding along the Upper Paraguay River plains in the Brazilian Pantanal wetland, *Geomorphology*, 350, 106906.

Sturzenegger, M., Holm, K., Lau, C.A. and Jakob, M. (2019) Semi-automated regional-scale debris-flow and debris-flood susceptibility mapping based on digital elevation model metrics and Flow-R software, *Association of Environmental and Engineering Geologists Special Publication*, 28, Colorado School of Mines.

Suresh, S., Rajesh, S. and Mani, K. (2018) Delineation of groundwater potential zones in Devikulam Taluk, Idukki District, Kerala, using remote sensing, GIS and MIF techniques, *Eco Chronicle*, 13, pp. 159–168.

Talukdar, S., Ghose, B., Shahfahad et al. (2020) Flood susceptibility modeling in Teesta River basin, Bangladesh using novel ensembles of bagging algorithms, *Stochastic Environmental Research and Risk Assessment*, 34, pp. 2277–2300.

Tehrany, M.S., Pradhan, B. and Jebur, M.N. (2013) Spatial prediction of flood susceptible areas using rule-based decision tree and novel ensemble statistical models in GIS, *Journal of Hydrology*, 504, pp. 69–79.

Tehrany, M.S., Kumar, L. and Shabani, F. (2019) A novel GIS-based ensemble technique for flood susceptibility mapping using evidential belief function and support vector machine: Brisbane, Australia, *PeerJ*, 7, e7653.

Tehrany, M.S., Shabani, F., Jebur, M.N., Hong, H., Chen, W. and Xie, X. (2017) GIS-based spatial prediction of flood prone areas using standalone and ensemble techniques, *Geomatics, Natural Hazards and Risk*, 8(2), pp. 1538–1561.

Thapa, N. and Prasai, R. (2022) Impacts of floods on land use land cover change: a case study of Indrawati and Melamchi River, Melamchi and Indrawati municipality, Nepal, *International Journal of Multidisciplinary Research and Growth Evaluation*, 3(5), pp. 374–384

Thomas, A., Saha, S., Danumah, J., Raveendran, S., Prasad, M., Ajin, R.S. and Kuriakose, S. (2021) Landslide susceptibility zonation of Idukki district using GIS in the aftermath of 2018 Kerala floods and landslides, *Journal of Geovisualization and Spatial Analysis*, 5, 16.

Uniyal, B., Jha, M.K., Verma, A.K. and Anebagilu, P.K. (2020) Identification of critical areas and evaluation of best management practices using SWAT for sustainable watershed management, *Science of the Total Environment*, 744, 140737.

Veerappan, R. and Sayed, S.I. (2020) Urban flood susceptibility zonation mapping using evidential belief function, frequency ratio and fuzzy gamma operator models in GIS: a case study of Greater Mumbai, Maharashtra, India, *Geocarto International*, 35(15), pp. 1679–1703.

Vijaykumar, P., Abhilash, S., Sreenath, A.V., Athira, U.N., Mohanakumar, K., Mapes, B.E., Chakrapani, B., Sahai, A.K., Niyas, T.N. and Sreejith, O.P. (2021) Kerala floods in consecutive years – its association with mesoscale cloudburst and structural changes in monsoon clouds over the west coast of India, *Weather and Climate Extremes*, 33, 100339

Wu, L., He, Y. and Ma, X. (2020) Can soil conservation practices reshape the relationship between sediment yield and slope gradient?, *Ecological Engineering*, 142, 105630.

Xu, K., Fang, J., Fang, Y., et al. (2021) The importance of digital elevation model selection in flood simulation and a proposed method to reduce DEM errors: a case study in Shanghai, International Journal of Disaster Risk Science, 12, pp. 890–902.

Yang, X.L., Ding, J. and Hou, H. (2013) Application of fuzzy analytical hierarchy process and triangular fuzzy numbers in flood risk assessment, *Natural Hazards*, 67(3), pp. 1295–1312.

Yilmaz, I. (2010) Comparison of landslide susceptibility mapping methodologies for Koyulhisar, Turkey: conditional probability, logistic regression, artificial neural networks and support vector machine, *Environmental Earth Sciences*, 61(4), pp. 821–836.

Young, J.C., Arthur, R., Spruce, M. and Williams, H.T.P. (2022) Social sensing of flood impacts in India: A case study of Kerala 2018, *International Journal of Disaster Risk Reduction*, 74, 102908.

Youssef, A.M., Pourghasemi, H.R., Pourtaghi, Z.S. and Al-Katheeri, M.M. (2016) Landslide susceptibility mapping using random forest, boosted regression tree, classification and regression tree, and general linear models and comparison of their performance at Wadi Tayyah Basin, Asir Region, Saudi Arabia, *Landslides*, 13(4), pp. 839–856.

Zhang, J., Wang, Y., Li, X. and Chen, L. (2022) Groundwater responses to recharge and flood interactions in riparian aquifers, Journal of Hydrology, 614, pp. 128540–128551.

Zhang, G., Xie, H., Chen, H. and Zhang, Y. (2017) Flood effects on groundwater recharge in silt-loam soils, Water, 9(7), pp. 523–534.

Zweig, M.H. and Campbell, G. (1993) Receiver-operating characteristic (ROC) plots: a fundamental evaluation tool in clinical medicine, *Clinical Chemistry*, 39(4), pp. 561–577.

ANNEXURE

PARAWISE RESPONSES BY MR. ZOHAIB AHMED KHAN (2K19/PHDCE/05) TO FOREIGN EXAMINER

Minor Revisions suggested by Foreign Examiner

Based on the work compiled by the Ph.D candidate, I have suggested some of the minor things (kindly see below) for further improvement of the quality and scientific clarity.

1. **Comment**: The candidate is advised to improve language clarity by simplifying long and complex sentences, reducing repetition across chapters (especially in Chapter 1), ensuring grammatical and formatting consistency throughout the chapters.

   Response: Thank you for the valuable suggestion. The suggestion has been duly noted. The thesis has been thoroughly reviewed to enhance language clarity by simplifying lengthy sentences, minimizing repetitive content particularly in Chapter 1 and improving grammatical accuracy. In addition, formatting consistency has been checked and corrected across all chapters.

2. **Comment**: A brief justification for the relative weighting of thematic layers used in the Analytical Hierarchy Process (AHP) should be strengthened (section 4.2.1) with latest literature support, along with a short discussion on the sensitivity of flood susceptibility results to changes in assigned weight.

   Response: Thank you for the valuable comment. The relative weights assigned to the thematic layers in the AHP model were determined based on the hydrological relevance of each parameter and supported by findings from recent studies on flood susceptibility mapping. Parameters that directly influence runoff generation and water accumulation, such as rainfall, elevation, slope, distance from river, and Topographic Wetness Index (TWI), were given comparatively higher importance as highlighted in previous literature. In addition, a sensitivity analysis has already been carried out and presented in Section 5.2.4 of the thesis, which confirms that rainfall, elevation, distance from river, slope, and TWI are the key contributing variables influencing flood susceptibility in the study area. The analysis also demonstrates

that moderate changes in parameter weights do not significantly alter the overall spatial pattern of flood-prone zones, indicating the robustness of the model. The requested clarification and discussion have been incorporated in the revised thesis.

3. **Comment**: The uncertainty associated with ML model outputs (AdaBoost, Gradient Boosting and Random Forest) should be discussed in Section 4.3, which includes limitations related to training data, model generalization and potential classification bias.

   Response: Thank you for the insightful comment. The uncertainty associated with the machine learning models (AdaBoost, Gradient Boosting, and Random Forest) has now been addressed in the revised thesis. A discussion outlining the possible sources of uncertainty particularly those related to the quality and representativeness of training data, the generalization capability of the models, and potential classification bias has been incorporated under the Methodology section (Sub Section 4.3.6). This section explains how limitations in training samples, variability in landscape conditions, and imbalanced data distributions may influence model outputs. It also highlights that the use of different machine learning algorithms which helps reduce individual model bias and improves the reliability of the groundwater potential zone predictions.

4. **Comment**: While the SWAT model results are convincing, a concise description of model calibration, validation strategy, and key performance indicators should be clearly highlighted, to improve transparency and reproducibility.

   Response: Thank you for the valuable suggestion. The procedures adopted for the calibration and validation of the SWAT model have already been described in Section 5.5.2 of the thesis. This section has been further revised to present the calibration approach, validation strategy, and the key performance indicators used for evaluating model performance in a clearer and more structured manner. The relevant statistical measures used to assess the reliability of the model simulations are now explicitly highlighted to enhance the transparency and reproducibility of the modelling process. These improvements have been incorporated in the revised Section 5.5.2 of the thesis.

5. **Comment**: The candidate may consider including a short discussion on the influence of extreme rainfall variability and possible future climate scenarios on flood susceptibility and runoff behaviour to enhance the national and/or global relevance of the study.

Response: Thank you for the valuable suggestion. The suggestion regarding the consideration of extreme rainfall variability and future climate scenarios is appreciated. The present study primarily focuses on assessing flood susceptibility and runoff behaviour using observed hydrological conditions in the Idukki district. In this context, the analysis already incorporates the extreme rainfall event of 2018, which represents one of the most severe precipitation events recorded in Kerala in recent decades. The flood susceptibility mapping and runoff modelling were carried out by considering the hydrological conditions associated with this extreme event, thereby reflecting the influence of high rainfall variability on flood generation and runoff response in the region. Since the scope of this research is centred on geospatial flood assessment and hydrological modelling rather than climate projection, future climate scenario simulations were not undertaken. However, a brief discussion has been incorporated in the thesis highlighting how increasing rainfall variability may influence flood susceptibility and runoff behaviour in the Western Ghats region. This clarification has been included in the section 5.5.5.

6. **Comment:** The linkage between repeated flooding, reduced infiltration, and constrained groundwater recharge should be supported with additional references or brief quantitative justification where possible.

   Response: Thank you for the valuable suggestion. The suggestion regarding the relationship between repeated flooding, reduced infiltration, and limited groundwater recharge has been carefully considered. To address this, additional references from relevant hydrological studies have been incorporated into the thesis to provide stronger support for the discussion on how flood events can influence infiltration processes and groundwater recharge conditions. These references reinforce the existing explanation presented in the study and improve the overall scientific grounding of the findings. The necessary revisions have therefore been incorporated in the relevant section of the thesis.

7. **Comment:** Figure captions, legends, and map layouts, should be reviewed to ensure clarity, uniform scale representation, and ease of interpretation for readers unfamiliar with the study area.

   Response: The suggestion has been noted. The figure captions, legends, and map layouts have been carefully reviewed and revised wherever necessary to improve clarity, maintain consistent scale representation, and enhance overall readability for readers who may not be familiar with the study area.

LIST OF PUBLICATIONS

- Khan, Z. A., & Jhamnani, B. (2023). Development of flood susceptibility map using a GIS-based AHP approach: a novel case study on Idukki district, India. *Journal of Spatial Science*, *69*(2), 409–442. https://doi.org/10.1080/14498596.2023.2236051 (SCI IF - 1.6)
- Zohaib Ahmed Khan, Bharat Jhamnani; Identification of groundwater potential zones of Idukki district using remote sensing and GIS-based machine-learning approach. *Water Supply* 1 June 2023; 23 (6): 2426–2446. doi: https://doi.org/10.2166/ws.2023.134 (SCI - IF 1.768)
- Zohaib Ahmed Khan, Bharat Jhamnani; Effects of Torrential Rainfall and Floods on the Changing Landscapes and their Impact Assessment in Idukki District, India. 4th International Conference on River Corridor Research and Management (RCRM- 2024), IIT Jammu, 7th – 9th March 2024.
- Zohaib Ahmed Khan, Bharat Jhamnani; Evaluation of Surface Runoff in the Periyar River Basin using SWAT Model. First International Conference on Advances in Energy and Environmental Engineering 2024, 17th – 18th December 2024.

JOURNAL OF SPATIAL SCIENCE
2024, VOL. 69, NO. 2, 409–442
https://doi.org/10.1080/14498596.2023.2236051

Development of flood susceptibility map using a GIS-based AHP approach: a novel case study on Idukki district, India

Zohaib Ahmed Khan and Bharat Jhamnani

Department of Civil Engineering, Delhi Technological University, Delhi, India

ABSTRACT

Flooding is a regular danger in the Idukki district of Kerala causing serious damage to life and property. An attempt has been undertaken in this research to identify crucial zones in the Idukki district that are more susceptible to flooding. The AHP technique was used to give relative weights to 12 flood contributing parameters. The resultant flood susceptibility map shows that 1346.4 km^2 of the total land in the Idukki district has a high to very high likelihood of flooding. Validation of the resultant map was achieved using the AUC-ROC approach, which showed good accuracy of 0.91.

ARTICLE HISTORY
Received 14 March 2023
Accepted 9 July 2023

KEYWORDS
Floods; analytical hierarchy process; susceptibility; mapping; remote sensing

1. Introduction

Flooding is a regular natural hazard that causes significant damage to people and property (Gabriels *et al.* 2022). Floods benefit the ecosystem in a number of ways at lower magnitudes, including by supplying water and nutrients to riparian corridors, eliminating pollutants from flood plain zones, recharging the groundwater table and enhancing soil fertility (Lyubimova *et al.* 2016, Zhang *et al.* 2017, Kraus *et al.* 2019, Abijith *et al.* 2020, Mahato *et al.* 2021). The lives, agricultural operations, residential areas, properties, roadways and natural ecosystems will all suffer enormous damage if the flood tolerance limit is exceeded (Pradhan and Youssef 2011, George *et al.* 2022). According to Kron (2005), this occurs due to heavy rain and melting of snow, which causes the river to overflow and stay momentarily stagnant, causing damage to the lands along the river. Flooding can be caused due to the overflowing of a river as well as other factors like abrupt cloudbursts in semi-arid locations, resulting in flash flood (Tehrany *et al.* 2013). Flooding is a very complicated occurrence that has always drawn researchers from all around the world to better understand and study different mechanisms for better management and avoidance of flood-related hazards. Several natural and human factors are to blame, all of which have the potential to cause a catastrophic flood disaster (Sholihah *et al.* 2020). There is an increase in frequencies of flood episodes and the causes are often associated with unsustainable industrial and farming practices such as cutting of trees, excessive utilisation of resources, improper planning of urbanised colonies and concretisation (Bradshaw *et al.* 2007).

CONTACT Zohaib Ahmed Khan zohaib098765@gmail.com

Check for updates

Water Supply

IWA PUBLISHING

Water Supply Vol 23 No 6, 2426 doi: 10.2166/ws.2023.134

Identification of groundwater potential zones of Idukki district using remote sensing and GIS-based machine-learning approach

Zohaib Ahmed Khan* and Bharat Jhamnani

Department of Civil Engineering, Delhi Technological University, Delhi, India
*Corresponding author. E-mail: zohaib098765@gmail.com

ABSTRACT

Kerala's Idukki district, which is situated on the Western Ghats of India, is susceptible to flooding and landslides. As a result of the 2018 Kerala floods, this disaster-prone region experienced drought conditions. In order to lessen the effects of future disasters, it is also necessary to identify and evaluate the district's groundwater potential (GWP). This work used three machine-learning (ML) algorithms – Random Forest (RF), Adaptive Boosting (AdaBoost), and Gradient Boosting (GB) – to model and produce GWP zonation maps for the Idukki district. Fourteen conditioning factors including elevation, slope, curvature, Topographic Roughness Index, lineament density, soil, geology, geomorphology, Topographic Wetness Index, Sediment Transport Index, drainage density, rainfall, land-use/land-cover (LULC), and Normalised Difference Vegetation Index were adopted as input parameters in the modelling. All showed prominence when they were examined for feature importance using the recursive feature elimination (RFE) method. The RF model outperformed the other two ML models in terms of fit, with an area under curve (AUC) value of 0.92, while the GB and AdaBoost models displayed less fit, with AUC values of 0.90 and 0.88, respectively. GWP maps produced by each model were reclassified into five zones – very high to very low – it was discovered that the zones were evenly spread throughout the Idukki region.

Key words: drinking water, groundwater, potential zones, rivers

HIGHLIGHTS

- Groundwater potential zones were identified using different machine-learning models such as Random Forest (RF), Adaptive Boosting (AdaBoost), and Gradient Boosting.
- Fourteen groundwater conditioning factors were utilised to evaluate the groundwater potential zones.
- Findings revealed that among all the machine-learning models Random Forest yields the most accurate results.
- Validation was performed using well locations.


भारतीय प्रौद्योगिकी संस्थान गुवाहाटी
Indian Institute of Technology Guwahati
विद्याधनं सर्वधन प्रधानम्
IIT JAMMU
CERTIFICATE
OF PARTICIPATION
This certificate is proudly presented to:
Zohaib Ahmed Khan
delivered a presentation during technical session on "River Corridor Issues and Challenges" for the abstract titled "Effects Of Torrential Rainfall And Floods On The Changing Landscapes And Their Impact Assessment" at the 4th International Conference on River Corridor Research and Management (RCRM-2024) jointly organized by the Indian Institute of Technology, Guwahati and the Indian Institute of Technology, Jammu held from March 7th to 9th 2024
Prof. Subashisa Dutta
Conference Chair
Dr. Vinay Chembolu
Conference Co-Chair

ICAEEE 2024

17-18 December 2024

First International Conference on

Advances in Energy and Environmental Engineering 2024

Certificate

This is to certify that the paper entitled

Evaluation of Surface Runoff in the Periyar River Basin Using SWAT Model

is presented by

Zohaib Ahmed Khan from Delhi Technological University, Delhi, India

at the **First International Conference on Advances in Energy and Environmental Engineering 2024** held on 17 - 18 December 2024, hosted by the Dr. Vithalrao Vikhe Patil College of Engineering, Ahilyanagar, India in association with Technology Research and Innovation Centre, Pune, India.

Dr. Kanif M. Markad	Dr. Ravindra R. Navthar	Dr. Sandip A. Kale	Dr. Sunday O. Oyedepo	Prof. Uday P. Naik
Convener	Scientific Chair	Scientific Chair	Chairperson	Chairperson

2307

Curriculum Vitae

Zohaib Ahmed Khan

Email: zohaib098765@gmail.com

Educational Qualifications

- Ph.D. in Civil Engineering (Water Resources Engineering) from Delhi Technological University.
- Completed M. Tech in Hydraulics and Water Resources Engineering from Delhi Technological University with 84.30 % in the year 2019.
- Completed B. Tech in Civil Engineering from Lovely Professional University, Punjab with 74.88 % in the year 2014.
- Completed 12th Standard in Science Stream from Ramjas School Pusa Road, Delhi (Central Board of Secondary Education) securing 81.60 % in the year 2010.
- Completed 10th standard from Ramjas School Pusa Road (Central Board of Secondary Education) securing 78.40 % in the year 2008.

Thesis

- **Ph.D. thesis title**: Study on Assessment of Floods & Groundwater Susceptible Zones in Idukki District, Kerala Using GIS Based Approach
  Supervisor: Dr. Bharat Jhamnani, Assistant Professor, Delhi Technological University
- **M.Tech thesis title**: CFD Analysis of Prismatic Compound Channels
  Supervisor: Dr. Bharat Jhamnani, Assistant Professor, Delhi Technological University
- **B.Tech Project title**: Construction of Underground Metro Station
  Supervisor: Mr. Tabish, Associate Professor, Lovely Professional University, Punjab

Certifications & Achievements

- Geographic Information Systems from NPTEL Microwave remote sensing in Hydrology from NPTEL.
- Groundwater Potential Zones Using GIS from UDEMY
- ArcSWAT model with ArcGIS from UDEMY
- SWATCUP Calibration and Validation from UDEMY
- Data Science Math Skills from Coursera
- Decision Making using Analytic Hierarchy Process (AHP)

PUBLICATIONS:

- Khan, Z. A., & Jhamnani, B. (2023). Development of flood susceptibility map using a GIS-based AHP approach: a novel case study on Idukki district, India. *Journal of Spatial Science*, *69*(2), 409–442. https://doi.org/10.1080/14498596.2023.2236051 (SCI IF - 1.6)
- Zohaib Ahmed Khan, Bharat Jhamnani; Identification of groundwater potential zones of Idukki district using remote sensing and GIS-based machine-learning approach. *Water Supply* 1 June 2023; 23 (6): 2426–2446. doi: https://doi.org/10.2166/ws.2023.134 (SCI - IF 1.768)
- Zohaib Ahmed Khan, Bharat Jhamnani; Effects of Torrential Rainfall and Floods on the Changing Landscapes and their Impact Assessment in Idukki District, India. 4th International Conference on River Corridor Research and Management (RCRM-2024), IIT Jammu, 7th – 9th March 2024.
- Zohaib Ahmed Khan, Bharat Jhamnani; Evaluation of Surface Runoff in the Periyar River Basin using SWAT Model. First International Conference on Advances in Energy and Environmental Engineering 2024, 17th – 18th December 2024.

Software Knowledge

- HEC-HMS
- HEC-RAS
- ArcMAP
- QGIS
- Ansys Fluent
- AutoCAD

- STAAD. Pro
- HY8
- Sewer Gems

References

1. Dr. Bharat Jhamnani

   Assistant Professor

   Department of Civil Engineering

   Delhi Technological University

   Email: bjhamnani@gmail.com

2. Dr. Ranganath M. Singari

   Department of Design

   Delhi Technological University

   Email: ranganath@dce.ac.in